JOURNAL OF FOOD PROCESS ENGINEERING

D.R. HELDMAN
and
R.P. SINGH
COEDITORS

FOOD & NUTRITION PRESS, INC.

VOLUME 20, NUMBER 3 JULY 1997

JOURNAL OF FOOD PROCESS ENGINEERING

All articles for publication and inquiries regarding publication should be sent to DR. D.R. HELDMAN, COEDITOR, *Journal of Food Process Engineering*, University of Missouri-Columbia, 214 Agricultural Engineering Bldg., Columbia, MO 65211 USA; or DR. R.P. SINGH, COEDITOR, *Journal of Food Process Engineering*, University of California, Davis, Department of Agricultural Engineering, Davis, CA 95616 USA.

All subscriptions and inquiries regarding subscriptions should be sent to Food & Nutrition Press, Inc., 6527 Main Street, P.O. Box 374, Trumbull, CT 06611 USA.

One volume of six issues will be published annually. The price for Volume 20 is $164.00, which includes postage to U.S., Canada, and Mexico. Subscriptions to other countries are $187.00 per year via surface mail, and $198.00 per year via airmail.

Subscriptions for individuals for their own personal use are $134.00 for Volume 20, which includes postage to U.S., Canada and Mexico. Personal subscriptions to other countries are $157.00 per year via surface mail, and $168.00 per year via airmail. Subscriptions for individuals should be sent directly to the publisher and marked for personal use.

The *Journal of Food Process Engineering* is listed in *Current Contents/Agriculture, Biology & Environmental Sciences (CC/AB)*, and SciSearch, and Research Alert.

The *Journal of Food Process Engineering* (ISSN:0145-8876) is published (February, April, June, August, October and December) by Food & Nutrition Press, Inc.—Office of Publication is 6527 Main Street, P.O. Box 374, Trumbull, Connecticut 06611 USA.

Second class postage paid at Bridgeport, CT 06602.

POSTMASTER: Send address changes to Food & Nutrition Press, Inc., 6527 Main Street, P.O. Box 374, Trumbull, Connecticut 06611 USA.

JOURNAL OF FOOD PROCESS ENGINEERING

Journal of FOOD PROCESS ENGINEERING

VOLUME 20
NUMBER 3

Coeditors: D.R. HELDMAN
R.P. SINGH

FOOD & NUTRITION PRESS, INC.
TRUMBULL, CONNECTICUT 06611 USA

ISSN 0145-8876

Printed in the United States of America

CONTENTS

A NONLINEAR PROGRAMMING TECHNIQUE TO DEVELOP LEAST COST FORMULATIONS OF SURIMI PRODUCTS

CHENG-KUANG HSU, EDWARD KOLBE[1] and MARSHALL ENGLISH

Department of Bioresource Engineering
Gilmore Hall
Oregon State University
Corvallis, OR 97331-3906

Accepted for Publication April 12, 1996

ABSTRACT

Optimization programming techniques were applied to develop the least cost formulations for Pacific whiting surimi-based seafood (PWSBS). To develop the quality constraint functions, texture and color of whiting surimi gels were determined by torsion test and colorimeter, respectively. Whiting surimi gels were produced by heating at 90C for 15 min with 2% NaCl, five final moisture contents (74, 76, 78, 80, 82%), and various combinations of beef plasma protein (0-2%), potato starch (0-8%), and two whey protein concentrates (0-8%). Due to the nonlinear constraint functions describing texture and color, a nonlinear programming search technique was required to solve the least cost model for PWSBS. Results for representative target quality constraints are reported in this study and show that whey protein concentrate both increases the texture properties and remains economically competitive with other ingredients which similarly influence functionality in PWSBS.

INTRODUCTION

Pacific whiting (*Merluccius productus*) was an underutilized species due to its soft texture caused by protease enzymes that may be related to parasites (Erickson *et al.* 1983). Whiting is commonly processed into surimi, a washed mince to which is added cryoprotectants, such as sorbitol and sucrose, which maintain protein quality during frozen storage. Surimi is then further processed into various surimi-based gelled products such as artificial crab legs and meats. It is well known that texture and color are the most important sensory factors affecting the consumer's acceptance of surimi-based seafood. During the

[1] To whom correspondence should be sent: Tel: (541) 737-6305, Fax: (541) 737-2082, E-mail: kolbee@ccmail.orst.edu

Journal of Food Process Engineering **20** (1997) 179–196.

processing of Pacific whiting surimi-based seafood (PWSBS), the addition of protease inhibitors and/or gel strength enhancers is generally required to maintain good texture characteristics (Morrissey *et al.* 1993). However, the addition of these food grade additives to enhance texture may increase the total cost of ingredients and/or change the color properties of final products, thereby reducing the market acceptance. Thus, it is necessary to determine the optimal formulation that leads to minimum cost of PWSBS while maintaining good texture and color.

Optimization techniques such as linear or nonlinear programming allow us to find a minimum cost while maintaining desired levels of product quality. This process, which includes experiments and application of quantitative models, additionally describes relationships among the costs of ingredients, the amount of ingredients in the formulation, and the quality of final products. The use of least cost formulation techniques has been found to improve the profitability and/or quality control for various food products (IBM 1966; Kramlich *et al.* 1973; Lanier and Park 1989; Park 1992).

Linear programming has been used to maintain minimum cost of surimi-based seafoods while blending different grades of surimi lots to reach a desired level of texture and color. Lanier and Park (1989) showed that the texture and color properties in blended surimi products are an approximate linear function of the mass of each surimi lot added to the formulation. However, questions arise concerning whether such linear relationships would still hold when protease inhibitors and/or gel strength enhancers are added to surimi products. In a study to optimize the texture properties of Alaska pollock surimi with the addition of starch and egg white, Chen *et al.* (1993) showed that a response surface methodology (which accounts for nonlinear relationships) provided a more accurate prediction of texture behavior than did a linear programming approach (which accounts only for linear relationships). Daley *et al.* (1978), optimizing a sausage product from minced fish using response surface methodology, showed that the relationships between texture properties and ingredient levels were nonlinear. Hastings and Currall (1989) also found significant interactions (both synergistic and antagonistic nonlinearities) between ingredients and the texture of cod surimi gels. Understanding the relationships between quality parameters and ingredient levels is necessary to allow selection of proper optimization techniques to develop least cost formulations of food products. This is particularly important in whiting surimi due to its intrinsic autoproteolytic activity. To control the protease activity in whiting surimi, a number of inhibitors or gel enhancers can be used. These include hydrolyzed beef plasma protein, potato starch, and whey protein concentrates.

The dairy industry annually produces thousands of tons of whey protein concentrate (WPC) world-wide, and this is available as a steady source of functional protein for the food industry. The use of WPC has been found to

improve the texture properties of PWSBS (Chung and Morrissey 1993). Piyachomkwan and Penner (1995) suggested that WPC may protect the myofibrillar proteins of surimi by acting as a true protease inhibitor or by serving as an alternative substrate. The use of WPC in PWSBS has therefore been found to be technically effective, however, its economic feasibility is subject to further study. The objectives of this study were to identify effective optimization approaches that will give least cost formulations of protease inhibitors and gel enhancement ingredients in PWSBS, and to evaluate the potential of using WPC as an economically viable gel enhancer in PWSBS.

MATERIALS AND METHODS

Washed and dewatered mince was made from Pacific whiting within 24 h of harvest at Point Adams Seafood Inc. in Hammond, Oregon. This mince was immediately transported, on ice, to the OSU Seafood Laboratory in Astoria, 30 min away by car. After mixing with cryoprotectants (4% sucrose, 4% sorbitol, and 0.3% sodium tripolyphosphate) in a cool room, the mince weighing about 650 g was vacuum-packaged in plastic bags. The packages were then frozen to a core temperature of -25C and stored in insulated boxes inside a blast freezer at -34C. Two packages of frozen surimi were removed from storage and used as one surimi sample.

Experimental Design

To develop the mathematical functions giving texture and color as a function of five ingredient variables, an appropriate experimental design was needed to limit the number of experimental points. Response surface methodology is the approach most commonly used for seeking optimal responses from experiments involving multiple variables (Box *et al.* 1978; Cochran and Cox 1957). In this study, a second-order central composite design for five variables was adopted (Cochran and Cox 1957) with some modifications. According to Chung and Morrissey (1993) and Morrissey *et al.* (1993), the maximum concentrations of BPP, PS, WPC33, and WPC72 that improve the texture properties of PWSBS are 2, 4, 4, and 4%, respectively, while not much improvement was observed beyond these concentrations.

Therefore in this study the levels for each ingredient were initially selected as 0, 0.5, 1, 1.5, and 2% for BPP; 0, 1, 2, 3, and 4% for PS, WPC33, and WPC72; and 74, 76, 78, 80, and 82% for moisture content. As shown in Table 1, the experimental points No. 1-27 included these combinations of ingredients based on the second order central composite design (Cochran and Cox 1957) for five variables at the five different levels given above. In central composite

TABLE 1.
THE EXPERIMENTAL DESIGN AND EXPERIMENTAL DATA

No.	Independent Variables					Color			Texture	
	BPP (%)	PS (%)	WPC33 (%)	WPC72 (%)	Moisture (%)	L*	a*	b*	Stress (kPa)	Strain
1	0.5	1	1	1	76	78.2	-4.4	4.1	42.7	2.23
2	1.5	1	1	1	80	79.9	-4.1	5.2	24.5	2.49
3	0.5	3	1	1	80	75.6	-4.6	1.9	24.7	2.38
4	1.5	3	1	1	76	78.8	-4.0	6.2	44.9	2.45
5	0.5	1	3	1	80	83.5	-3.8	5.4	17.6	2.15
6	1.5	1	3	1	76	78.1	-4.7	5.8	47.3	2.35
7	0.5	3	3	1	76	80.4	-4.0	5.3	37.9	2.18
8	1.5	3	3	1	80	77.5	-5.0	4.9	19.9	2.43
9	0.5	1	1	3	80	82.7	-3.8	5.2	19.9	2.20
10	1.5	1	1	3	76	79.6	-4.2	7.2	44.9	2.11
11	0.5	3	1	3	76	79.7	-4.0	5.3	45.5	2.18
12	1.5	3	1	3	80	75.7	-4.7	4.9	26.4	2.17
13	0.5	1	3	3	76	79.3	-4.7	5.3	41.6	2.29
14	1.5	1	3	3	80	84.9	-3.8	7.9	14.8	2.07
15	0.5	3	3	3	80	81.6	-4.1	5.2	18.3	2.17
16	1.5	3	3	3	76	77.5	-4.8	6.3	45.5	2.24
17	0	2	2	2	78	77.9	-4.6	3.2	29.5	2.25
18	2	2	2	2	78	82.8	-3.7	8.3	27.6	2.20
19	1	0	2	2	78	79.4	-4.4	5.1	27.4	2.15
20	1	4	2	2	78	81.5	-3.5	6.6	30.8	2.25
21	1	2	0	2	78	78.1	-4.4	4.6	40.2	2.62
22	1	2	4	2	78	80.0	-4.6	6.2	27.5	2.27
23	1	2	2	0	78	78.8	-4.2	4.5	34.1	2.51
24	1	2	2	4	78	82.2	-4.2	6.9	31.9	2.04
25	1	2	2	2	82	85.1	-3.2	6.3	11.8	2.23
26	1	2	2	2	74	76.3	-4.8	5.2	62.3	2.36
27	1	2	2	2	78	80.6	-3.9	6.0	27.1	2.34
	1	2	2	2	78	81.1	-3.9	6.2	32.5	2.27
28	0	0	0	0	74	80.5	-3.5	4.1	22.0	1.07
	0	0	0	0	74	78.6	-3.6	2.9	21.3	1.03
29	2	0	0	0	82	81.0	-3.8	6.1	14.6	2.44
	2	0	0	0	82	80.0	-3.6	6.7	20.8	2.23
30	0	4	0	0	82	80.4	-3.2	1.0	7.1	1.68
	0	4	0	0	82	79.0	-3.5	1.5	9.5	1.50
31	2	4	0	0	74	79.3	-3.4	7.9	62.3	2.36
32	0	0	4	0	82	82.5	-3.9	3.2	7.1	1.69
	0	0	4	0	82	82.9	-3.7	3.6	6.2	1.45
33	2	0	4	0	74	79.6	-4.2	7.9	35.4	2.11
34	0	4	4	0	74	80.4	-3.7	S.0	31.7	1.87
35	2	4	4	0	82	85.6	-3.3	7.0	7.8	1.98
36	0	0	0	4	82	83.2	-3.7	4.9	10.0	1.97
	0	0	0	4	82	82.0	-3.4	4.5	13.0	1.91
37	2	0	0	4	74	79.8	-4.1	8.5	54.6	1.99

38	0	4	0	4	74	75.0	-4.7	3.2	75.6	2.41
39	2	4	0	4	82	84.4	-3.2	7.8	14.9	2.01
40	0	0	4	4	74	81.3	-4.5	6.6	39.8	1.95
41	2	0	4	4	82	88.4	-3.5	9.3	3.6	1.31
	2	0	4	4	82	87.7	-3.5	9.5	3.7	1.33
42	0	4	4	4	82	85.4	-3.7	5.6	8.4	1.74
43	2	4	4	4	74	78.8	-4.2	8.1	56.7	2.01
	2	4	4	4	74	78.8	-4.4	8.7	48.8	2.05
44	0	0	0	0	78	80.2	-3.4	3.5	19.5	1.12
	0	0	0	0	78	79.8	-3.2	3.3	16.9	0.98
45	0	0	0	0	82	80.6	-3.7	1.3	6.0	1.17
	0	0	0	0	82	82.3	-3.3	2.2	6.2	1.38
46	0	0	0	8	78	81.1	-4.7	5.5	37.3	1.80
	0	0	0	8	78	80.0	-4.3	6.0	43.6	1.59
47	0	0	8	0	78	81.9	-4.4	8.4	8.2	1.57
	0	0	8	0	78	82.9	-4.7	8.9	9.5	1.65
48	0	8	0	0	78	75.2	-3.8	0.6	19.0	1.53
	0	8	0	0	78	77.0	-3.4	1.3	16.1	1.39
49	1	2	2	6	78	81.3	-4.5	7.9	24.0	1.64
50	1	2	6	2	78	82.2	-4.1	9.5	13.9	1.73
51	1	6	2	2	78	75.4	-5.0	4.6	32.9	2.20
52	1	2	6	6	74	83.8	-4.1	11.7	19.8	1.35
53	1	6	2	6	74	78.5	-4.6	8.6	53.1	1.67
54	1	6	6	2	74	78.5	-4.6	10.0	36.5	1.81
55	2	0	4	8	74	83.5	-4.0	11.6	27.7	1.27
56	0	4	0	8	76	78.2	-4.9	5.6	66.0	1.77
57	2	0	8	4	74	82.9	-4.0	12.4	14.9	1.30
58	0	4	8	0	76	79.5	-4.6	8.6	18.9	1.65
59	2	8	4	0	74	73.2	-4.8	7.2	75.8	2.42
60	0	8	0	4	76	74.2	-4.4	3.0	62.7	2.29
61	1	2	2	8	76	81.7	-4.4	9.2	37.8	1.37
	1	2	2	8	76	83.6	-4.1	10.1	32.3	1.44
62	1	2	8	2	76	82.9	-4.1	11.1	13.3	1.49
	1	2	8	2	76	83.2	-3.5	11.4	12.8	1.50
63	1	8	2	2	76	73.0	-4.9	4.8	57.4	2.35
	1	8	2	2	76	74.1	-4.0	6.1	39.2	2.31

design, it is assumed that the optimum is located at the center level of each variable. So additional experimental points are selected about this center level, allowing us to accurately pinpoint the optimum while taking only a few experimental points at the end-levels of each variable.

Since a major objective of this study was to investigate methods to minimize the cost of PWSBS rather than simply to optimize the quality of texture and color, it was desired to derive mathematical functions of texture and color having the same level of accuracy over the expected experimental range of each variable. Although a "rotatable" central composite (Cochran and Cox 1957)

allows us to obtain uniform accuracy around the neighborhood of the central level, it has poor prediction at the end-levels of each variable. Thus, adding extra experimental points, No. 28-45 (Table 1), to increase accuracy of prediction at the end-levels of each variable was found to be necessary. All experimental runs were performed in a random order. After initial analysis, it was learned that a broader range of ingredient levels was needed to reach the optimum solution because the use of PS and WPC33 higher than 4% appears to further lower the formulation cost of PWSBS. Thus, the upper levels of PS, WPC33, and WPC72 were further increased from 4% to 8% (experimental points No. 46-63).

Surimi Gel Preparation

Frozen surimi was thawed at room temperature for 2 h. A Stephan vacuum mixer (Model UM5 Universal, Stephan Machinery Corporation, Columbus, OH) was used to mix approximately 1 kg of whiting surimi with 2% NaCl and various combinations of beef plasma protein (BPP, American Meat Protein Corp. Inc., IA) (0-2%), potato starch (PS, Avebe America, Inc., NJ) (0-8%), and two kinds of whey protein concentrate: WPC33 (with 33% protein content, Avonmore West, Inc., ID) and WPC72 (with 72% protein content, New Zealand Milk Products, Inc., CA) (0-8%). The mixture was chopped for 4 min with the addition of ice (versus water) to adjust the final moisture content to five different levels (74, 76, 78, 80, and 82%) while maintaining a low temperature (below 10C).

A 5-lb-capacity sausage stuffer (The Sausage Maker, Buffalo, NY) was used to extrude the mixture into stainless steel cooking tubes (inside diameter 1.9 cm, length 17.8 cm). Surimi gels were produced by heating in a 90C water bath for 15 min, followed by cooling in ice water for 10 min. They were then stored in ziplock bags at a refrigerated temperature of about 5C. Gels were removed from a refrigerated storage within 48 h, and allowed to set at room temperature for 1 h before slicing into small sections (diameter 1.9 cm, length 2.9 cm). These served as samples for color and texture measurement.

Color Measurement

The color of surimi gels was measured using a Minolta CR-200 colorimeter (El Monte, CA) calibrated with a standard hitch tile (Hunter Associates Laboratory, Inc., Reston, Virginia) specified for testing the color of surimi gels (NFI 1991). The L*, a*, and b* values were recorded, with L* denoting lightness on a 0 to 100 scale from black to white; a*, red (+) or green (-); and b*, yellow (+) or blue (-). A "whiteness" index for overall color evaluation of surimi is also used and calculated as: L* - 3b* (Park 1994). Each experimental point had eight replicates.

Torsion Test

The gels were cut into hourglass shapes, then subjected to twisting in a torsion gelometer (Gel Consultants, Raleigh, NC) to the point of failure, following the procedures described in NFI (1991). The results of the torsion test for our experiments were defined as shear stress and shear strain at failure, calculated from the equations provided by Hamann (1983). Eight replicate samples were tested for each experimental point.

Composition Analysis

The analysis of protein and moisture contents of whiting surimi and of each ingredient was performed according to standard AOAC methods (1984).

Model and Validation

A stepwise regression procedure in the SAS package (SAS Institute, Inc., Cary, NC) was used to fit the texture and color data into second order polynomial equations with interaction terms:

$$Z=A_o+\sum_{i=1}^{5} A_i Y_i+\sum_{i=1}^{5} A_i Y_i^2+\sum_{i=1}^{5}\sum_{j=1}^{5} A_{ij} Y_i Y_k (i\neq j)$$

where Z is the dependent variable, A_o, A_i, A_{ij} are regression coefficients of the model, and Y_i are concentrations (in weight percent) of each ingredient (subscripts i, j = 1..5 represent BPP, PS, WPC33, WPC72, and the final moisture content, respectively). An F test for lack of fit was used to determine whether the regression models adequately fit the experimental data. Once the regression models were developed, 14 new experimental points determined randomly in separate experiments were then used to test the models.

Least Cost Model of PWSBS

The objective function to be minimized in the least cost model of PWSBS, was the total cost of ingredients. The cost of each ingredient was collected from the commercial suppliers. Cost of ingredients and the experimental values of ingredient protein and moisture contents are reported in Table 2. Using results of Table 2, the final moisture content of PWSBS (Y_5) in the regression models of texture and color can be substituted by the summation of moisture contents of each ingredient as the following equation:

$$Y_5 = 0.076X_1 + 0.17\ X_2 + 0.064\ X_3 + 0.052\ X_4 + X_5 + 0.751\ X_6$$

where X_1, X_2, X_3, X_4, X_5, and X_6 are the weight percent of BPP, PS, WPC33, WPC72, water, and surimi, respectively.

TABLE 2.
THE PROTEIN CONTENT, MOISTURE CONTENT, AND THE COST (IN 1993) OF EACH INGREDIENT IN PWSBS

Ingredient	Protein (%)	Moisture (%)	Cost (per lb)
BPP	68.7	7.6	$2.50
PS	0.0	17.0	$0.39
WPC33	33.0	6.4	$0.60
WPC72	72.3	5.2	$2.05
Water	0.0	100.0	$0.00
Surimi	15.7	75.1	$1.00
NaCl	0.0	0.0	$0.22

Upper and lower boundaries of the parameter which defines each constraint function (i.e. texture, color, and ingredients) were used to define the quality of PWSBS. According to Lanier (1988) and Park (1993), one example of a set of constraints depicting high quality PWSBS are listed in Table 3. Hamann and MacDonald (1992) and Park (1992) define a texture mapping procedure that might be used to identify boundaries of constraints which would simulate certain textural characteristics (One example might characterize properties of a given frankfurter product). The example constraints given in Table 3 simulate a good quality surimi seafood and were used in this study to develop the least cost formulations for PWSBS.

TABLE 3.
GENERAL CONSTRAINTS DEPICTING HIGH QUALITY SURIMI-BASED SEAFOODS

Quality Index	Low- and/or High-boundary Values
Protein content	$\geq$ 10%
Moisture content	$\geq$ 74% and $\leq$ 77%
Surimi content	$\geq$ 40%
Salt	= 2%
Texture	
Shear stress (kPa)	$\geq$ 36 and $\leq$ 44
Shear strain	$\geq$ 2.0 and $\leq$ 2.6
Color	
Yellowness	$\leq$ 7
Whiteness	$\geq$ 60

Nonlinear and Linear Programming

A primal simplex method (Dantzig 1963) was used to solve the linear programming problem. In the case of solving a nonlinear programming problem with nonlinear constraint functions, they were transformed with the augmented Lagrangian procedures described by Robinson (1972) and Murtagh and Saunders (1982), into a sequence of linearly constrained subproblems which could be solved by using a reduced gradient algorithm (Wolfe 1967). In solving nonlinear programming problems, 20 different starting quests were randomly used to avoid getting local minima instead of a global minimum. The random number function in the commercial spreadsheet, Quattro Pro (Borland International, Inc., Scotts Valley, CA), was used to generate these starting quests. A commercial linear and nonlinear programming package "AMPL" (The Scientific Press, San Francisco, CA) (Murtagh and Saunders 1978, 1982) was used to search least cost formulations of PWSBS with varied composition, texture, color, and constraints. The linear and nonlinear optimization solvers in Quattro Pro were also used to verify the results obtained from the AMPL program.

RESULTS AND DISCUSSION

Texture of Whiting Surimi Gels

The effects of ingredient levels on the texture properties of whiting surimi gels are presented in Table 1. The regression coefficients (R^2) of the models for shear stress and shear strain were 0.92 and 0.85, respectively (Table 4). To show the results graphically, the response surface plots of shear stress and shear strain (Fig. 1 and 2) were derived from the regression models in Table 4. It was found that adding BPP, WPC72, and PS while maintaining constant moisture content (78%) increased the shear stress values, however a reverse effect was found with the addition of WPC33 (Fig. 1). As shown in Fig. 2, the addition of all the ingredients increased the shear strain values. The addition of WPC72 in quantities to 5% has been found to improve the texture properties of whiting surimi gels (Chung and Morrissey 1993). The results of this study showed, however, that as WPC72 concentrations exceeded 6%, shear strain values began to decrease. The regression models of shear stress and shear strain were clearly nonlinear (Table 4) with interactions between ingredients being statistically significant. As shown in Fig. 1, for example, the addition of WPC72 increased shear stress at low BPP levels but not at high BPP levels, indicating an antagonistic interaction between BPP and WPC72.

The ability of WPC and BPP to improve the texture properties in surimi gels has been related to its ability to inhibit the protease activity in surimi (Chang-Lee *et al.* 1990; Akazawa *et al.* 1993). In this study, WPC72 had more

influence on texture properties of PWSBS than did WPC33. The study of Piyachomkwan and Penner (1995) also suggests that the extent of inhibition by the WPC on the protease activity in whiting surimi is dependant upon the protein content of WPC. Thus, the protein content of WPC is shown not only to influence its cost (Table 2) but also its ability to improve the texture properties of whiting surimi gels.

TABLE 4.
REGRESSION COEFFICIENTS OF THE SECOND ORDER POLYNOMIALS FOR TEXTURE AND COLOR OF PWSBS

	L*	a*	b*	whiteness	stress	strain
Intercept	601.3994	92.2516	10.4949	18.4010	202.1753	-1.4390
BPP	------	------	2.1424	-9.7260	58.5442	0.6923
PS	-5.9840	------	-0.2027	-4.9118	33.3563	0.1264
WPC33	0.5669	-0.2235	0.0878	0.5107	1.2762	1.3320
WPC72	0.3995	-1.8800	0.4964	-1.1134	42.2810	1.4146
Moisture	-13.8035	-2.4921	- 0.1021	0.6831	-2.3675	0.0339
BPP^2	------	------	------	1.8087	------	-0.1175
PS^2	------	------	------	-0.0842	------	-0.0086
$WPC33^2$	------	0.0171	0.0849	-0.2911	-0.3481	-0.0223
$WPC72^2$	------	0.0152	------	------	-0.5245	-0.0301
$Moisture^2$	0.0911	0.0162	------	------	------	------
BPP x PS	------	------	------	------	------	------
BPP x WPC33	------	------	-0.1576	0.5018	------	-0.0538
BPP x WPC72	------	-------	------	------	-1.9289	-0.0941
BPP x Moisture	------	------	------	------	-0.6565	------
PS x WPC33	------	------	-0.0448	-0.1223	------	-0.0158
PS x WPC72	------	------	------	------	------	0.0137
PS x Moisture	0.0705	------	------	0.0719	-0.4186	------
WPC33 x WPC72	------	0.0441	------	------	-1.0516	-0.0298
WPC33 x Moisture	------	------	------	------	------	-0.0143
WPC72 x Moisture	------	0.0215	------	------	-0.4477	-0.0142
R^2	0.69	0.53	0.93	0.97	0.92	0.85
F test for lack of fit						
F statistic[1]			2.99	1.31	1.65	4.56
F critical value[1]			~2.99	~3.01	~3.01	~3.04
Test result			adequate	adequate	adequate	inadequate

------the coefficient is not significant ($p > 0.05$)
[1] with significance level, $\alpha = 0.01$

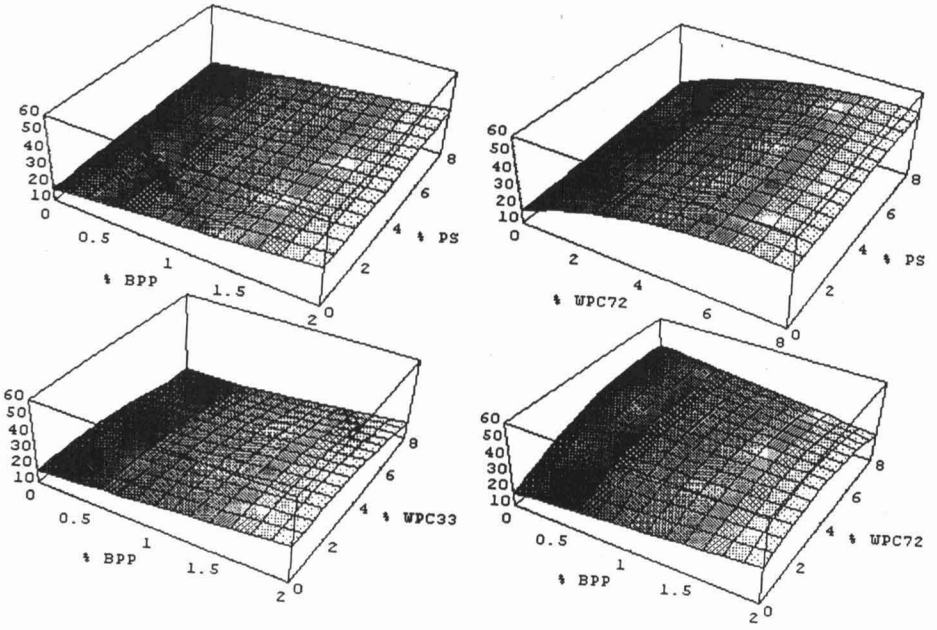

FIG. 1. THE RESPONSE SURFACES OF THE SHEAR STRESS (kPa) OF WHITING SURIMI GELS WITH 78% MOISTURE CONTENT

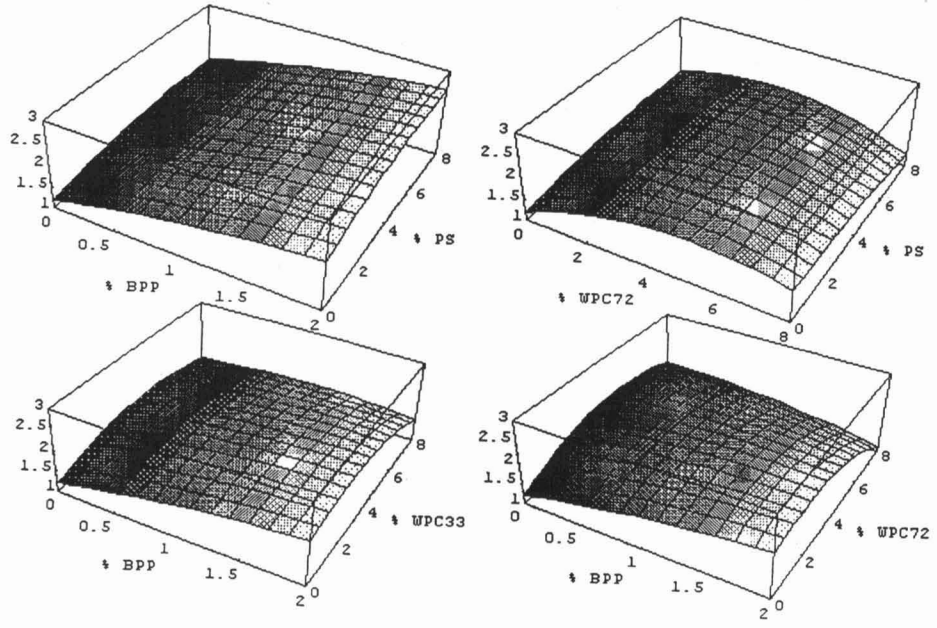

FIG. 2. THE RESPONSE SURFACES OF THE SHEAR STRAIN OF WHITING SURIMI GELS WITH 78% MOISTURE CONTENT

Color of Whiting Surimi Gels

The effects of ingredient levels on the color properties of whiting surimi gels are presented in Table 1. The regression coefficients (R^2) of the regression models for L*, a*, b* and whiteness (L* - 3b*) were 0.69, 0.53, 0.93 and 0.97, respectively as shown in Table 4. This indicates that b* (an indictor of yellowness or blueness) and whiteness are parameters capable of describing significant color changes of PWSBS, with the ingredients used in this study. Adding BPP, WPC72, and WPC33 was found to decrease the whiteness and increase the yellowness of surimi gels. However, the addition of PS decreased the yellowness and showed little effect on the whiteness of surimi gels. The low R^2 value for the regression models of a* (an indictor of redness or greenness), indicated that a* was little affected by the addition of ingredients used in this study. Park (1994, 1995) also reported the independence of a* values of surimi gels upon protein addition and changing processing variables.

Nonlinear Versus Linear Model

The results of the analysis of lack of fit and variance for b*, whiteness, shear stress, and shear strain are shown in Table 4 and 5, respectively. The F test for lack of fit (with significance level 0.01) indicated that the second order

TABLE 5.
THE ANALYSIS OF VARIANCE FOR TEXTURE AND COLOR OF PWSBS

	Source of Variation	df	Sum of Squares	Mean Squares	F	p
Yellowness (b*)	Regression	8	510.83	63.85	111.34	0.0001
	Error	70	40.14	0.57		
	Total	78	550.97			
Whiteness	Regression	11	3880.31	352.76	218.85	0.0001
	Error	67	107.99	1.61		
	Total	78	3988.30			
Shear Stress	Regression	12	22299	1858.3	60.0	0.0001
	Error	66	2043	31.0		
	Total	78	24342			
Shear Strain	Regression	16	11.837	0.740	22.67	0.0001
	Error	62	2.024	0.033		
	Total	78	13.861			

regression models of b*, whiteness, and shear stress adequately fit the experimental data. However, the F test indicated that the model of shear strain did not adequately fit its experimental data (Table 4). Various transformations (logarithmic, square, square root) on the data of shear strain were applied and showed no significant improvement. The lack of fit of strain data relative to that of stress data, appears to result from a variation among samples. Such variation would give a relatively greater error, and lack of fit, for the strain model whose value is relatively uniform.

Table 4 (and Fig. 1-2) indicates that the relationships between either texture or color of PWSBS and its ingredient levels are clearly nonlinear. To examine the predictive capability of both nonlinear and linear regression models of texture and color, 14 separate experiments using randomly selected variables were run, and results appear in Table 6. The nonlinear models of shear strain, whiteness, and b* provided quite reasonable estimates, but the nonlinear model for shear stress slightly underestimated the experimental results. As shown in Table 6, the mean errors between experimental data and estimated values from linear models of b*, shear stress, and shear strain were all significantly higher than that of nonlinear models. Thus, the predictive capability of linear models of texture and color for the new data set was less than that of nonlinear models.

The least cost model of PWSBS is shown in Table 7. Due to the nonlinearity of the functions of texture and color, nonlinear programming techniques must be used to search the solution of the least cost model of PWSBS. As shown in Table 8, the levels of WPC33 and WPC72 in the least cost formulation which included BPP were 4.08 and 2.98%, respectively, with the total concentration of WPC reaching 7.06%. When BPP was not used in the formulation, the amount of WPC33 and WPC72 became 2.72 and 3.82%, respectively. This indicated that WPC is economically competitive with PS and BPP under the quality constraints listed in Table 3. A comparison between the least cost formulations using nonlinear and linear models is listed in Table 8. To determine whether it is possible to produce PWSBS without using BPP, the least cost formulations with and without BPP were also reported in Table 8. It was found that the percentages of BPP and WPC33 in the formulation were quite different between nonlinear and linear models. It was also found that the least cost of PWSBS obtained from linear models was higher than that from nonlinear models and could not be treated as the true least cost in this case. The results of Table 8 further suggest that BPP may be excluded from the least cost formulation, with only a slight increase of the ingredient cost (0.5¢/lb of PWSBS), particularly when the use of BPP presents some difficulty with product labeling and sensory requirements (Akazawa *et al.* 1993).

However, the use of a linear model may require us erroneously to include BPP in the formulation to avoid a significant predicted increase in total ingredient cost. This indicates that the linear assumption needs to be checked out

TABLE 6.
VALIDATION OF REGRESSION MODELS FOR THE TEXTURE AND COLOR OF PWSBS

Independent Variables					Color						Texture					
					b*			Whiteness			Stress (kPa)			Strain		
BPP	PS	WPC33	WPC72	Moisture		Non-linear	Linear		Non-linear	Linear		Non-linear	Linear		Non-linear	Linear
(%)	(%)	(%)	(%)	(%)	Exp.[1]	Esti.[2]	Esti.[3]	Exp.[1]	Esti.[2]	Esti.[3]	Exp.[1]	Esti.[2]	Esti.[3]	Exp.[1]	Esti.[2]	Esti.[3]
0	0	4	2	74	5.4	5.6	6.4	63.5	64.1	60.7	47.9	34.3	33.3	2.15	2.18	1.58
0	0	7	3	75	9.4	9.1	8.7	54.4	55.6	56.4	20.0	15.8	20.9	1.65	1.98	1.42
0	1	1	4	76	4.4	4.7	5.0	65.7	66.4	64.8	53.9	45.1	37.5	2.16	2.14	1.69
0	4	1	0	80	0.7	1.7	2.3	74.7	74.8	71.7	14.9	13.2	21.4	1.85	1.74	1.93
0	5	6	2	74	7.9	7.8	7.0	54.8	55.6	57.2	45.0	37.6	35.8	1.79	1.97	1.72
0.5	2	4	2	82	5.1	5.5	6.0	67.9	66.8	65.4	10.0	6.7	3.8	2.03	1.91	1.77
0.5	2	4	8	78	9.2	8.9	9.1	54.1	56.8	56.2	8.4	6.1	27.0	1.26	0.98	1.59
1	5	3	3	75	6.3	6.7	6.9	58.4	57.3	57.1	54.0	50.6	44.7	2.30	2.29	2.02
1.5	3	2	3	78	6.8	6.9	7.0	58.7	59.8	59.3	41.2	34.2	32.9	2.25	2.29	2.08
2	0	3	1	76	7.5	7.6	8.3	57.1	58.9	56.1	44.1	41.0	33.0	2.06	2.29	2.07
2	1	6	6	75	10.2	11.9	12.4	52.4	49.0	46.1	14.0	12.7	34.8	1.20	0.87	1.84
2	2	3	4	74	8.3	9.2	9.5	52.7	54.0	51.3	68.8	52.5	48.0	2.08	2.15	2.07
2	3	3	3	82	9.0	7.8	8.0	57.7	61.9	59.2	9.2	6.2	14.2	1.80	1.89	2.14
2	7	1	1	76	6.0	6.3	5.9	58.3	57.1	58.1	49.0	54.1	51.0	2.38	2.51	2.46
						non-linear Esti.	linear Esti.		non-linear Esti.	linear Esti.		non-linear Esti.	linear Esti.		non-linear Esti.	linear Esti.
Mean error between estimate and experimental values						17.7%	26.2%		2.7%	3.4%		18.6%	50.9%		8.6%	14.8%

[1]experimental values
[2]estimated values from the nonlinear regression model (Table 4)
[3]estimated values from the linear regression model (not shown)

TABLE 7.
THE LEAST COST MODEL OF PWSBS

Note that 2% NaCl was added to each formulation

Objective Function

Cost: $c_1 X_1+c_2 X_2+c_3 X_3+c_4 X_4+c_5 X_5+c_6 X_6+2c_7$

Where

X_1:BPP (%) X_2: PS (%) X_3: WPC33 (%)
X_4: WPC72 (%) X_5: Water (%) X_6: Surimi (%)
c_1, c_2, c_3, c_4, c_5, c_6 are costs of each ingredient; c_7 = cost of salt

Constraint Functions

Note: l, m, n, p, q, r, s are low- or high-boundary parameters defined by the quality target

Weight Constraint: $X_1+X_2+X_3+X_4+X_5+X_6+2 = 100$

Surimi Constraint: $X_6 \geq l$

Protein Constraint: $0.687 X_1+0.33 X_3+0.723 X_4+0.157 X_6 \geq m$

Moisture Constraint: $0.076X_1+0.17X_2+0.064 X_3+0.052X_4+X_5+0.751X_6 \geq n_1$ and $\leq n_2$

Stress Constraint:

$$202.17532+58.36425 X_1+32.95384 X_2+1.12465 X_3+42.15790 X_4-2.36747 X_5$$
$$-1.77797 X_6-0.04989 X_1^2-0.07116 X_2^2-0.34813 X_3^2-0.54781 X_4^2-0.14341 X_1 X_2$$
$$-0.04201X_1 X_3-1.99703 X_1 X_4-0.65647 X_1 X_5-0.49301 X_1 X_6-0.02679 X_2 X_3$$
$$-0.09787 X_2 X_4-0.41861 X_2 X_5-0.31438 X_2 X_6-1.08021 X_3 X_4-0.44768 X_4 X_5$$
$$-0.33621 X_4X_6 \geq p_1 \text{ and } \leq p_2$$

Strain Constraint:

$$-1.43904+0.69489 X_1+0.13215 X_2+1.33419 X_3+1.41631 X_4+0.03385 X_5+0.02542 X_6$$
$$-0.11746 X_1^2-0.00861 X_2^2-0.02325 X_3^2-0.03087 X_4^2-0.05489 X_1 X_3-0.0952 X_1 X_4$$
$$-0.01824 X_2 X_3-0.01611 X_2 X_4-0.03148 X_3 X_4-0.01428 X_3 X_5-0.01072 X_3 X_6$$
$$-0.01422 X_4X_5-0.01068 X_4X_6 \geq q_1 \text{ and } \leq q_2$$

b* Constraint:

$$10.49493+2.13462 X_1-0.22006 X_2+0.08131 X_3+0.49107 X_4-0.10214 X_5-0.07671 X_6$$
$$+0.08494 X_3^2-0.15758 X_1 X_3+0.04475 X_2 X_3 \leq r$$

Whiteness Constraint:

$$18.4010-9.67407 X_1-4.79570 X_2+0.55437 X_3-1.07783 X_4+0.68307 X_5+0.51298 X_6$$
$$+1.80867 X_1^2-0.07201 X_2^2-0.29106 X_3^2+0.00547 X_1 X_2+0.50178 X_1 X_3-0.11770 X_2X_3$$
$$+0.00374 X_2 X_4+0.07193 X_2 X_5+0.05402 X_2 X_6 \geq s$$

TABLE 8.
THE LEAST COST FORMULATION OF PWSBS

Ingredient	Nonlinear Model		Linear Model	
	With BPP	Without BPP	With BPP	Without BPP
BPP:	0.32%	0.00%	0.75%	0.00%
PS:	5.67%	5.76%	5.67%	6.74%
WPC33:	4.08%	2.72%	2.85%	0.31%
WPC72:	2.98%	3.82%	3.13%	2.91%
Water:	44.95%	45.33%	45.59%	38.40%
Surimi:	40.00%	40.37%	40.00%	49.64%
NaCl	2.00%	2.00%	2.00%	2.00%
Total Cost per lb.	$0.520	$0.525	$0.527	$0.589

seriously before it can be applied to least cost food formulations, otherwise inaccuracies may result.

The application of the least cost formulation model allows us to obtain more insight regarding the relationships among ingredient costs, ingredient percentage, and the desired quality levels. Results are presented in a separate article (Hsu and Kolbe 1996).

CONCLUSION

The relationships between the quality properties of texture and color for Pacific whiting surimi-based seafood (PWSBS) and its ingredient levels are nonlinear. Nonlinear programming techniques thus provided a better method than linear programming to solve the least cost model. The use of WPC was found to be promising in terms of improving texture properties of PWSBS while remaining economically competitive. It was found that WPC could be a potential replacement of BPP based on the quality constraints and 1993 prices.

ACKNOWLEDGMENT

Major funding for this work was provided by the National Dairy Promotion and Research Board. Support was also provided by Oregon Sea Grant. The authors are grateful for the valuable assistance from Dr. J.W. Park, Dept. of Food Science & Technology, Oregon State University.

REFERENCES

AKAZAWA, H., MIYAUCHI, Y., SAKURADA, K., WASSON, D.H. and REPPOND, K.D. 1993. Evaluation of protease inhibitors in Pacific whiting surimi. J. Aquatic Food Prod. Technol. *2*, 79.

AOAC. 1984. Official Methods of Analysis of the Association of Official Analytical Chemists, 14th Ed., Washington, D.C.

BOX, G.E.P., HUNTER, W.G. and HUNTER, J.S. 1978. Statistics for Experimenters. John Wiley & Sons, New York.

CHANG-LEE, M.V., LAMPILA, L.E. and CRAWFORD, D.L. 1990. Yield and composition of surimi from Pacific whiting (Merluccius productus) and the effect of various protein additives on gel strength. J. Food Sci. *55*, 83.

CHEN, J.S., LEE, C.M. and CRAPO, C. 1993. Linear programming and response surface methodology to optimize surimi gel texture. J. Food Sci. *58*(3), 535.

CHUNG, Y.C. and MORRISSEY, M.T. 1993. Effect of whey protein concentrates on gel strength of Pacific whiting surimi. Presented at the 1993 Annual Meeting of the Institute of Food Technologists, Chicago, IL.

COCHRAN, W.G. and COX, G.M. 1957. *Experimental Designs*. John Wiley & Sons, New York.

DALEY, L.H., DENG, J.C. and CORNELL, J.A. 1978. Development of sausage-type product from minced mullet using response surface methodology. J. Food Sci. *43*, 1501.

DANTZIG, G.B. 1963. *Linear Programming and Extensions*. Princeton University Press, Princeton, NJ.

DAVIDON, W.C. 1959. Variable metric methods for minimization. A.E.C. Res. and Develop. Report ANL-5990, Argonne National Laboratory, Argonne, IL.

ERICKSON, M.C., GORDON, D.T. and ANGLEMIER, A.F. 1983. Proteolytic activity in the sarcoplasmic fluid of parasitized Pacific whiting (Merluccius productus) and unparasitized true cod (Gadus macrocephalus). J. Food Sci. *48*, 1315–1319.

FISHKEN, D. 1983. Consumer-oriented product optimization. Food Technol. *37*, 49.

HAMANN, D.D. 1983. Structural failure in solid foods. In *Physical Properties of Foods*. (M. Peleg and E. Bagley, eds.) pp. 351, Chapman & Hall, New York.

HAMANN, D.D. and MACDONALD, G.A. 1992. Rheology and texture properties of surimi and surimi-based foods. In *Surimi Technology*. (T.C. Lanier and C.M. Lee, eds.) pp. 427, Marcel Dekker, New York.

HASTING, R.J. and CURRALL, J.E.P. 1989. Effects of water, oil, egg white and starch on the texture of cod surimi gels by response surface

methodology. J. Texture Studies *19*, 431–451.
HSU, C.K. and KOLBE, E. 1996. Market potential of whey protein concentrate as a functional ingredient in surimi seafoods. J. Dairy Sci. *79*, 2146-2151.
IBM. 1966. Linear Programming-Meat Blending. IBM Data Processing Application. IBM Corp., White Plains, NY.
KRAMLICH, W.E., TAUBER, F.W. and PEARSON, A.M. 1973. Least cost formulation and preblending of sausage. In *Processed Meats*. First Ed. Chapter 8. Chapman & Hall, New York.
LANIER, T.C. 1988. Least-cost linear programming of surimi-based food products. Food Technol. Aug., p. 24. New Zealand.
LANIER, T.C. and PARK, J. 1989. Application of surimi quality measurements to least-cost linear programming of surimi product formulations. Report to the Alaska Fisheries Development Foundation, Inc., Anchorage, AK.
MORRISSEY, M.T., WU, J.W., LIN, D. and AN, H. 1993. Protease inhibitor effects on torsion measurements and autolysis of Pacific whiting surimi. J. Food Sci. *58*, 1050-1054.
MURTAGH, B.A. and SAUNDERS, M.A. 1978. Large-scale linearly constrained optimization, Math. Prog. *14*, 41–72.
MURTAGH, B.A. and SAUNDERS, M.A. 1982. A projected Lagrangiar algorithm and its implementation for sparse nonlinear constraints, Math. Prog. Study *16*, 84–117.
NFI 1991. A manual of standard methods for measuring and specifying the properties of surimi. Prepared by the Technical Subcommittee of the Surimi and Surimi Seafoods Committee; (T.C.Lanier, K. Hart and R.E. Martin, eds.) National Fisheries Institute, Washington, D.C.
PARK, J.W. 1992. Use of various grades of surimi with an application of least cost formulation. In *Pacific Whiting: Harvesting, Processing, Marketing, and Quality Assurance*. (G. Sylvia and M.T. Morrissey, eds.) pp. 17.
PARK, J.W. 1993. Oregon State University, Astoria OR. Personal communication.
PARK, J.W. 1994. Functional protein additives in surimi gels. J. Food Sci. *59* 525–527.
PARK, J.W. 1995. Surimi gel colors as affected by moisture content and physical condition. J. Food Sci. *60*, 15-18.
PIYACHOMKWAN, K. and PENNER, M.H. 1995. Inhibition of Pacific whiting surimi-associated protease by whey protein concentrate. J. Food Biochemistry *18*, 341–353.
ROBINSON, S.M. 1972. A quadratically convergent algorithm for general nonlinear programming problems. Math. Prog. *3*, 145.
WOLFE, P. 1967. Methods of nonlinear programming. In *Nonlinear Programming*. (J. Abadie, ed.).

A NONINVASIVE STUDY OF MILK CLEANING PROCESSES: CALCIUM PHOSPHATE REMOVAL

CHRISTINE S. GRANT[1], GREGORY E. WEBB and YOUNG W. JEON[2]

Department of Chemical Engineering
North Carolina State University
Raleigh, North Carolina 27695-7905

Accepted for Publication June 17, 1996

ABSTRACT

High temperature, high pH milk processing results in the formation of mineral rich deposits that are > 70% mineral and < 30% protein by weight. This research investigates the removal of P^{32} labeled mixtures of calcium phosphate dihydrate (brushite, $CaHPO_4 \cdot 2H_2O$) and hydroxyapatite ($Ca_5(PO_4)_3OH$) from stainless steel tubes using a solid scintillation technique. Experiments were performed at pH values ranging from 2.86-7.82 and flow rates from 3.8-11.4 L/min. Previous cleaning models are reviewed and a mass transfer model is proposed which, when compared to the experimental results suggests that film removal is due to both dissolution and mechanical effects due to shear stress. A modified first order model is presented which incorporates the effects of the solvent flow rate and pH on decontamination rates. This first order model is in agreement with the experimental results over the range of pH and flow rates investigated.

INTRODUCTION

Cleaning Processes

The fouling and cleaning of stainless steel surfaces is a large problem in food processing. These fouled surfaces lead to increased costs due to energy losses, maintenance, additional heat transfer surface area and process downtime (Perka *et al.* 1993). Sandu and Singh (1991) report that the cost of cleaning agents to remove milk deposits in pasteurization plants in the fluid milk industry is over 20 million dollars per year. In a recent study on the cleaning of heat exchangers and evaporators fouled with milk and whey, Jeurnink and Brinkman

[1] Correspondence concerning this paper should be addressed to Christine S. Grant
[2] Current Address: Department of Environmental Engineering, Kyungpook National University, Taegu, Korea

Journal of Food Process Engineering **20** (1997) 197–230. *All Rights Reserved.*

(1994) speculated that an optimal cleaning procedure could result in an annual savings of over 5 million Dutch guilders. These savings would result from a reduction in energy costs, cleaning agents and product losses. Pritichard *et al.* (1988) state that in the dairy industry, up to 42% of the available production time may consist of cleaning and sterilization processes. These potential economic and performance improvements are the driving force for the development of methods to both reduce and/or eliminate fouling and clean fouled surfaces more efficiently.

There are two general classes of contaminant residues; solids and liquids. These contaminants can be further classified as homogeneous or heterogeneous mixtures. In the food industry, surface cleaning is particularly challenging due to the heterogeneity of the fouling residues. This heterogeneity makes it difficult to design a standard protocol consisting of a single solvent or surfactant system to completely clean all surfaces. In the food industry, most cleaning and sanitation procedures consist of a series of steps (Plett 1985) which may include: pre-rinse, cleaning, inter-rinse, sanitizing, and post-rinse processes.

Cleaning in place (CIP) procedures minimize the requirements of time, labor, cleaning solvent, and energy associated with the dismantling of processing equipment (Wennerberg 1981). During CIP procedures while cleaning efficiency is maintained, it is difficult to verify the degree of internal surface cleanliness and the rate at which contaminants are removed from the surface. This limitation causes the chemical and food industries to use cleaning reagents and solvents inefficiently.

A quantitative description of cleaning techniques useful for food and chemical processing requires an understanding of the fundamental steps that govern the process. On a macroscopic scale, the following factors influence the degree of decontamination or cleaning achieved: (1) the physical and chemical properties of the substrate (e.g., morphology, hydrophobicity), (2) the chemical composition, microscopic crystal structure of the contaminant and its film thickness, (3) the temperature, composition and concentration of the decontamination reagents, (4) the contact time between solutions and contaminants, (5) the solubility of the residue in the solvents (6) the fluid microstructure and the degree of turbulence promoted during the decontamination operation and (7) interfacial phenomena. This research investigates how some of the aforementioned factors affect the removal of solid residues from metal surfaces.

In a typical cleaning experiment, an evaluation is made of the amount of contaminant either remaining on the surface or removed from the solid substrate. Approaches to the determination of contaminant remaining after cleaning include: the direct measurement of the amount left on the surface (e.g., gravimetric), an assessment of a physical property of the surface related to the amount of contaminant remaining (e.g., color, wettability, reflectance) or an evaluation of a characteristic contaminant component (e.g., chemical analysis,

the presence of spores) (Jennings 1963; Kulkarni *et al.* 1975; Corrieu 1981; Plett 1985; LeClercq-Perlat and Lalande 1994). The aforementioned techniques, however, are limited to periodic inspection of closed vessels or disassembled equipment.

A number of early research methods have been discontinuous or invasive in nature. Continuous evaluation of the cleaning process may be done by monitoring the contaminant in the effluent (e.g., chemical analysis, fluorescence, conductivity). The pressure drop in the system may also provide an indication of the amount of residue present. The major drawback of these monitoring techniques is that in spite of an indication that no further soil is being removed, there is no guarantee that complete cleanliness has been achieved (Plett 1985). The main obstacle in the study of cleaning processes is the accurate assessment of the transport phenomena at the substrate-residue interface. Given the level of complexity associated with heterogeneous residues, it is not surprising that cleaning processes have so far eluded detailed quantification and modeling.

Milk Residue Formation and Cleaning

Milk fouling can be described as a heterogeneous reaction that causes the aggregation of β-lactoglobulin, α-lactoglobulin, caseins, and fat globules to a solid surface. Calcium phosphate contributes to growth of the deposit by creating "carboxylate" bonds between protein aggregates and precipitated minerals. The most common mineral components are calcium phosphate dihydrate (brushite) ($CaHPO_4 \cdot 2H_2O$) and octocalcium phosphates ($Ca_8H_2(PO_4)_6 \cdot 5H_2O$) with hydroxyapatite ($Ca_5(PO_4)_3OH$), the least soluble form of calcium phosphate in milk, on the surface (Sandu and Lund 1985). These mineral deposits readily form on heat transfer surfaces because raw milk exhibits a high degree of supersaturation with respect to calcium phosphates. For operating temperatures close to 100C, the milk fouling deposits are composed of 50 to 60% protein, 30 to 35% minerals, and 15 to 20% fat (LaLande and Rene 1988). During high temperature processing (130-140C) the resulting high density deposit is composed of up to 75% minerals.

The mechanism of milk deposition on metal surfaces has been represented by several fouling models. There is still a great deal of debate as to whether the initial layer formed on stainless steel consists of protein or minerals (Belmar-Beiny and Fryer 1993). A defect-growth model considers the fouling of milk proteins and mineral salts to occur in three steps: development of a compact sublayer, granule formation, and deposit growth (Sandu 1989). The compact sublayer formed at metal surfaces is composed of calcium phosphate and protein. Active sites on the surface of the sublayer (called protuberances) provide anchors for the granules of large protein aggregates, causing the growth

of a porous, spongy deposit with low density and high moisture content. Fat globules and microorganisms are also entrapped in this matrix.

There are several cleaning processes commonly used for milk residues. For example, a two-stage process removes proteins and fats with an alkaline solvent (e.g., NaOH) and mineral deposits by an acidic solution (e.g., HNO_3 or H_3PO_4). In contrast, during single-stage cleaning the residues are removed by use of formulated detergents, which may contain surface active agents, chelating agents, or sequestering compounds (Timperley and Smeulders 1987; Jeurnink and Brinkman 1994). Several cleaning studies have focused on the removal of heterogeneous mixtures of fats and proteins as a function of alkali concentration (Grabhoff 1989; de Goederon and Pritchard 1989).

The removal of milk proteins from stainless steel surfaces has been studied extensively; below 100C, the protein represents the majority of the milk fouling deposit and is easy to detect. At high temperatures, the milk fouling deposit consists primarily of minerals. The presence of a mineral residue after cleaning can provide nucleation sites for subsequent fouling (Fryer 1989). Bird and Fryer (1991) state that in cleaning milk fouling residues the removal of mineral films is an area that needs further investigation. The first phase of our research focuses on the removal of calcium phosphate residues representative of those formed during high temperature processing of dairy based products. The rate of contaminant removal was studied in the region of fully developed turbulent flow; the region of industrial cleaning processes.

The effects of pH, surface finish, and flow rates on the cleaning rates are examined in an effort to develop a mechanistic model to describe the cleaning process. We have developed a noninvasive technique wherein the radioactivity of fouling deposits on the internal surface of a cylindrical flow cell is monitored continuously using solid scintillation. The experimental system consists of a flow cell coated with calcium phosphate. As the cleaning solvent flows through the cell a solid scintillation detector measures beta emissions from P^{32} radio-labeled calcium phosphate films. Dissolution and shear models are developed to describe the removal of calcium phosphate from a cylindrical hard surface into a flowing solvent. This research will provide information to the food process industry for the development of improved methods of estimating milk deposit removal, and a better understanding of the mechanisms that govern the removal of contaminants from hard surfaces.

BACKGROUND AND PREVIOUS WORK

In 1961, Bourne and Jennings reported that the majority of cleaning studies had been performed in the textile/fiber industry (Bourne and Jennings 1961). They were among the first in the food processing industry to investigate the

removal of food related residues from solid surfaces. Since that time, several studies have been published on the cleaning of pipes, again emanating from the food processing industry. Timperley (1981) showed that the cleaning achieved in a pipe could be related to the shear stress at the laminar boundary layer under turbulent flow conditions. He reported that the shear stress, and therefore the cleaning efficiency, in pipes of different diameters scales with linear velocity rather than Reynolds number. In another study, the soil removal rate and turbulent shear stress in pipes were simultaneously measured using a constant-temperature anemometer (Paulsson and Tragardh 1985).

In addition to the residue removal studies described above, several works have focused on the mechanisms by which residues are bound to solid surfaces. Bourne and Jennings (1961) studied and examined the relative influence of electrostatic and van der Waals forces on the adsorption behavior of proteins. They presented evidence that two kinds of bonding exist in soil systems. The first is a soil-soil cohesion bond, which is relatively weak compared to the second, soil-surface adhesion bond. In a related study, Nassauer and Kessler (1985) concluded that globular proteins with hydrophilic groups were bound to a surface primarily by electrostatic forces, whereas denatured whey proteins were primarily bound by van der Waals forces between the surface and hydrophobic groups.

There are several general and very pertinent reviews of cleaning in the food industry. Plett (1985) reviewed the cleaning of fouled surfaces in food processing equipment, focusing on equipment design, operating parameters, and surfactant solution characteristics. Another review, by Kulkarni *et al.* (1975), provides a comprehensive summary of cleaning in the food (especially dairy) industry. Corrieu (1981) discusses methods of evaluating cleanliness, cleaning mechanisms and kinetics, and the role of parameters such as: detergent nature and concentration, temperature, mechanical action, surface finish, type of soil. His conclusion was that a systematic, fundamental approach to understanding cleaning is still needed.

The main limitation to a number of the aforementioned studies is that the experiments are either discontinuous or invasive in nature. Gallot-LaVallee *et al.* (1982), used an optical detector to continuously and noninvasively measure the turbidity of the solvent after passing over a surface contaminated with milk. These authors, however, noted possible problems with the turbidity measurements taken downstream from the surface being cleaned. Noninvasive discontinuous techniques to evaluate the contaminant remaining on the surface include: gravimetric analysis, FTIR and the use of radioactive tracers. For example, Ottesen (1986) used infrared reflection spectroscopy to evaluate stainless steel tubing contaminated with thin films of hydrocarbon lubricants and metal oxides.

Several researchers have looked at the relative contributions of solubility (Linton and Sherwood 1950; Harriott and Hamilton 1965), dissolution (Murray 1987a,b) and shear-stress or mechanical effects (Beaudoin *et al.* 1995a,b; Jackson 1984; Timperley 1981) to the removal of contaminants from solid surfaces. Jackson (1984) found that significant cleaning required a minimum velocity; below the minimum velocity the fluid does not provide enough shear to remove a significant portion of the contaminant.

The Use of Radiotracers in Cleaning Studies

The use of radioactive tracers to study the cleaning of metal surfaces was first reported by Harris *et al.* (1950) as an alternative to the fluorescent dye, copper plate, and water spreading analytical tests. The sensitivity of the radioactive tracer technique was reported to be up to 100 times better than other methods in use at that time. In early studies, Jennings (1961) reported an extremely high correlation between the gravimetrically determined percent soil removed and the percent radioactivity removed from stainless steel. In one of the first models describing the removal of food products from solid surfaces, Jennings *et al.* (1957) studied the effects of time, temperature, and solvent type (e.g., pH) on the removal of P^{32}-labeled dried milk from solid surfaces. Peters and Calbert (1960) also reported that when P^{32} was incorporated into bacterial cells that were suspended in the test milk soil, there was a linear response between the weight of soil removed and the radioactive count removal.

Radiotracers have also been utilized to study the rate of deposition and removal of contaminants as a function of the nature of the surface (e.g., morphology) (Pflug *et al.* 1961; Peters and Calbert 1960; Perka *et al.* 1996). Masurovsky and Jordan (1960) investigated the removal of P^{32} labeled bacteria from stainless steel, aluminum, glass and Teflon during ultrasonic cleaning. They reported that the type of surface roughness influenced the degree of bacterial retention and the subsequent growth of the organisms.

More recently, radioactive species have been used to study the decontamination of nuclear facilities prior to decommissioning. In these studies, the contaminant species (e.g., metal oxides) is already radioactive. The main goal of these studies has been to investigate the chemical reactivity of the decontamination reagents with the contaminant films (Bradbury *et al.* 1983; Murray 1986). In contrast to earlier radioactive tracer studies, a solid scintillation technique will enable us to continuously evaluate the interface between the substrate and the contaminant during the decontamination process. This approach will eliminate disturbance of the contaminant-solvent interface when the substrate is removed from the cleaning solution prior to evaluation.

MATERIALS AND METHODS

A heterogeneous mixture of P^{32} labeled calcium phosphate in slurry form is used to coat a stainless steel experimental tube cell. The P^{32} labeled residues emit energy in the form of beta particles. The amount of P^{32} species present on the pipe surface can be detected using solid scintillation. The fraction of β-particles transmitted through the stainless steel is defined as

$$N(t')/N(0)=\exp(-\mu_m t') \quad (1)$$

where N(0) is the number of incident beta particles, N(t') is the number of beta particles transmitted through a thickness t', and μ_m is the mass absorption coefficient (Tsoulfanidis 1983).

The following sections describe the experimental cleaning apparatus, the method used to prepare the calcium phosphate coatings, the chemical properties of the slurries and the physical nature of the resulting residues. Presentation of the results of the decontamination experiments are followed by a discussion of the application of theoretical kinetic and mass transfer models to the experimental data.

Experimental Apparatus

The aqueous cleaning solvent was placed in a solvent feed tank and pumped through the 304 stainless steel piping by a Micropump Model 101-415 pump (see Fig. 1). The flow rate was monitored by an Omega flow meter. The spent solvent is collected in an effluent storage tank. The 304 stainless steel tube cell (see Fig. 2) consisted of a thin inner sheath (thickness = 0.1016 mm) and an outer protective tube (OD = 12.7 mm, length 60 mm) with a window opening for connection to the scintillator detector. The inner diameter of the system piping was the same as the ID of the tube cell. The test cell is placed far enough downstream of the inlet to insure fully developed turbulent flow. Two types of surface finishes were used in the tube cell; a #4 finish, which is a finely polished surface, and a #63 finish, which is visibly rough. The precision engineered stainless steel tube cell was designed to allow a high transmission rate of beta particles through the cell window. The rate at which beta particles leave the tube cell window is measured by a CaF_2 solid-scintillation detector (Fig. 2). Using the approximation from Eq. 1, 48% of the β-particles emitted from the inner surface of the window were able to pass through the stainless steel.

The light signal from the CaF_2 scintillation detector (Bicron) is sent to a photo-multiplier tube, amplified and converted to an electronic signal. The amplified signal is transmitted through a Tennelec TC145 preamplifier, a Tennelec TC241 amplifier, and an Oxford multi-channel scalar that converts the

raw signal to net counts. This signal is sent in digital form to an IBM 386 compatible personal computer which displays and stores the signals.

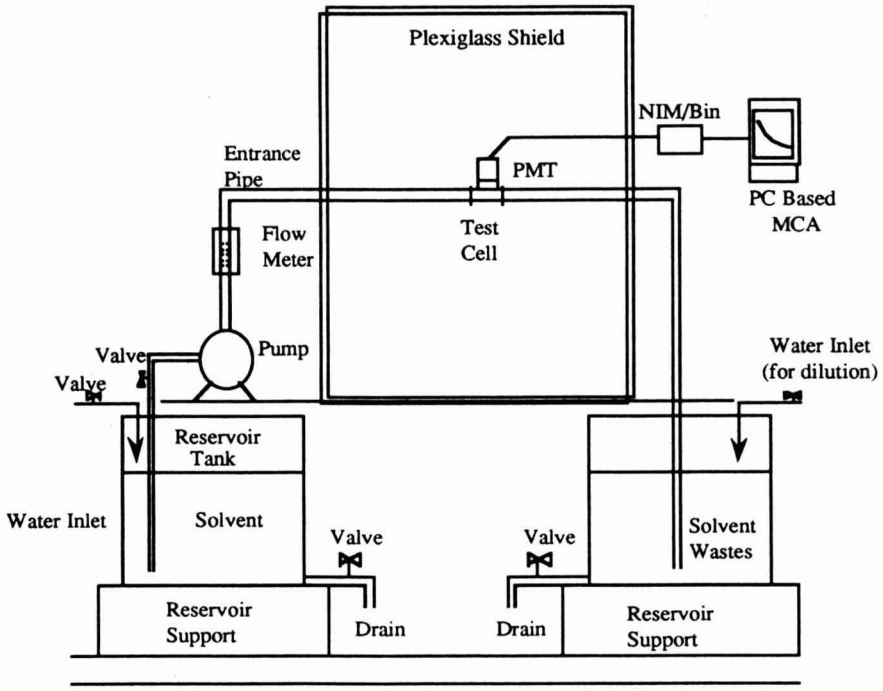

FIG. 1. SOLID SCINTILLATION EXPERIMENTAL FLOW SYSTEM

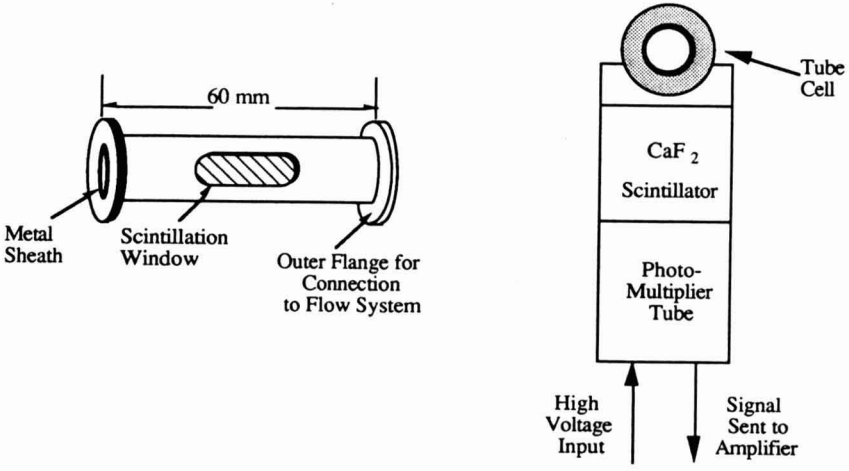

FIG. 2. EXPERIMENTAL TUBE CELL FOR SOLID SCINTILLATION EXPERIMENTS

Preparation of Calcium Phosphate Slurry and Cleaning Experiments

The calcium phosphate slurry is a mixture of the hydroxyapatite and the brushite compounds commonly found in milk fouling residues. The Ca/P ratios in this study were selected to represent calcium phosphate formulations found in high temperature fouling residues.

The coatings in the tube cell were formed by drying calcium phosphate slurries made from phosphoric acid and calcium hydroxide. One hundred μL of radio-labeled 2×10^{-7} M phosphoric acid (DuPont Chemical) and 100 μL of unlabeled 1 M phosphoric acid (Fisher Scientific) were mixed with 5.3 mL of a 1.057×10^{-2} M calcium hydroxide solution (Fisher Scientific). The phosphoric acid/calcium hydroxide mixture was allowed to equilibrate in a centrifuge tube for 24 h at 25C. The resulting solution was centrifuged (Fisher Scientific; Marathon 6K) for 50 min at 5000 rpm and the supernatant was drained. A 250-watt infrared lamp (Fisher Scientific; Infra-Rediator) was used to dry the calcium phosphate slurry at approximately 89C for 2 h. The slurry was reconstituted by adding 2 mL of distilled water to the centrifuge tube and stirring with a micro-stir bar for 15 min.

The coating in the test cell was created by injecting 1 mL of the reconstituted calcium phosphate slurry into a stainless steel tube cell capped at both ends. The slurry was dried by rotating the tube cell horizontally at 60 rpm under the 250 watt infrared heat lamp at 89C for 12 h. To test the uniformity of the film, a tube cell without a window was coated with radio-labeled calcium phosphate and allowed to dry. The counts emitted from the cell were measured at different angles using the solid scintillation technique. The rotational coating varied only 1.33% over the range of angles measured. The error associated with measuring the coatings is approximately 1.0%.

The average mass of calcium phosphate mixtures used to coat the tube cell was 3.14 ± 0.198 mg. The thickness, t_{film}, on the surface of the tube cell was estimated from the dimensions of the cell and the density of the calcium phosphate (2.306 g/cm^3):

$$M=\rho_o\pi(R^2-r_0^2)L \tag{2}$$

$$t_{film}=R-r_0=0.692\mu m \tag{3}$$

where M is the total dry mass of the film deposited in the tube cell, ρ_o is the density of calcium phosphate, R is the radius of the tube cell, and r_0 is the initial distance from the center of the tube cell to the solid surface of the film. This value for r_0 was used for model calculations.

The tube cell was tightly secured in the flow apparatus so that the window was flush against the solid scintillation detector (Fig. 2). Before the flow was started, the activity of the coating was measured for one minute. When the pump

was turned on, the activity was measured in 10 s intervals. In initial cleaning studies, fresh solvent (reverse osmosis water) was used; the length of the experimental run was limited by the size of the solvent reservoir (189 L) and the flow rate of the solvent (3.8-11.4 L/min). Changes in the pH values of the solutions were achieved by adding a solution of 12.1 normal hydrochloric acid, HCl (Fisher Scientific) to the water. Experiments were conducted at flow rates and pH values ranging from 3.8-11.4 L/min and 2.86 to 7.82, respectively. The majority of the experiments occurred on a #63 test cell. Duplicate runs were performed under all conditions except the flow rate of 3.8 L/min for the #4 cell at a pH of 3.24. All experiments were conducted at room temperature.

Solubility Determination

Studies were performed using P^{32} radio-labeled calcium phosphate to determine equilibrium solution concentrations. The solubility value can be used in the dissolution based model to define the concentration at the interface between the solid and the solution. Calcium phosphate slurries were prepared in an identical manner to that used in coating the experimental flow cell. All samples (i.e., for calibration and solubility studies) were equilibrated for three weeks at room temperature, followed by liquid scintillation measurements. The calibration solutions were prepared by completely dissolving a specific amount of calcium phosphate in a strongly acidic solution (pH=2.0). Different amounts of this calibration solution were then pipetted into a liquid scintillation cocktail (ICN; CytoScint™) and counted using a liquid scintillator (Packard 1500 Tri-Carb® Liquid Scintillation Analyzer).

Four solubility studies were performed over an eight month period over the range of solution pH values used in the cleaning studies. There was limited reproducibility in the four studies conducted (see Fig. 3). The solubility experiments reported here are presented as a function of the pH of the solvent before it was added to the calcium phosphate mixture. The experimental solubility was compared with literature solubility values for brushite (Driesseus and Verbeek 1990). The literature solubility values are at the pH of the solvent after equilibrium was reached. The differences in the solubility values of pure brushite in the literature are most likely a result of the calcium phosphate being a mixture of brushite and hydroxyapatite and the difference in the reporting of the solvent pH values. The solubilities were measured at the following pH values: Study A-> 2.65-3.88; Study B-> 2.0-4.0; Study C-> 2.72-3.36; Study D-> 2.72-3.36; Study E-> 2.81-3.24.

Determination of Calcium Phosphate Formulation

The Ca/P ratio in heterogeneous milk deposits has been reported to be approximately 1.5 (Lyster 1965; Jeurnink and Brinkman 1994). Brushite has a

Ca/P ratio of 1.0 and the Ca/P ratio of hydroxyapatite is 1.67. It has been reported in the literature that calcium phosphates created under acidic conditions generally form brushite ($CaHPO_4$)·2 H_2O and hydroxyapatite $Ca_{10}(PO_4)_6(OH)_2$ (Driesseus 1990). Hence, a solution with an initial $Ca(OH)_2/H_3PO_4$ ratio equal to 0.5 leads to a brushite-rich precipitate. A solution with an initial $Ca(OH)_2/H_3PO_4$ ratio of 2.0 results in a hydroxyapatite-rich precipitate.

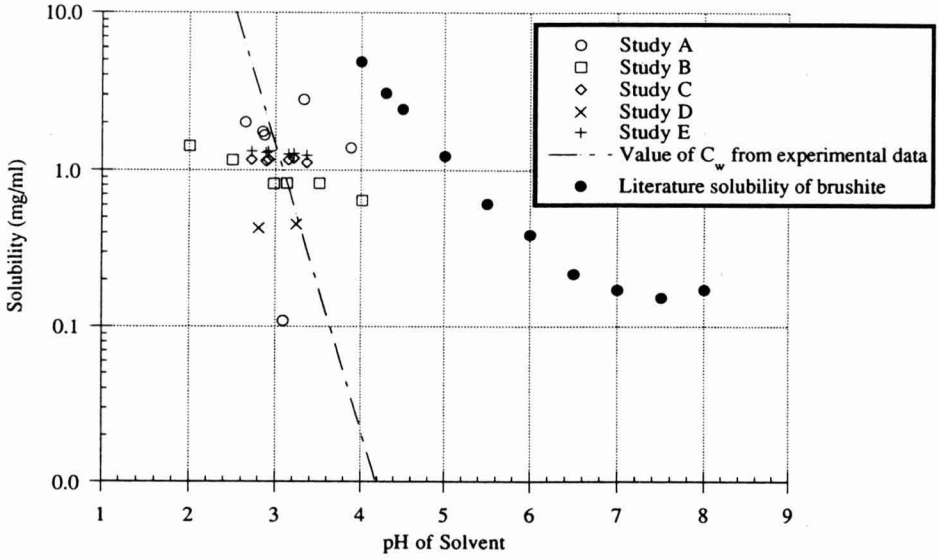

FIG. 3. CHANGES IN CALCIUM PHOSPHATE SOLUBILITY WITH pH (COMPARED WITH LITERATURE SOLUBILITY FOR BRUSHITE) (DRIESSEUS AND VERBEEK 1990)
Calcium phosphate solubility determined using liquid scintillation techniques.
Literature solubility of brushite presented at equilibrium pH values.

To determine the type of calcium phosphate mixture used in the decontamination experiments, the Ca/P ratios of unlabeled slurries were measured. The precipitates were analyzed for calcium and phosphorus contents using atomic absorption (AA) and UV-visible spectrometry, respectively. Initial solution molar ratios of $Ca(OH)_2/H_3PO_4$ of 0.5, 1.0, and 2.0, resulted in Ca/P ratios of the precipitates of 1.00, 1.12, and 1.51, respectively. The Ca/P ratio in all slurries used in the decontamination experiments was approximately 1.1.

The solution in equilibrium with the precipitated calcium phosphate was also analyzed to ascertain the calcium phosphate formulation. Inductively coupled plasma atomic emission (ICPAE) spectrometry analysis (Perkin Elmer; Plasma 2000) was performed on dilutions of supernatant in equilibrium with calcium phosphates with DI water. In this test, calcium phosphate was made by mixing

100 μL of unlabeled 1 M phosphoric acid with 5.3 mL of 1.057×10^{-2} M calcium hydroxide solution. One hundred microliters of DI water were added to compensate for the 100 μL of labeled phosphoric acid. This combination of calcium hydroxide and phosphoric acid yields an initial $Ca(OH)_2/H_3PO_4$ ratio of 0.56. The supernatant had a phosphorus concentration of 7.17×10^{-3} M and a calcium concentration of 7.62×10^{-3} M. The measured pH of the supernatant solution was 5.45. A study by Patel *et al.* (1974) found the calcium concentration of brushite in equilibrium with a solution having a pH of 5.41 to be 3.74×10^{-3} M; their value is slightly lower than those found in this study.

RESULTS AND DISCUSSION

Cleaning Experiments

The effect of the following parameters on the removal rate of calcium phosphate were studied: solvent type, flow rate, solvent pH, drying temperature of tube cell and surface finish. In the cleaning experiments, the net counts detected by the solid scintillator were assumed to correspond to the amount of calcium phosphate film on the cell window. Water is a low density material and absorbs the energy of beta particles; hence there will be a reduction in the signal when water is present in the cell. An experiment was performed to measure the signal dampening associated with a solvent blocking beta particle emissions. A flow cell was coated with 6.28 mg of P^{32} labeled calcium phosphate. The flow cell was then mounted vertically against the solid scintillator, and the signal was measured from the dry cell and after the cell was slowly filled with 4 mL of DI water. Approximately 60% of the signal was blocked by the DI water. This is on top of the 48% detectable signal mentioned earlier due to the density of the stainless steel.

Because of the water dampening effects, the data collected during decontamination experiments have been normalized to the signal strength after 30 s of solvent flow. Hence, the beginning of the run (i.e., time equal to zero on the plots) is actually 30 s into the collection of experimental data. This normalized (or time modified) signal indicates the amount of P^{32} remaining, which is proportional to the fraction of calcium phosphate remaining on the stainless steel. The half-life of P^{32} is 14 days; hence, the decontamination data are presented as fraction remaining versus time to eliminate the variation in the initial counts between experiments.

Reverse osmosis water was used in the cleaning experiments; the large differences in the tap water quality caused variations in the cleaning results. The reproducibility of the decontamination experiments is presented for runs using RO water as the solvent. Figure 4 shows the results of decontamination

experiments performed at flow rates of 3.8 L/min and 11.4 L/min. This data indicates that the use of the rotational coating technique and RO water as a solvent produced consistent, reproducible cleaning results.

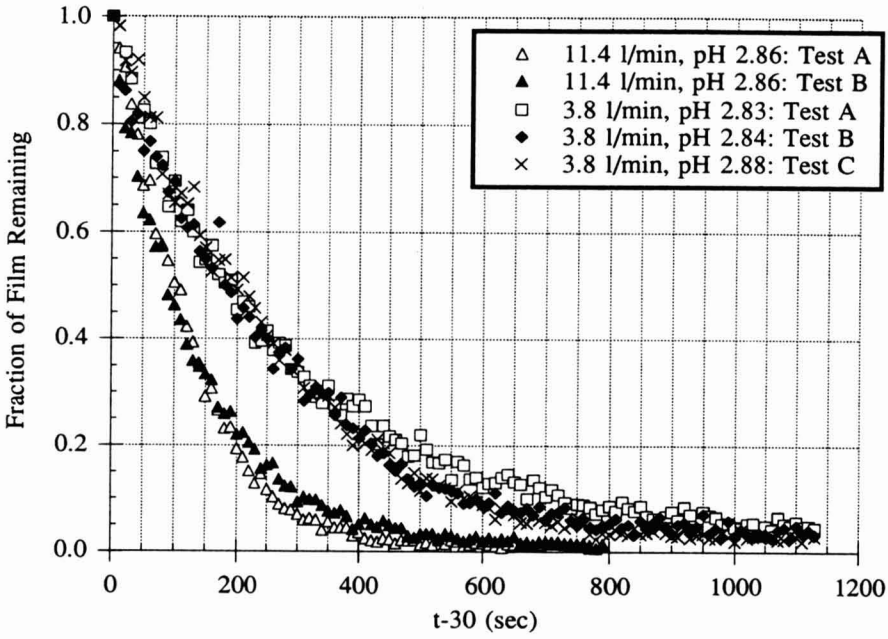

FIG. 4. REPRODUCIBILITY OF RO WATER EXPERIMENTS PREPARED USING A ROTATIONAL COATING, SOLVENT FLOW RATES OF 3.8 L/MIN AND 11.4 L/MIN (#4 TUBE CELL)

Initial decontamination rates were determined by performing a linear regression over the first 100 s of a particular decontamination experiment. The effect of pH and flow rate on decontamination rates is illustrated in Fig. 5; as the solvent flow rate is increased from 3.8 L/min to 11.4 L/min there is a 65% increase, in the initial cleaning rate. The increase in removal of calcium phosphate with decreasing pH can be attributed to the dependence of calcium phosphate solubility on pH. At the highest pH value (7.82) there is no significant removal in the first 100 s. It should be noted that the scatter at the high pH is due to the scatter in the raw data at low count rates. The benefits of a low pH on cleaning rates is also observed at lower flow rates. This is consistent with observations made by Jeurnink and Brinkman (1994) and others on the use of an acidic solution to remove mineral films produced in milk fouling.

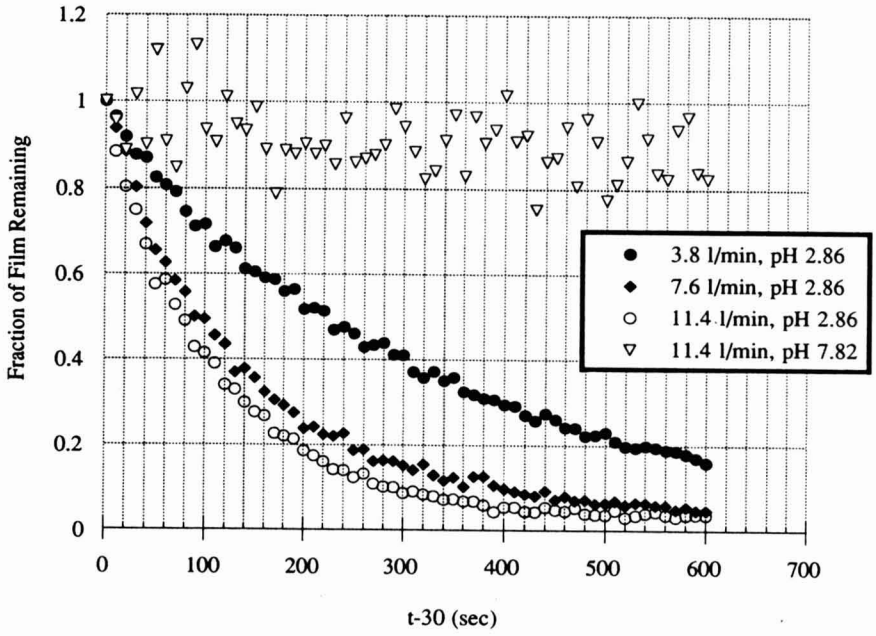

FIG. 5. EFFECT OF FLOW RATE AND pH ON DECONTAMINATION
Note: scatter in high pH data due to low activity and corresponding low count rate of sample.

A limited number of tests were done to evaluate the role of surface finish (#63 and #4 finishes) on the rate and extent of surface cleaning. Under the experimental conditions of our tests in the removal of solid calcium phosphate residues, Fig. 6 suggests that the surface finish had little effect on both the initial and final decontamination rates.

Scanning Electron Microscopy (SEM) Studies

The morphology of the calcium phosphate films was determined indirectly from scanning electron micrographs (SEMs). In this study, 1 cm square stainless steel coupons made of the same 304 stainless steel as the experimental tube cells were coated with calcium phosphate slurries and dried under the infrared heat lamp to evaporate the water, producing a solid residue. After drying, the coated samples were suspended in solutions of varying pH; the pH was adjusted by mixing HCl acid in distilled water at 25C. To simulate the cleaning process a constant flow of solvent was provided by a magnetic stirbar. After cleaning, the test coupons were removed and allowed to dry overnight at room temperature. Scanning electron micrographs of the dried samples are shown in Fig. 7.

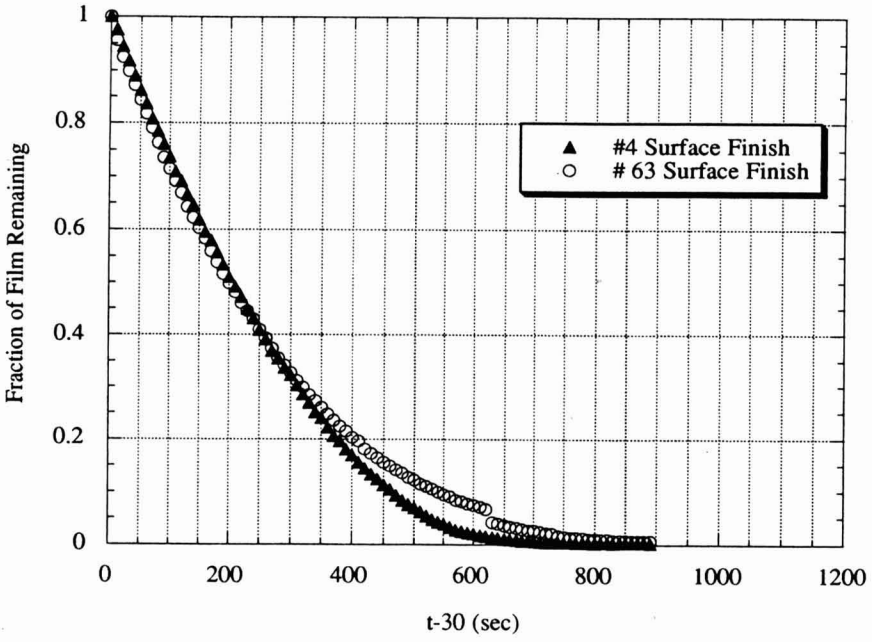

FIG. 6. EFFECT OF SURFACE FINISH ON RO WATER EXPERIMENTS PERFORMED AT A SOLVENT FLOW RATE OF 7.6 L/MIN AND AN AVERAGE SOLVENT pH OF 2.86

The pH values of the solutions were selected based on the pH values of solvents used in decontamination experiments. After 30 s of cleaning at a pH of 2.89, Fig. 7a indicates that there are several particles of calcium phosphate present and the stainless steel is visible. Figure 7b represents twenty minutes of cleaning in a solution with a pH of 2.89. Under these conditions, the majority of the calcium phosphate has been removed from the stainless steel surface.

The removal of the residue is due to the dissolution of the calcium phosphate on the surface and the breaking of the bonds between the residue and the stainless steel. The projected surface area of the crystals was found to range from 2.5×10^4 to $1.0 \times 10^5 \mu m^2$ with an average area of $6.5 \times 10^4 \mu m^2$. The morphology of the calcium phosphate residue is similar to that reported by Timperley and Smeulders (1987) for mineral residues.

MECHANISMS OF DEPOSIT REMOVAL AND DECONTAMINATION MODELS

The theoretical models used to describe cleaning in the chemical, nuclear and food industries range from purely empirical relationships to models based

(a)

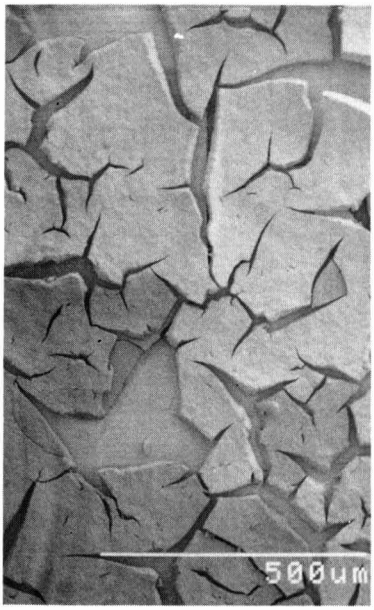

(b)

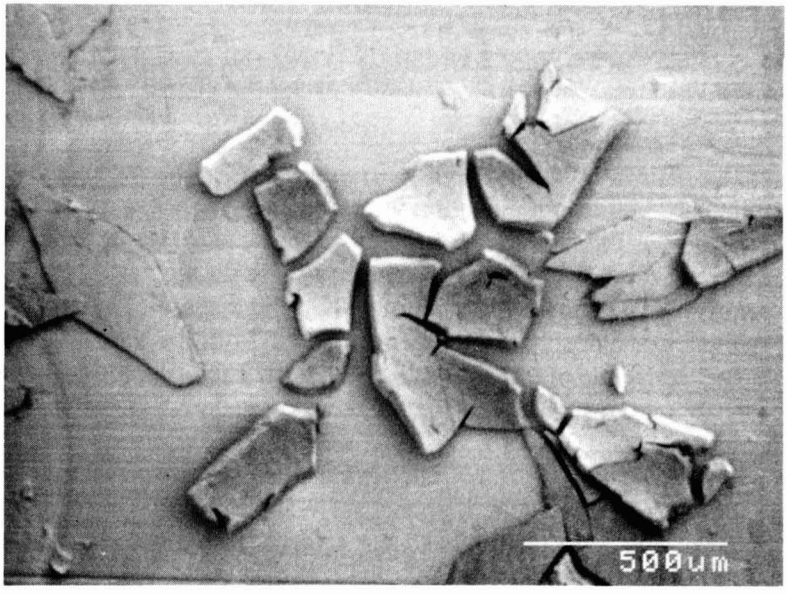

FIG. 7. SCANNING ELECTRON MICROGRAPHS: (a) CALCIUM PHOSPHATE COATING AFTER 30 S OF CLEANING AT A pH OF 2.89 (30/300 X) MAGNIFICATION, (b) CALCIUM PHOSPHATE COATING AFTER 20 MIN OF CLEANING AT A pH OF 2.89 (30X MAGNIFICATION)

on mass transfer principles. There are three basic approaches used to model contaminant removal: (1) an empirical model which attempts to fit the data based on solvent or solute concentrations (2) a dissolution based mass transfer model that accounts for the contaminant solubility, and the transport of material away from the surface and (3) models which evaluate the removal of large aggregates of contaminant as a function of shear stress. Table 1 contains a brief summary of some models along with the contaminants to which the models have been applied. Jennings (1957) was one of the first to develop models to describe the removal of food products from solid surfaces. Jennings used a first order (in

TABLE 1.
EXAMPLES OF DECONTAMINATION MODELS USED IN FOOD, CHEMICAL AND NUCLEAR INDUSTRIES

Contaminant Type	Reaction Order	Model	Author(s)
Dried Milk	*1st Order* Limited by Reaction	$\frac{dC_x}{dt} = -k C_x C_{OH,B}$	Jennings (1957)
Dirt and Scale Formed in Condensers	Dependent upon kinetic energy of fluid and deposit thickness	$\frac{dM}{dt} = -k \tau x_{thick}$	Kern and Seaton (1959)
Milk Residues	*Two stage cleaning model* 1st stage: zero order 2nd stage: removal of intermediates	$\frac{dM}{dt} = b_5[1 - \exp(b_6 t)]$ for $t < M_0 / b_5$ $\frac{dM}{dt} = b_5[\exp(b_6(M_0 / b_5)) - 1]\exp(-b_5 t)$ for $t > M_0 / b_5$	Gallot-LaVallee *et al.* (1982)
Metal Oxides	*Zero Order* Limited by dissolution *1st Order* Limited by dissolution	Dense film no pores $\frac{dM}{dt} = -k_1$ Porous film $\frac{dM}{dt} = -kM$	Murray (1987)

contaminant concentration) empirical model for the rate of removal of milk residues as a function of the concentration of hydroxyl ions ($C_{OH,B}$) and the concentration of the contaminant to be removed (C_x):

$$\frac{dC_x}{dt} = -kC_xC_{OH,B} \tag{4}$$

where k is an empirical rate constant. When compared to experimental data, Jennings found that the model is only valid up to the removal of 60% of the initial contaminant. In their study, the lack of continuous measurements of the mass of contaminant made it difficult to make an accurate assessment of cleaning kinetics.

The cleaning process is often represented as occurring in four distinct stages (Harper 1972): (1) transport of the solvent to the surface of the contaminant to be removed, (2) wetting and penetration of the contaminant by the solvent, (3) transport of the contaminant away from the solid-liquid interface, and (4) prevention of contaminant redeposition onto the clean, solid surface. Although, each of the aforementioned stages can be described using transport phenomena, researchers find it difficult to accurately model each stage using fundamental transport phenomena.

Schlussler (1970) attempted to simplify the mechanisms of Harper with the objective of developing a transport based model to describe cleaning behavior:

$$\frac{dN}{dt} = -\frac{D_{soil}A}{z_w}(C_w - C_b) \tag{5}$$

where dN/dt is number of moles dissolved per unit time, C_w is the concentration of contaminant in equilibrium with solvent, C_b is the concentration of soil in bulk solution, A is the surface area of soil, D_{soil} is the diffusivity of the contaminant in the solvent, and z_w is the thickness of the equivalent boundary layer. Schlussler's model assumed the following: (1) the first and third stages were controlled by diffusional mechanisms across an equivalent hydrodynamic boundary layer created by the fluid stream, (2) the dissolved contaminant diffuses more slowly than the solvent itself and (3) stage three, the transport of contaminant away from the solid-liquid interface was the rate-limiting step for the overall removal of contaminant.

Gallot-LaVallee *et al.* (1982), were among the first to develop a continuous, noninvasive technique for measuring the removal of contaminant films. They applied their optical technique to measure the decontamination of fouled tubes and proposed a two-stage cleaning model (see Table 1). The first stage, a zero-order step, represents the formation of an intermediate component, similar to an active site complex in a heterogeneous catalytic reaction. The second stage represents the removal of intermediate components through the equivalent concentration boundary layer.

Kern and Seaton studied the fouling and cleaning of heat transfer equipment in the nuclear industry (Kern 1959; Murray 1987). Kern and Seaton's model is

based on the assumptions that: (1) contaminant removal is due to the shearing action of fluid passing the surface; (2) the contaminant film is removed as chunks of material at random planes of weakness; and (3) these planes of weakness are likely to occur at any depth in the residue. The rate of deposit removal is described in terms of the thickness of the deposit, x_{thick} (see Table 1). In this relationship k is an arbitrary rate constant, τ is the shear stress at the interface, and M is the mass of the deposit. Rewriting the shear stress in terms of the velocity, the rate of deposit removal is:

$$\frac{dM}{dt} \propto v^{1.75}. \tag{6}$$

Studies performed by Jackson (1984) on the removal of tomato paste from heat exchanger plates found that significant cleaning required a minimum velocity; below the minimum velocity the fluid does not provide enough shear to remove a significant amount of the particular contaminant.

Models of Calcium Phosphate Decontamination

The data from the calcium phosphate decontamination studies in this work will be evaluated using two different approaches. The first approach starts with a model for the dissolution of a solid cylindrical surface into a flowing solvent. This approach is often used to describe the removal of individual molecules of a species into a fluid. The second technique is based on the kinetic modeling work of Jennings; the resulting modified first order model is an empirical fit of the data as a function of pH and velocity.

Dissolution Model of Contaminant Removal. A standard mass transfer model can be used to describe the dissolution of a solid from the inside of a cylindrical surface. The following assumptions are made in the development of the model: (1) a smooth contaminant surface, (2) fully developed flow, and (3) a concentration at the solid-liquid interface equal to the solubility of the contaminant in the solvent. The molar flux, J, of a contaminant species into a bulk solvent can be described as:

$$J = -k_m(C_b - C_w) \tag{7}$$

where C_b is the bulk concentration of the contaminant (e.g., calcium phosphate), C_w is the concentration of contaminant at the solid-liquid interface (assumed to be the solubility), and k_m is the mass transfer coefficient. A mass balance performed on a differential volume element of solid within the pipe results in the local rate of change of the mass within the differential control volume (see Fig. 8):

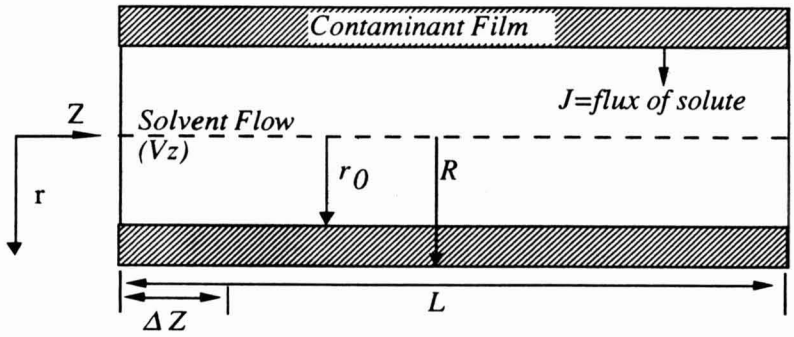

FIG. 8. CYLINDRICAL CONTROL VOLUME USED FOR DISSOLUTION MODEL

$$\frac{\partial M'(z)}{\partial t} = -J(z)A\bar{M} \tag{8}$$

where A is the surface area of the control volume, and $\bar{M}$ is the average molecular weight of the material in the film. Using the parameters indicated on the control volume in Fig. 8, Eq. (8) can be written as:

$$\frac{\partial}{\partial t}\left[\rho_o \Delta z \pi (R^2 - R_i^2)\right] = -J(z)\bar{M}2\pi R_i \Delta z \tag{9}$$

where ρ_o is the density of the calcium phosphate film, R is the radius of the cylinder, and R_i is the radius of the film at a given axial position and time. Incorporating the definition of the molar flux into Eq. (9) results in the following expression for the rate of change in the radius of the film:

$$\frac{\partial R_i}{\partial t} = \frac{-k_m(C_b - C_w)\bar{M}}{\rho_o} \tag{10}$$

The radius of the film at a dimensionless distance Z:

$$Z = \frac{z}{L} \tag{11}$$

from the inlet to the tube can be expressed as a dimensionless parameter:

$$\phi = \frac{R_i}{r_o} \tag{12}$$

where r_o is the initial radius of the solid and L is the length of the tube cell. Equation 10 can be expressed as:

$$\frac{\partial \phi}{\partial \eta} = \frac{-k_m \bar{M} L}{\rho_o \langle v_z \rangle r_o} \theta(Z,\eta) \tag{13}$$

where Θ is the concentration gradient:

$$\theta = (C_b - C_w) \tag{14}$$

and the dimensionless time is expressed as:

$$\eta = \frac{t \langle v_z \rangle}{L} \tag{15}$$

The concentration, Θ, can be expressed as a differential equation from a mass balance on the contaminant in the liquid phase:

$$\frac{\partial \theta}{\partial \eta} + \frac{\partial \theta}{\partial Z} = -\frac{2k_m}{r_o} \frac{L}{\langle v_z \rangle} \theta \tag{16}$$

The boundary conditions and the initial condition for Eq. 16 are:

$$\begin{aligned} \theta &= -C_w \qquad @Z=0 \\ \theta &= -C_w \qquad @\eta=0 \end{aligned} \tag{17}$$

Equation 16 can be expressed in terms of dimensionless correlation's as:

$$\frac{\partial \theta}{\partial \eta} + \frac{\partial \theta}{\partial Z} = -2 \left[\frac{Sh}{ReSc} \right] \frac{L}{r_o} \theta \tag{18}$$

where

$$Sh = 0.0172(Re)^{0.86}(Sc)^{0.33} \text{ and } Sc = \frac{\mu}{\rho D_{AB}} \tag{19}$$

Solving Eq. 18 using Laplace Transforms

$$\begin{aligned} \theta &= -C_w e^{-\beta Z} \text{ for } Z < \eta \\ \theta &= -C_w e^{-\beta \eta} \text{ for } Z > \eta \end{aligned} \tag{20}$$

where

$$\beta = 2 \left[\frac{Sh}{ReSc} \right] \frac{L}{r_0}. \tag{21}$$

At long times ($\eta > 1$) the average dimensionless radius of the solid phase over the length of the film is

$$\bar{\phi} = 1 + \frac{\bar{M} C_w}{2\rho_0} \left[1 - e^{-\beta} \right] \eta \text{ for } Z < \eta \tag{22}$$

The total mass of the film can be expressed as:

$$M(\eta)=\rho_0\pi L r_0^2\left[\left(\frac{R}{r_0}\right)^2-\bar{\phi}^2\right] \tag{23}$$

(Grant *et al.* 1996). The normalized film residual is defined as the mass of film remaining divided by the mass of initial film and can be written as (Webb 1994):

$$\frac{M(\eta)}{M(0)}=\frac{\left[\left(\frac{R}{r_0}\right)^2-(1+\kappa\eta)^2\right]}{\left[\left(\frac{R}{r_0}\right)^2-1\right]} \tag{24}$$

where:

$$\kappa=\frac{\bar{M}C_w}{2\rho_0}[1-e^{-\beta}] \tag{25}$$

and β is defined as a function of key dimensionless transport variables. Incorporating the definitions for Re, Sc an expression for the effect of bulk velocity on the rate of removal can be defined as

$$\frac{\partial M(t)}{\partial t}=-\pi L r_0 \bar{M} C_w \frac{[2^b a R^{b-1} v_z^b \rho^{b-1} Sc^{c-1}]}{\mu^{b-1}}. \tag{26}$$

The rate of removal of calcium phosphate is a function of the velocity of the bulk fluid raised to the *b* power. The dissolution model developed indicates that if dissolution is the sole mechanism of removal, the rate of removal should be approximately proportional to the velocity to the 0.86 power.

Development of a Modified First-Order Decontamination Model. The velocity dependence in the first model is used to describe molecular diffusion of CaP molecules from the surface to the bulk solution. The dissolution model does not account for the role of shear in removing large contaminant aggregates. The SEMs, however, indicate that during the cleaning process, the calcium phosphate is dislodged from the metal surface as large aggregates. Several researchers have reported that both mechanical and dissolution mechanisms are involved in the removal of contaminant films (Jennings 1965; Linton and Sherwood 1950; Harriott and Hamilton 1965). Even though it is clear that both mechanical and

dissolution mechanisms are important, most cleaning studies focus on a single mechanism.

The rate of cleaning of various fouled surfaces has been reported by several authors to have a first order behavior (Jennings 1957; Kern 1959; Gallot-LaVallee 1982; Murray 1987a,b). The proposed rate equation usually has the following form:

$$\frac{dM}{dt} = -kM, \tag{27}$$

where k is a first-order rate constant. The initial mass on the surface is defined as:

$$M = M_0 \qquad @t=0. \tag{28}$$

Incorporating the initial conditions into the rate equation, results in the following expression for the fraction of the film remaining:

$$\frac{M(t)}{M_0} = \exp(-kt). \tag{29}$$

In the modified first order model, a numerical fit of the decontamination data has been made which incorporates the velocity and pH effects. The first order rate constant, k, is expanded to account for the pH of the solvent and the flow rate. Since the experimental data has been normalized to the mass of the film at 30 s (instead of the mass of film at t=0), the least square fit was performed using a function of the following form based on the exponential behavior of the data:

$$\frac{M(t)}{M(30s)} = \exp[\alpha v_z^n (t-30)], \tag{30}$$

where α and n are fitted parameters (based on the experimental data), v_z is the velocity of the fluid, and t is the time in seconds. The statistical analysis of the data was conducted using an EXCEL spreadsheet program. The same program was used for the curve-fitting presented later in this paper. The parameter α was determined separately for each unique solvent pH so that a dependence of α on hydronium concentration could eventually be determined. The parameters α and n were calculated by minimizing the sum of the squares of the relative error over the first 600 s of a cleaning experiment. The parameter n was determined by fitting both α and n to 27 experiments performed at pH values of 2.81, 2.86, and 2.93. A weighted average was found for n (0.70); this value was used to independently determine the values of α. After computing values for α, the parameter was fit to an equation of the following form:

$$\alpha = a' \exp(b'[H^+] + c') \tag{31}$$

In this equation a′, b′, and c′ are constants determined by minimizing the sum of the square of the weighted-relative error (SSWRE); the weights were determined by the number of experiments representing each of the calculated α values from the SSWRE equation. The weights were determined by the number of experiments representing each of the calculated α values; the result of this fit was:

$$\alpha = 0.008092 \exp(-371.272[H^+] - 1.01692) \tag{32}$$

The final expression for the fraction of the calcium phosphate material remaining at time, t is:

$$\frac{M(t)}{M(30s)} = \exp\left[\alpha v_z^{0.70}(t-30)\right]. \tag{33}$$

Comparison of Theoretical Models to Experimental Data. The mass transfer model describes the molecular dissolution of calcium phosphate in a well defined flow field. In the dissolution based model, an important parameter in predicting the theoretical removal rate is the calcium phosphate solubility. In spite of the variation in the experimental solubility data, an attempt was made to assess how well the model predicted changes in experimental conditions. The scatter seen in experimental solubility studies required us to obtain a value for C_w derived from the dissolution model. C_w was obtained by finding the average slope of the fraction remaining versus time data generated in the decontamination experiments and calculating a C_w value that provided a similar slope. For example, at a pH of 2.85 the value of C_w was calculated to be 1.77 mg/mL. The dissolution model (Eq. 24) is compared to the decontamination rates for RO experiments having a solvent pH's of 2.85 and 3.24 and a flow rates ranging from 3.8 to 11.4 L/min (see Fig. 9). It can been seen that the region of applicability of the model is limited; the model slightly under predicts initial cleaning rates and over predicts cleaning rates over long periods of time. This deviation may be due to the rapid removal of calcium phosphate aggregates in the initial state of cleaning and the adhesion of residual deposits to the stainless steel at long times. These deviations could also be related to uncertainties in the coating thickness and variations in the quality of the water. Although there are variations, the model does show, the general trends in initial decontamination rates as a function of solvent flow rate and pH.

Many researchers have described cleaning processes in terms of the removal of large aggregates. Visual observation of the calcium phosphate films indicates that the surface of the film is nonuniform. Furthermore, the results reported here strongly suggest that the removal of the calcium phosphate is due to both residue dissolution and shearing of large chunks of the residues.

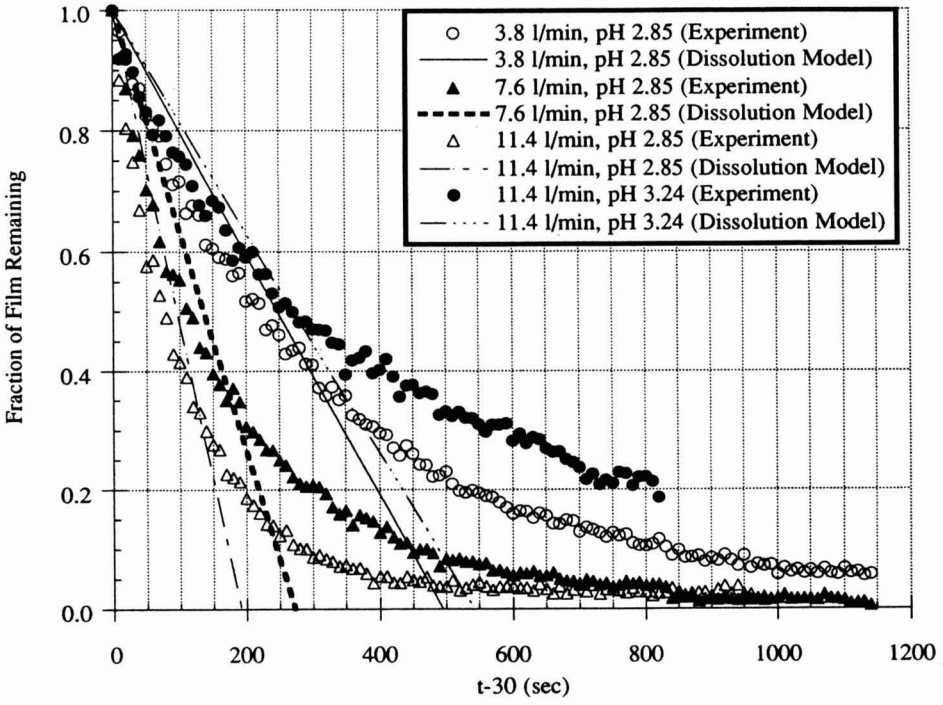

FIG. 9. COMPARISON OF DISSOLUTION MODEL (EQ. 24) TO DECONTAMINATION DATA FOR EXPERIMENTS PERFORMED AT A RANGE OF SOLVENT FLOW RATES (3.8-11.4 L/MIN) AND SOLVENT pHS (2.85-3.24)

Plots have been constructed to compare the modified first order model to the experimental data. The overall average error was determined by weighting the average errors according to the number of experiments performed at the different conditions. This error was found to be 6.70 for a pH range of 2.35 - 7.82 and a flow rate range of 3.8 to 11.4. Figure 10 compares the model empirical approximation (Eq. 33) with experimental runs at three solvent pH values and two flow rates. Although there are some deviations, the first order model predicts the removal of calcium phosphate relatively well; it captures the trends found with changing solvent flow rate and pH. Some of the deviations in the fit may be attributed to scatter in the original experimental data.

The application of a dissolution model versus the modified first-order model to a cleaning process can be discussed in terms of the velocity function. Kern and Seaton's model describing the removal of aggregates indicated that pure mechanical or shear based cleaning would result in a cleaning rate proportional to the amount of kinetic energy the solvent possessed (Kern 1959). They showed

that cleaning from purely hydrodynamic effects (i.e., shear stress) would yield a cleaning rate with a velocity term to a power close to 2.0. In the modified first order model a cleaning rate proportional to the velocity to the 0.70 power suggests that the calcium phosphate/water system does not depend solely upon mechanical cleaning mechanisms. It appears that the dissolution model predicts the velocity trend more closely than that of a mechanical based cleaning model. However, the implementation of the model depends upon the accuracy of solubility measurements.

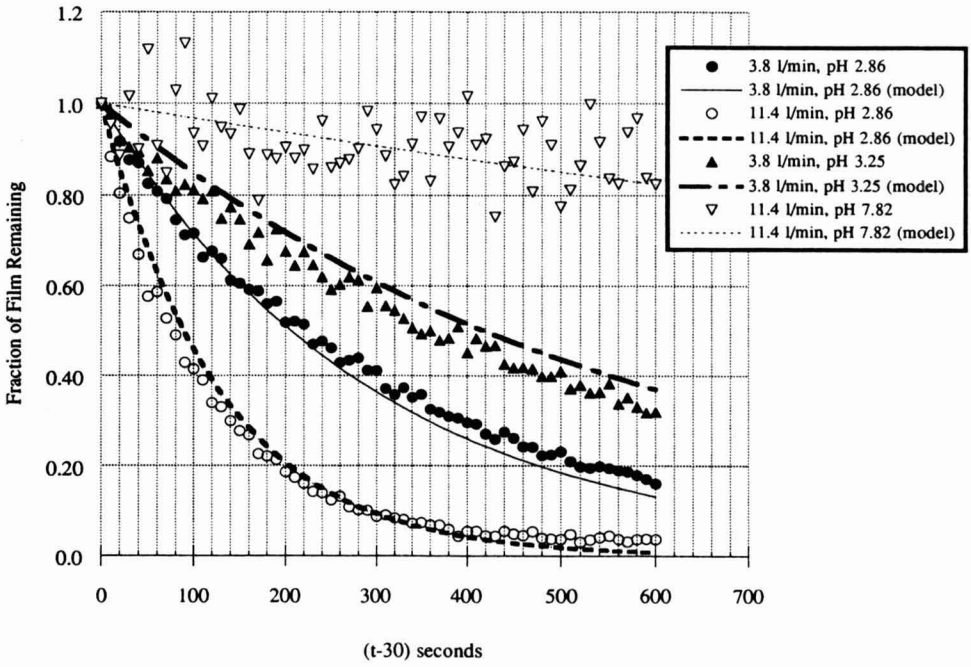

FIG. 10. COMPARISON OF MODIFIED FIRST ORDER MODEL (EQ. 33) TO EXPERIMENTS PERFORMED AT A RANGE OF pH AND FLOW RATES

Application of Calcium Phosphate Cleaning Studies to Protein Removal. The majority of industrial milk fouling is heterogeneous in nature. The next step in this research is a study of heterogeneous contaminants. Measuring real-time decontamination kinetics of these compounds may be done if a single component were radio-labeled and mixed with other unlabeled compounds. The observed cleaning mechanism for the removal of calcium phosphate is very different from studies on protein removal. In studies on the removal of milk deposits from

stainless steel Jeurnink and Brinkman (1994) observed that the deposit is a spongy protein matrix with associated minerals and fat globules. In their study, the removal of the deposit with alkaline solutions proceeded by a two step mechanism. Initial contact with the alkaline solution caused the residue to swell and form cracks. Subsequent removal of the spongy, primarily protein layer was due to the shear stresses imparted by the cleaning solutions. The subsequent removal of the residual mineral layer was achieved using an acidic solution. The development of a model for protein removal similar to the modified first order model for calcium phosphate would require cleaning data as a function of velocity and alkali concentration. The application of this model could, however, be limited by the formation of a protein gel layer at high alkali concentrations (Jeurnink and Brinkman 1994).

The calcium deposit matrix often encountered during HTST processing is heterogeneous; it contains proteins and other milk components. The mineral residue that remains after removal of the other major components (e.g., protein via alkaline solutions) is often described as a hard, sandy deposit. The residues found in an actual processing facility are also created at a higher temperature; this may change the nature of the bonds formed between the residues and the stainless steel substrate. However, the Ca/P ratio of these deposits is approximated by our experimental conditions.

Because of the bonds that form during the development of the fouling residues from a bulk solution - the calcium phosphate films we developed will have a different chemical structure than an actual deposit. The removal of the spongy heterogeneous protein film by an alkali solution is often described in terms of both dissolution and spalling mechanisms. Spalling is the removal of large aggregates of material based on the breaking of bonds in the protein/mineral/fat residues. While the mechanism that we describe has these elements; it appears to be due primarily to the dissolution process.

There may be a difference in the mechanism and kinetics associated with the decontamination due to small differences in the solubility and the physical structure of the deposits. Although we do not have any direct experimental evidence, we are continuing to conduct experimental studies on the removal of mixed films (e.g., calcium phosphate and protein) from stainless steel surfaces using the solid scintillation technique.

CONCLUSIONS

SEM photographs of partially cleaned test coupons show that large aggregates of calcium phosphate are detached from the surface of test coupons during the cleaning process. This indicates that the calcium phosphate films are not removed solely by dissolution, but by a process that removed individual

particles of calcium phosphate from the surface. It is believed that these particles are lifted from the hard surface by shear forces imparted by the fluid. This behavior is consistent with studies by Jeurnink and Brinkman (1994) on the spalling of milk deposits during the cleaning process.

In this project, our initial assumption was that the calcium phosphate would be removed solely through the process of dissolution. The flow of solvent past the solid residues was thought only to facilitate the removal of calcium phosphate by maintaining a concentration driving force for the dissolution process. The experimental data showed a large increase in decontamination rate with a decrease in solvent pH. The dissolution model based on the mass transfer of calcium phosphate predicted that if dissolution was the only film removal mechanism, the rate of removal would actually increase slightly over time because of the increase in surface area in contact with the solvent as layers of contaminant were removed. The decontamination data, however, showed that the rate of film removal did not increase over time, but instead showed a marked decrease.

The dissolution model also predicts the cleaning rate would be proportional to velocity raised to a power less than one. According to Kern and Seaton, if mechanical cleaning were the primary mechanism, the cleaning rate would be proportional to the kinetic energy of the fluid or the velocity to a power slightly less than two. Experiments have indicated that the cleaning rate is proportional to the velocity to the 0.70 power, suggesting that dissolution plays a significant role in the removal of calcium phosphate.

The dissolution based model, although theoretically sound, was difficult to test due to the absence of reliable solubility data. If, however, the solubility could be accurately determined, this model would still over predict the latter stages of calcium phosphate removal. The modified first order model developed in this work provided a more complete overview of the role of velocity and pH on the decontamination process.

An understanding of the mass transfer and hydrodynamic mechanisms governing the cleaning of contaminated surfaces is important in the development of efficient cleaning operations. This research has provided information on the mechanism of calcium phosphate removal by examining decontamination rates under various experimental conditions. It has also introduced a useful solid scintillation technique for noninvasively and continuously obtaining a measurement of the amount of material remaining on a solid surface. The accuracy of the decontamination experiments depends on the activity, uniformity and the initial mass and physical nature of the coating.

Many challenges still exist in the modeling of decontamination rates including the incorporation of surface morphology, effects of solvent additives (e.g., pH), the role of heterogeneous contaminants, and the geometry of the fouled surface into the models. The work presented here represents a first step

to investigate the use of dissolution, shear stress and empirical based models to describe the removal of heterogeneous solid contaminants from stainless steel.

ACKNOWLEDGMENTS

This research was supported by a grant from the Center for Aseptic Processing and Packaging Studies an NSF-University-Industrial Center located at North Carolina State University, and the National Science Foundation, Grant No. EID-9115327. We also thank R. Carbonell for helpful technical advice, R. Caton and M. Britt for experimental assistance.

NOMENCLATURE

Dimensions are given in terms of mass (M), length (L), time (t), and moles.

A	surface area of film, L^2.
a', b', c'	fitted dimensionless parameters (Eq. 31).
a, b, c	exponents in Eq. 26.
b_5	rate constant, M/t (see Table 1).
b_6	rate constant, l/t (see Table 1).
C_b	bulk concentration of contaminant, moles/L^3.
$C_{OH,B}$	hydroxyl ion concentration in solvent, moles/L^3 (Eq. 4).
C_w	concentration of calcium phosphate at liquid - solid interface, moles/L^3.
C_x	concentration of contaminant to be removed, moles/L^3 (Eq. 4).
D_{soil}	diffusivity of film, L^2/t (Eq. 5).
g	gravitational acceleration, L/t^2.
J	molar flux @ liquid - solid interface, moles/tL^2.
k_m	effective mass transfer coefficient, L/t.
k	empirical rate constant, t^{-1}, (see Table 1); L^3/t moles (Eq. 4).
k_1	empirical rate constant, M/t (see Table 1).
L	length of mass transfer region, L.
M	mass of film, M.
M'	local mass, M.
M_0	initial mass of film, M.
$\bar{M}$	average molecular weight of film, M/moles.
N	moles of film, moles.
n	fitted dimensionless parameter (Eq. 30).
$N(0)$	number of incident beta particles (Eq. 1).
$N(t')$	number of particles transmitted through thickness t' (Eq. 1).
r_0	initial radius of liquid solid interface, L (Eq. 2).

R radius of pipe, L.

Re Reynolds number = $\frac{\rho v D}{\mu}$.

R_i radius of film, L.

Sc Schmidt number = $\frac{\mu}{\rho D_{AB}}$

Sh Sherwood number = $\frac{kD}{D_{AB}}$

t time, t.

t′ thickness of stainless steel window, L (Eq. 1).

t_{film} thickness of film, L.

v velocity of bulk solvent, L/t (Eq. 6).

$<v_z>$ average fluid velocity, L/t^2.

z axial distance, L.

Z dimensionless distance, $\frac{z}{L}$

z_w thickness of film, L (Eq. 5).

x_{thick} thickness of deposit, L

Greek Symbols

α fitted parameter defined by Eq. 30, 31

β dimensionless variable, $\beta = 2\left[\frac{Sh}{ReSc}\right]\frac{L}{r_0}$ (Eq. 21)

η dimensionless time, $\eta = t < v_z > /L$ (Eq. 15).

κ dimensionless variable, $\kappa = \frac{\bar{M}C_w}{2r_0}(1 - e^{-\beta})$ (Eq. 25).

ϕ dimensionless radius, $\frac{R_i}{r_0}$ (Eq. 12)

$\bar{\phi}$ average dimensionless radius

μ_m mass absorption coefficient, L^2/M (Eq. 1).

μ viscosity, M/L t.

ρ density of solvent, M/L^3.

ρo density of film, M/L^3 (Eq. 2).

Θ $C_b - C_w$, concentration gradient, moles/L^3.

τ shear stress, M/t^2L (see Table 1).

REFERENCES

BEAUDOIN, S.P., GRANT, C.S. and CARBONELL, R.G. 1995a. Removal of organic films from solid surfaces using aqueous solutions of nonionic surfactants I: Experiments. Ind. Eng. Chem. Res. *34*, 3307-3317.

BEAUDOIN, S.P., GRANT, C.S. and CARBONELL, R.G. 1995b. Removal of organic films from solid surfaces using aqueous solutions of nonionic surfactants II: Theory. Ind. Eng. Chem. Res. *34*, 3318–3325.

BELMAR-BEINY, M.T. and FRYER, P.J. 1995. Preliminary stages of fouling from whey protein solutions. J. Dairy Res. *60*, 167–183.

BIRD, M.R. and FRYER, P.J. 1991. An experimental study of the cleaning of surfaces fouled by whey proteins. Trans I ChemE *69*, 13–21.

BOURNE, M.C. and JENNINGS, W.G. 1961. Some physico-chemical relationships in cleaning hard surfaces. Food Tech. *15*, 495–499.

BRADBURY, D., SELLERS, R.M., SWAN, T., LARGE, N.R. and MONAHAN, J. 1983. Experience of plant decontamination with LOMI reagents. In *Water Chemistry of Reactor Systems 3 - Vol. 1: Proceedings of British Nuclear Energy Society Conferences*.

CORRIEU, G. 1981. State-of-the-art of cleaning surfaces. In *Fundamentals and Applications of Surface Phenomena Associated with Fouling and Cleaning in Food Processing*. (B. Hallstrom, D.B. Lund and C. Tragardh, eds.) pp. 90-114, University of Lund, Sweden.

dE GOEDEREN, G. and PRITCHARD, N.J. 1989. Improved cleaning processes for the food industry. In *Fouling and Cleaning in Food Processing*. (H.G. Kessler, K. Welchner and D.B. Lund, eds.) pp. 115–130, Bavaria, Germany.

DRIESSEUS, F.C.M. and VERBEEK, R.M.H. 1990. Biominerals. pp. 37–58, CRC Press, New York.

FRYER, P.J. 1989. The use of fouling models in the design of food process plant. J. Soc. Dairy Technol. *42* (1), 23–29.

GALLOT-LAVALLEE, T., LALANDE, M. and CORRIEU, G. 1982. An optical method to study the kinetics of cleaning milk deposits by sodium hydroxide. J. Food Eng. *5*, 131–143.

GRABHOFF, A. 1989. Environmental aspects of the use of alkaline cleaning solutions. In *Fouling and Cleaning in Food Processing*. (H.G. Kessler, K. Welchner and D.B. Lund, eds.) pp. 107–114, Bavaria, Germany.

GRANT, C.S., PERKA, A., THOMAS, W.D. and CATON, R. 1996. Cleaning of solid behenic acid residue from stainless steel surfaces. AIChE J. *42* (5), 1465–1477.

GRANT, C.S., WEBB, G.E. and JEON, Y. 1996. Calcium phosphate decontamination of stainless steel surfaces. AIChE J. *42* (1), 861–876.

HARPER, W.J. 1972. *Sanitation in Dairy Food Plants*, Chapman & Hall, New York.

HARRIOTT, P. and HAMILTON, R.M. 1965. Solid-liquid mass transfer in turbulent pipe flow. Chem. Engin. *Sci. 20*, 1073–1078.

HARRIS, J.C., KAMP, R.E. and YANKO, W.H. 1950. Detection of soil removal in metal cleaning by the radioactive tracer technique. J. Electrochem. Soc. *97*, 430–432.

JACKSON, A.T. 1984. Cleaning characteristics of a plate heat exchanger fouled with tomato paste using 2% caustic soda solution In *First U.K. National Conference on Heat Transfer*, pp. 465–472, University of Leeds, Pergamon Press.

JENNINGS, W.J. 1961. A critical evaluation of in vitro radioactive phosphorus additions for estimating soil deposits. J. Daily Sci. *44*, 258-268.

JENNINGS, W.G. 1963. An interpretive review of detergency for the food technologist. Food Tech. *17* (7), 53–61.

JENNINGS, W.G. 1965. Theory and practice of hard surface cleaning. Adv. Food Res. *14*, 325–458.

JENNINGS, W.G., MCKILLOP, A.A. and LUICK, J.R. 1957. Circulation cleaning. J. Dairy Sci. *40*, 1471–1479.

JEURNINK, T.J.M. and BRINKMAN, D.W. 1994. The cleaning of heat exchangers and evaporators after processing milk or whey. Int. Dairy J. *4*, 347–368.

KERN, D.Q. and SEATON, R.E. 1959. A theoretical analysis of thermal surface fouling. Brit. Chem. Eng. *12*, 258–262.

KULKARNI, S.M., MAXCY, R.B. and ARNOLD, R.G. 1975. Evaluation of soil deposition and removal processes: An interpretive review. J. Dairy Sci. *58*, 1922–1936.

LALANDE, M. and RENE, F. 1988. Fouling by milk and dairy product and cleaning of heat exchange surfaces. In *Fouling Science and Technology* (L.F. Melo *et al.*, eds.) pp. 557–578, Kluwer Academic Publishers, Amsterdam.

LECLERCQ-PERLAT, M.N. and LALANDE, M. 1994. Cleanability in relation to surface chemical composition and surface finishing of some materials commonly used food industries. J. Food Eng. *23*, 501–517.

LENGES, J. 1982. Study of Diffusion Coefficients and of the Kinetics of Micellization of a Colorant, Sc.D. Thesis, University of Brussels.

LINTON, W.H. and SHERWOOD, T.K. 1950. Mass transfer from solid shapes to water in streamline and turbulent flow. Chem. Eng. Prog. *46*, 258–264.

LYSTER, R.L.J. 1965. The composition of milk deposits in an ultra-high-temperature plant. J. Dairy Res. *32*, 203–208.

MASUROVSKY, E.B. and JORDAN, W.K. 1960. Studies on the removal of staphylococcus aureus from milk-contact surfaces by ultrasonic cleaning methods. J. Dairy Sci. *43*, 1545–1559.

MURRAY, A.P. 1986. A chemical decontamination process for decontaminating and decommissioning nuclear reactors. Nuclear Technol. *74*, 324–332.

MURRAY, A.P. 1987a. Mathematical modeling of the chemical decontamination of boiling water reactor components. Nuclear Technol. *79*, 359–370.

MURRAY, A.P. 1987b. Modeling nuclear decontamination processes. Nuclear Technol. *79*, 194–209.

NASSAUER, J. and KESSLER, H.G. 1981. Determination of residues in tubes and fittings after rinsing in dependence of several parameters. In *Fundamentals and Applications of Surface Phenomena Associated with Fouling and Cleaning in Food Processing*. (B. Hallstrom, D.B. Lund and C. Tragardh, eds.) pp. 348–355, University of Lund, Sweden.

OTTESEN, D.K. 1986. Detection of contaminants in steel tubing using infrared reflection spectroscopy. SPIE: Optical Techniques for Industrial Inspection. *665*, 226–233.

PATEL, P.R., GREGORY, T.M. and BROWN, W.E. 1974. Solubility of $CaHPO_4 \cdot 2H_2O$ in the quaternary system of $Ca(OH)_2$-H_3PO_4-NaCl-H_2O at 25C. J. Res. National Bureau of Standards, *78*A(6), 675–681.

PAULSSON, B. and TRAGARDH, C. 1985. A method for the measurement of hydrodynamic effects during cleaning of a solid surface. In *Fouling and Cleaning in Food Processing* (D.B. Lund, C. Sandu and E.A. Plett, eds.) pp. 358–373, University of Wisconsin, Madison, WI.

PERKA, A.T., GRANT, C.S. and OVERCASH, M.R. 1993. Waste minimization in batch vessel cleaning. Chem. Eng. Commun. *119*, 167–177.

PETERS, J.J. and CALBERT, H.E. 1960. Use of P^{32} in the study of the cleanability of milk handling surfaces. J. Dairy Sci. *43*, 857.

PFLUG, I.J., HEDRICK, T.I., KAUFMANN, O.W., KEPPELER, R.A. and PHEIL, C.G. 1961. Studies on the deposition and removal of radioactive soil. J. Milk and Food Tech. *24*, 390–396.

PLETT, E.A. 1984. Rinsing kinetics of fluid food equipment. Eng. and Food *2*, 659–668.

PLETT, E.A. 1985a. Cleaning of fouled surfaces. In *Fouling and Cleaning in Food Processing* (D.B. Lund, C. Sandu and E.A. Plett, eds.) pp. 288–311, University of Wisconsin, Madison, WI.

PLETT, E.A. 1985b. Relevant mass transfer mechanisms during rinsing. In *Fouling and Cleaning in Food Processing*. (D.B. Lund, E.A. Plett and C. Sandu, eds.) pp. 395–409, University of Wisconsin, Madison, WI.

PRITCHARD, N.J., dE GOEDEREN, G. and HASTING, A.P.M. 1988. The removal of milk deposits from heated surfaces by improved cleaning processes. In *Fouling in Process Plant*. (A.M. Pritchard, ed.) pp. 465–475, Inst. of Corrosion Sci. and Technol., London.

SANDU, C. 1989. Chemical reaction fouling due milk: defects-growth model. In *Fouling and Cleaning in Food Processing*. (H.G. Kessler, K. Welchnel and D.B. Lund, eds.) pp. 46–58, Bavaria, Germany.

SANDU, C. and LUND, D. 1985. Fouling of heating surfaces - chemical reaction fouling due to milk. In *Fouling and Cleaning in Food Processing*. (D.B. Lund, E.A. Plett and C. Sandu, eds.) pp. 122–168, University of Wisconsin, Madison, WI.

SANDU, C. and SINGH, R.K. 1991. Energy increase in operation and cleaning due to heat Exchanger fouling in milk pasteurization. Food Technol. *45*, 84–91.

SCHLUSSLER, H.J. 1970. Cleaning of hard surfaces in the food industry. Milchwissenschaft, *25*(3), 133–149.

TIMPERLEY, D.A. 1981. The effects of Reynolds number and mean velocity of flow on the cleaning in-place of pipeline. In *Fundamentals and Applications of Surface Phenomena Associated with Fouling and Cleaning in Food Processing*. (B. Hallstrom, D.B. Lund and C. Tragardh, eds.) pp. 402–412, University of Lund, Sweden.

TIMPERLEY, D.A. and SMEULDERS, C.N.M. 1987. Cleaning of dairy HTST plate heat exchangers: comparison of single- and two-stage procedures. J. of Soc. of Dairy Tech. *40* (1), 4–7.

TSOULFANIDIS, N. 1983. *Measurement and Detection of Radiation*. Hemisphere, New York.

WEBB, G. 1994. Kinetics and Modeling of Calcium Phosphate Film Decontamination from Hard Surfaces, Masters thesis, North Carolina State University, Raleigh, North Carolina.

WENNERBERG, J. 1981. Observations on the behaviour of fouling and cleaning in industrial processes. In *Fundamentals and Applications of Surface Phenomena Associated with Fouling and Cleaning in Food Processing*. (B. Hallstrom, D.B. Lund and C. Tragardh, eds.) pp. 76–89, University of Lund, Sweden.

DYNAMIC GAIN MATRIX APPROACH TO MODELING OF DYNAMIC MODIFIED ATMOSPHERE PACKAGING SYSTEMS[4]

E. ÖZER[1], J.H. WELLS[1,3], K.W. McMILLIN[2], C.-P. HO[2] and N.-Y. HUANG[2]

[1]*Department of Biological and Agricultural Engineering*
[2]*Department of Animal Science*
Louisiana Agricultural Experiment Station
Louisiana State University Agricultural Center
Baton Rouge, LA 70803

ABSTRACT

Variations in food and biological systems create nonlinear interactions that increase complexity of mathematical models. A multivariable correlative mathematical modeling strategy, dynamic gain matrix (DGM) method, was derived using advanced process control concepts and it was applied to describe quality changes in beef loin steaks with postmortem fabrication time and modified atmosphere packaging (MAP) conditions altered by dynamic gas exchange. DGM was used for modeling of dynamic MAP to satisfy the special modeling requirements of relationships between the processing and packaging variables and quality parameters through consideration of multivariable interacting deterioration mechanism in mathematical terms. A normalization method was also developed and applied to eliminate initial condition effects arising from meat source differences. A total of 960 data points were analyzed, and the model is reported as a series of first order differential equations with respect to retail display time to describe changes in color, pH and microbial population as functions of postmortem fabrication time, distribution gas composition, gas exchange time and retail gas composition. The model was optimized to minimize prediction sum of residual errors, and a pairing and control strategy was proposed to be used for optimum control of quality parameters for a chosen display time by manipulation of processing and packaging variables. The strategy developed has specific use for prediction and design of dynamic gas exchange MAP systems as well as potential use in similar biological engineering systems.

[3] Corresponding author.

[4] Approved for publication by the Director of Louisiana Agricultural Experiment Station as Manuscript No. 95-07-9236.

Journal of Food Process Engineering **20** (1997) 231–248. *All Rights Reserved.*

INTRODUCTION

Quantitation of biology for engineering purposes has many challenging theoretical and practical problems due to complexities of biological systems (Gold 1977) and complicated interactions of biological materials and the surrounding microenvironment (Pons 1992). Mathematical interpretations of nonlinear, multivariable biological systems incorporate difference and differential equations with the notion of a governing control system (Eisen 1988). Control theory is useful for analyzing complex systems in biological engineering and biomedical engineering (Swan 1984), as well as chemical engineering and economics (Eisen 1988). There are few areas in biology that have been described on such mathematical procedures and laws to predict the outcome of a large number of different processes (Eisen 1988). A correlative mathematical model, previously validated to reflect observed relations between variables, is useful for prediction of the outcomes of biological processes as a basis for prediction and control (Gold 1977). There are no such correlative models reported that can be used for design, prediction, optimization and control of modified atmosphere packaging (MAP) systems.

Dynamic gas exchange in MAP systems have been demonstrated to extend the shelf-life of fresh meat while providing a means for retail merchandising of meat with the bloomed color desired by consumers (Wells and McMillin 1990; Nunes 1992; McMillin 1994). Commercial application of dynamic gas exchange MAP (known as the Windjammer Case-Ready Packaging System) uses a dynamic two-stage gas exchange system (Zhao *et al.* 1994). In such a system, an initial CO_2 atmosphere, $\geq 20\%$, is used for reduction of microorganism growth during distribution and storage, followed by a physical exchange of the in-package gaseous environment with one of $\geq 60\%$ O_2 prior to retail display. The exchange of a package atmosphere with high O_2 concentration achieves fresh meat color, therefore increasing consumer acceptability compared with extended product storage in conventional O_2 permeable packages (Zhao *et al.* 1995). Initial (distribution) gas composition, gas exchange time and subsequent (retail) gas composition, as well as total storage time have a complex relationship with important quality parameters of color, pH and microbial content (McMillin *et al.* 1991). Dynamic gas exchange MAP is the prototypical system to provide immediate changes compared with static or passive modifications for active packaging systems.

The processing variable-quality relationships for dynamic MAP meats have been addressed by McMillin *et al.* (1990 and 1994). Analysis of packaging/quality relationships indicates that there is a system of nonlinear interactions that require description prior to process optimization (Zhao *et al.* 1995). Mixed microbial species found in meat can variously inhibit or promote the growth of one another thereby creating complex effects on quality with respect to

postslaughter and postprocessing storage time (Marshall *et al.* 1991). Parallel to microbial activity, there are active decoupled enzyme systems and chemical reactions within meat during package storage and display (Lee 1983). Accordingly, dynamic MAP procedures pose challenging modeling problems due to the complexity of chemical and biochemical interactions within meat. One special modeling difficulty in dynamic MAP meat is the initial condition problem arising from meat source differences. It is almost impossible to predict future course of biological changes without considering the initial state (conditions) of the biological systems (Pennycuick 1992). A reliable multivariable correlative mathematical model that relates processing and packaging variables to meat quality at retail display could be useful for design of dynamic MAP systems.

A strategy for optimization and control of dynamic MAP is to express the changes in the targeted outputs as functions of deviations in manipulated inputs. In the case of dynamic MAP systems, packaging and processing variables are the manipulated inputs while quality parameters at retail display are the controlled outputs. A common modeling method based on an input-output deviations relationships is the Process Reaction Curve Method (PRCM) (Pons 1992; Seborg *et al.* 1989; Stephanopoulos 1984). The PRCM approach relates changes in outputs to the corresponding step changes in input variables as a set of first order differential equations in terms of three approximated parameters: (1) static gain (output change at steady state divided by corresponding input change), (2) dead time (time elapsed until the system responded), and (3) time constant (time elapsed until the output comes to a new steady state) (Stephanopoulos 1984). This modeling strategy is a practical tool for analysis and modeling of multivariable linear systems. The PRCM approach is used extensively in the chemical industry to obtain transfer functions for controller design purpose (Seborg *et al.* 1989) but is typically applied to defined chemical processing systems at stable operating regions for a linear approximation.

A common practice with the PRCM approach is to use steady state gain parameters of defined transfer functions to determine the optimum input-output variable pairings for control (McAvoy 1983; Seborg *et al.* 1989). A modeling approach named input-output coefficient matrix, analogous to the steady state gain array in process control, has been used to analyze interdependencies of various sectors of economy (Searle 1982). However, such an approach has not been used for control and therefore for pairing purposes to determine the most effective pairing of manipulated inputs and controlled outputs in economics. There is no such correlative modeling methodology reported relating quality changes in dynamic MAP meats during retail display to corresponding changes in processing and packaging variables.

The specific objective of this study was to develop a correlative mathematical modeling strategy and to apply it to relate quality changes in beef loin steaks with typical packaging and processing variables manipulated within a dynamic

MAP system. Such a model is suitable for design, prediction, optimization and control purposes to relate time dependent changes in meat color, pH and microbial content with postmortem fabrication time and modified atmosphere packaging conditions.

THEORY

Dynamic Gain Matrix (DGM) Approach

Individual relationships between quality parameters and packaging and processing variables can be expressed in terms of dynamic gains for the multivariable, highly interacting, nonlinear (i.e. dynamic MAP) system. A dynamic gain, $D_{ij}(t)$, is defined as the ratio of relative change in a quality parameter, $Y_{i,t}$, at a given display time, t, resulting from a step change in a processing variable, X_j, to the magnitude of that processing variable change. Accordingly, the relationship between the i'th quality parameter and the j'th processing variable is expressed as:

$$\frac{\Delta Y_{i,t}}{Y_{i,t}} = D_{ij}(t) \quad \Delta X_j \tag{1}$$

where change in the quality parameter i for the display time t is

$$\Delta Y_{i,t} = Y_{i,t}^{(new)} - Y_{i,t} \tag{2}$$

and the corresponding change in the processing and packaging variable j is

$$\Delta X_j = X_j^{(new)} - X_j \tag{3}$$

In Eq. (2) and (3), $Y_{i,t}^{(new)}$ and $X_j^{(new)}$ represent the new value of quality variable i at a chosen display time t and the corresponding new set value of processing and packaging variable j, respectively. A sample calculation for a gain is also presented in Appendix Example A1.

Gains can be expressed as second order polynomial functions of display time, Eq. (4), since functional nonlinearity is anticipated within meat products because of the enzymatic and microbial interactions within dynamic MAP (Zhao *et al.* 1995). Thus individual gain functions, $D_{ij}(t)$, can be described as:

$$D_{ij}(t) = d_{ij} + d_{ij}' t + d_{ij}'' t^2 \tag{4}$$

where the coefficients of Eq. (4) can be calculated from a second order polynomial fitted to the observed gains with respect to display time.

Individual dynamic gain functions, $D_{ij}(t)$, for $j=m$ processing variables and $i=n$ quality parameters can be stated in matrix notation as an $m \times n$ dynamic gain matrix (DGM):

$$D = \begin{bmatrix} D_{11}(t) & \cdots & D_{1m}(t) \\ \cdot & \cdots & \cdot \\ \cdot & \cdots & \cdot \\ \cdot & \cdots & \cdot \\ D_{n1}(t) & \cdots & D_{nm}(t) \end{bmatrix} \tag{5}$$

The DGM approach can be considered as a modified version of the "steady state gain array" concept in chemical process control. However, the dynamic gains are time dependent, and not constants as in steady state gain array. The dynamic gains are obtained similar to PRCM except output values are normalized and the gains are not steady state values but are pre-specified to a retail display time. Changes in quality parameters are normalized through division by the initial value to eliminate the effect of the differences in the initial conditions on the magnitude of responses for the same specific input change. The DGM would specifically relate changes in quality parameters during retail display to corresponding changes in processing and packaging variables in nonlinear processing and packaging systems. Using the DGM approach and the normalization method Eq. (1) can be restated in matrix notation as:

$$\begin{bmatrix} \dfrac{\Delta Y_{1,t}}{Y_{1,t}} \\ \cdot \\ \cdot \\ \cdot \\ \dfrac{\Delta Y_{n,t}}{Y_{n,t}} \end{bmatrix} = D \begin{bmatrix} \Delta X_1 \\ \cdot \\ \cdot \\ \cdot \\ \Delta X_m \end{bmatrix} \tag{6}$$

From Eq. (5) and (6) it can be seen that if a processing variable had no effect on a quality parameter then the dynamic gain function for that relationship would be equal to zero.

Bristol's Relative Gain Array (BRGA) Analysis

Analyzing the severity of processing and packaging variable and quality parameter interactions in dynamic MAP systems is possible by use of dynamic gains. Such information would be needed to recommend the most effective pairing of manipulated processing and packaging variable and controlled quality parameter for an intended display time. The BRGA method can be used for such determinations (Seborg *et al.* 1989). Bristol's approach is based on the relative gain concept (Bristol 1966). A relative gain array, Λ, for a 2 by 2 system is

expressed as:

$$\Lambda = \begin{bmatrix} \lambda & 1-\lambda \\ 1-\lambda & \lambda \end{bmatrix} \tag{7}$$

where λ, the relative gain, can be defined using dynamic gains as

$$\lambda = \frac{1}{1 - \dfrac{D_{12}(t)D_{21}(t)}{D_{11}(t)D_{22}(t)}} \tag{8}$$

The relative gain array is normalized since the sum of each row or column is one. Relative gains are dimensionless and not affected by units. The optimum pairing is such that the diagonal elements of the BRGA are positive and close to 1. If $\lambda >> 1$ or $\lambda \cong 0.5$, then interaction is severe (Seborg *et al.* 1989) between those processing variables and the quality parameters. A sample calculation using the BRGA and DGM to analyze interactions and pairings in a 2×2 dynamic MAP system is presented in Appendix Example A2.

Control Strategy

There are few techniques to remanipulate or alter packaging variables once meat is displayed for retail sale. This means that the inputs can be realistically manipulated only before display to achieve the desired outcome. Therefore, control would be accomplished with a no system/model mismatch assumption. A zero offset internal model controller designed based on the dynamic gains can be used for that (Garcia and Morari 1985). Such a controller that would relate the desired change in quality parameters to processing and packaging variables for a targeted display time would be simply the model inverse. This is a straight forward and practical strategy that gives a realizable controller (Garcia and Morari 1985). Therefore, the controller array in matrix notation is

$$C = D^{-1} \tag{9}$$

for the controller model expressed as

$$\Delta X = C \Delta \varepsilon \tag{10}$$

where ΔX is array of changes in processing and packaging variables

$$\Delta X = \begin{bmatrix} X_1^{(new)} - X_1 \\ \cdot \\ \cdot \\ X_m^{(new)} - X_m \end{bmatrix} \tag{11}$$

and $\Delta\varepsilon$ is the relative error vector

$$\Delta\varepsilon = \begin{bmatrix} (Y_{1,t}^{(new)} - Y_{1,t}) / Y_{1,t} \\ \cdot \\ \cdot \\ (Y_{n,t}^{(new)} - Y_{n,t}) / Y_{n,t} \end{bmatrix} \tag{12}$$

An example to demonstrate the design of a controller based on actual data is presented at Appendix Example A3.

Dynamic Model

A dynamic model can be obtained using the input-output model, Eq. (6), for a constant retail temperature and a set of constant input variable values. The differentiated model with respect to time gives a first order differential equation for a constant retail temperature and a set of constant input variable values since the dynamic gains were defined as quadratic with respect to time, Eq. (4). The reference values for each output and input is determined within the range where the model is valid and such that the residual sum of prediction errors is minimum for all the experimental data. Therefore, change in the quality parameter i, with respect to display time t for a set of processing and packaging parameters X_j (j=1,2,3,4), is expressed as

$$\left(\frac{dY_i}{dt}\right)_{X1,X2,X3,X4} = c_i + c_{X1,i}X_1 + c_{X2,i}X_2 + c_{X3,i}X_3 + c_{X4,i}X_4 + 2(c_i + c_{X1,i}X_1 + c_{X2,i}X_2 + c_{X3,i}X_3 + c_{X4,i}X_4)t \tag{13}$$

where the initial display condition for quality parameter i depends on processing and packaging variables,

$$Y_{oi} = c_{oi} + c_{X1,oi}X_1 + c_{X2,oi}X_2 + C_{X3,oi}X_3 + c_{x4,oi}X_4 \tag{14}$$

Equations (13) and (14) comprise the predictive models that resulted from this study.

METHODS

Sample Preparation and Quality Parameter Determination

Strip loin steaks obtained from 4 cattle of the same breeding, finished on grain rations for 200 days were fabricated at 48 and 96 h postmortem. After fabrication, steaks were packaged in 80% N_2: 20% CO_2 or 50% N_2: 50% CO_2. After 15 or 22 days storage at simulated distribution temperature of 2C, MAP atmospheres were exchanged for 80% O_2: 20% CO_2 or 60% O_2: 40% CO_2 with a prototype Windjammer (Pakor Inc., Livingston, TX) before display at simulated retail conditions, 4C under 550 lux cool white fluorescent lighting for 1, 3 or 5 days. The total number of processing and packaging value sets for each animal was 16. Color analyses of L* (lightness), a* (red/green) and b* (yellow/blue) values (LABSCAN-2 0/45, Hunter Laboratory, Inc., Reston, VA) were averaged on each strip loin steak by rotating 90° between three readings for each sample. The surface pH was measured with a probe electrode (Extech Instruments Corp., Waltham, MA) at three random locations. Psychrotrophic plate counts were determined as $\log_{10}$ colony forming units (CFU)/g by plate count procedures using pour-plates (APHA 1976) with standard plate count agar (Difco), incubated at 6C for 8 to 10 days. The total number of quality data for each animal was 240 (16 processing sets × 5 quality variables × 3 display times). Data were previously reported in McMillin *et al.* (1994).

DGM Application

The packaging variables and quality parameters considered in model development are indicated in Tables 1 and 2, respectively. Applying the DGM approach, one processing variable was changed at a time and the average changes in all quality parameters were observed for display times of 1, 3 and 5 days. Dynamic gains were calculated using Eq. (1), (2) and (3) to obtain the DGM, Eq. (5), and the whole input-output model, Eq. (6). The dynamic model equations obtained as stated in the theoretical considerations Eq. (13) and (14) were simulated using FORTRAN on a 486-25 MHz Personal Computer using the Euler numerical-integration method with an integration interval of 0.005 display days chosen as recommended (Chandra and Singh 1995; Luyben 1990).

RESULTS AND DISCUSSION

The gains with respect to display time obtained from experimental data using Eq. (1) are presented in Table 3. An analysis of Table 3 discloses the interacting and nonlinear nature of the processing-quality variable relationships for the dynamic MAP beef loin steaks. Eleven of the twenty gain sets had elements with

differing signs for different display times for the same quality parameter - processing variable pair. A negative gain indicated that an increase in the processing variable would produce a decrease in the corresponding quality for the targeted display time. In the present study, this indicates that the effect of an input can dramatically change the response of a quality parameter with respect to the chosen display time. In some cases (Table 3), the processing variable may have the opposite effect for the following chosen display time.

TABLE 1.
PACKAGING AND PROCESSING VARIABLES, X_j, AND ABSOLUTE DEVIATIONS, $|\Delta X_j|$

j	X_j	set values	$\|\Delta X_j\|$
1	Retail Gas Composition (mol O_2/mol CO_2)	4.0 O_2/CO_2 (80% O_2:20% CO_2) or 1.5 O_2/CO_2 (60% O_2:40% CO_2)	2.5
2	Distribution Gas Composition (mol N_2/mol CO_2)	4.0 N_2/CO_2 (80% N_2:20% CO_2) or 1.0 N_2/CO_2 (50% N_2:50% CO_2)	3.0
3	Gas Exchange Time (days)	15 or 22	7
4	Postmortem Time (hours)	48 or 96	48

TABLE 2.
QUALITY PARAMETERS, Y_i, AND THEIR RANGES

i	Y_i	range
1	L (HunterLab L color value)	21 - 38
2	a (HunterLab a color value)	11 - 24
3	b (HunterLab b color value)	6 - 11
4	pH	5.3 - 6.4
5	Microbial Content (log (CFU) / g)	4 - 7

TABLE 3.
OBSERVED (EXPERIMENTAL) GAINS, $D_{ij}(t)$, OBTAINED BY USE OF EQ. (1) AND THE EXPERIMENTAL DATA

		j			
i	t	1	2	3	4
	1	106.206[a]	-8.178	-14.840	3.934
1	3	111.816	-23.374	-84.150	3.668
	5	-14.674	-33.458	107.195	-1.073
	1	-376.864	30.513	3.425	5.906
2	3	-265.147	113.141	64.874	6.756
	5	-143.489	114.550	-17.988	12.797
	1	-199.293	-1.974	-26.432	2.949
3	3	-95.836	26.577	30.014	6.135
	5	-9.671	69.998	-38.047	7.283
	1	-46.272	13.142	56.616	1.656
4	3	-5.081	15.703	20.770	-0.522
	5	-9.114	16.526	0.169	0.011
	1	80.415	-0.315	-14.958	-4.057
5	3	-83.775	-47.633	249.352	-0.448
	5	-9.411	7.529	255.521	4.964

[a]All values to be multiplied by a factor of 10^{-4}.

The coefficients of predictive model Eq. (13) and (14) obtained from theoretical derivations using the observed gains for each display day are tabulated in Tables 4 and 5. The predictive model expressed color values, pH and microbial population of dynamic MAP beef loin steaks as a function of retail gas concentration, gas exchange time, distribution gas concentration and postmortem time as well as display time. Figures 1, 2 and 3 show observed quality data with respect to retail display time together with predicted curves. Twelve experimental data points (4 different animals at each of 3 display days) are plotted to illustrate how well the predicted curves fit with the experimental data for microbial content, pH and L color values. Each of the predictions were developed for corresponding specific processing and packaging variables and the effects of the differences in the initial conditions on the magnitude of responses arising from the meat source differences were eliminated by the normalization method. Furthermore, the model obtained through the developed DGM method was optimized to minimize sum of residual errors. The observed sum of residual errors between model predicted values and all 960 experimental data points are near to zero (Table 6).

TABLE 4.
INITIAL CONDITION COEFFICIENTS, EQ. (12)

	i				
	1	2	3	4	5
c_o	22380.304[a]	26445.456	12134.069	4870.998	7046.403
$c_{X1,o}$	175.144	-927.135	-257.466	-48.380	137.472
$c_{X2,o}$	-0.981	-47.997	-9.507	6.759	37.145
$c_{X3,o}$	333.202	-149.565	-94.127	46.772	-143.492
$c_{X4,o}$	7.546	15.563	0.972	2.153	-2.411

[a]All values to be multiplied by a factor of 10^{-3}.

TABLE 5.
MODEL COEFFICIENTS, EQ. (11)

	i				
	1	2	3	4	5
c	7073.554[a]	-5043.605	-2266.510	165.339	-2024.462
c_{X1}	179.919	160.974	68.811	24.981	-113.518
c_{X2}	-23.658	122.667	5.872	0.892	-45.001
c_{X3}	-470.161	189.852	82.757	-15.350	154.956
c_{X4}	5.475	-4.706	2.066	-1.392	0.163
c'	-1355.071	641.0063	26.740	-4.952	216.922
c'_{X1}	-44.755	-5.374	-3.812	-3.265	16.977
c'_{X2}	0.746	-12.202	1.728	-0.078	7.696
c'_{X3}	93.600	-33.274	-14.158	1.203	-19.078
c'_{X4}	-1.526	1.234	-0.190	0.192	0.184

[a]All values to be multiplied by a factor of 10^{-3}.

Figure 4 is a plot of predicted values versus actual values for the case of retail gas composition of 1.5:1.0 O_2:CO_2, distribution gas concentration of 4.0: 1.0 N_2:CO_2, gas exchange time of 15 days, and postmortem time of 48 h to illustrate the goodness of prediction. For a perfect prediction the predicted values should be identical to observed values and therefore on the diagonal. There is a symmetry across the diagonal, parallel to the observed value axis, since there was one predicted value for each of 4 different animals.

The DGM analysis of the dynamic MAP system can be used for the prediction of quality variables in response to processing parameters and display time as well as for analysis of interactions between all quality parameters and the processing variables. Additionally, such an analysis can be conducted for each individual processing parameter - quality variable pairing with respect to display time, thus enabling control of the quality for a targeted display time by

appropriate manipulation of the processing parameters through an advanced model predictive control method.

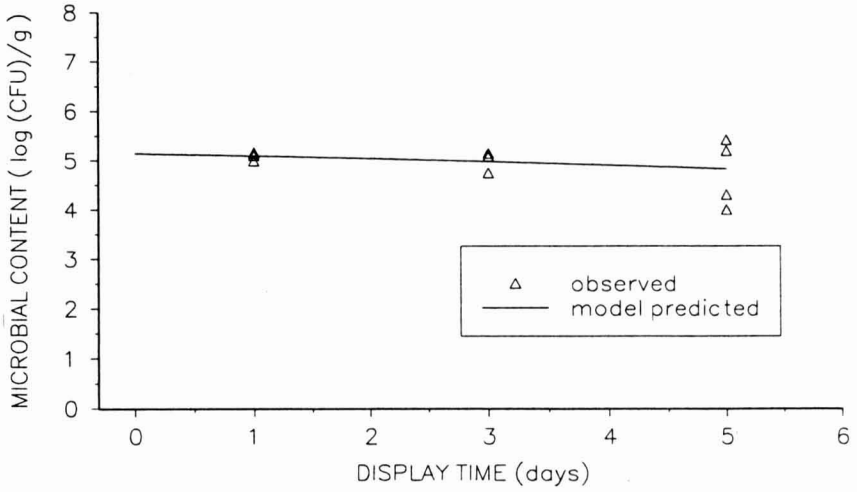

FIG. 1. COMPARISON OF MODEL PREDICTED CURVE OF MICROBIAL CONTENT WITH THE EXPERIMENTAL DATA FOR THE PROCESSING AND PACKAGING SET OF RETAIL GAS COMPOSITION (X_1)=1.5 O_2/CO_2, DISTRIBUTION GAS COMPOSITION (X_2) =4 N_2/CO_2, GAS EXCHANGE TIME (X_3)=15 DAYS AND POSTMORTEM TIME (X_4)=48 H

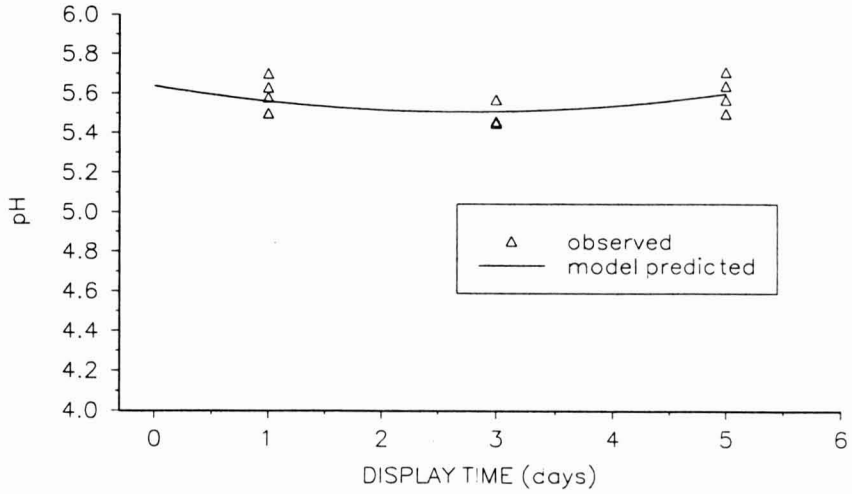

FIG. 2. COMPARISON OF MODEL PREDICTED CURVE OF pH WITH THE EXPERIMENTAL DATA FOR THE PROCESSING AND PACKAGING SET OF RETAIL GAS COMPOSITION (X_1) = 1.5 O_2/CO_2, DISTRIBUTION GAS COMPOSITION (X_2) = 4 N_2/CO_2, GAS EXCHANGE TIME (X_3) = 15 DAYS AND POSTMORTEM TIME (X_4) = 48 H

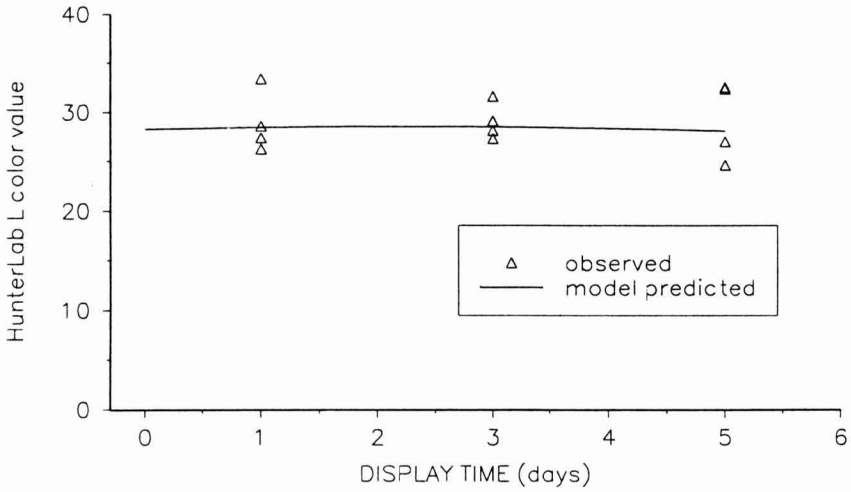

FIG. 3. COMPARISON OF MODEL PREDICTED CURVE OF HUNTERLAB L COLOR VALUE WITH THE EXPERIMENTAL DATA FOR THE PROCESSING AND PACKAGING SET OF RETAIL GAS COMPOSITION (X_1) = 1.5 O_2/CO_2, DISTRIBUTION GAS COMPOSITION (X_2) = 4 N_2/CO_2, GAS EXCHANGE TIME (X_3) = 15 DAYS AND POSTMORTEM TIME (X_4) = 48 H

TABLE 6.
MODEL PREDICTION SUM OF RESIDUAL ERRORS

i	Y_i	t	sum of residual errors for prediction of Y_i
		1	0.08
1	L	3	0.44
		5	-0.01
		1	0.06
2	a	3	-0.10
		5	-0.32
		1	-0.24
3	b	3	0.01
		5	-0.06
		1	-0.03
4	pH	3	0.01
		5	0.01
		1	-0.04
5	MO	3	-0.17
		5	0.31

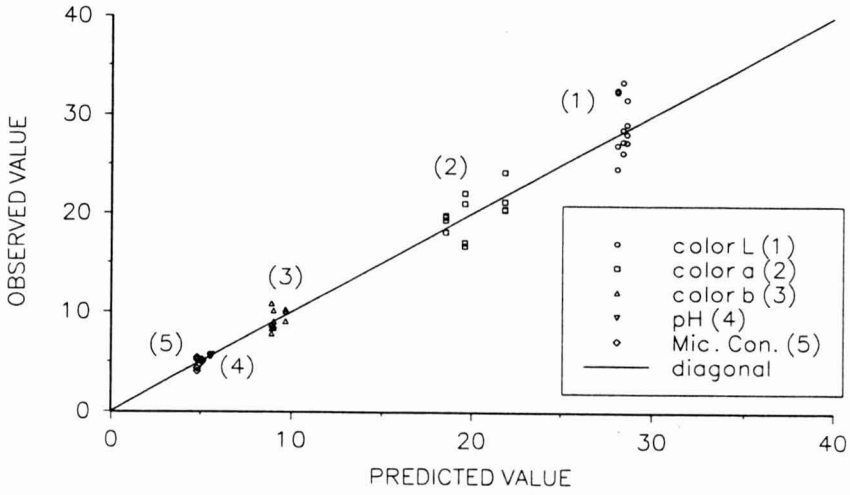

FIG. 4. COMPARISON OF MODEL PREDICTED VALUES OF ALL QUALITY VALUES WITH THE EXPERIMENTAL DATA FOR THE PROCESSING AND PACKAGING SET OF RETAIL GAS COMPOSITION (X_1) = 1.5 O_2/CO_2, DISTRIBUTION GAS COMPOSITION (X_2) = 4 N_2/CO_2, GAS EXCHANGE TIME (X_3) = 15 DAYS AND POSTMORTEM TIME (X_4) = 48 H

CONCLUSIONS

The derived DGM theory was verified on experimental data obtained in an earlier study. Equations (13) and (14) with Tables 4 and 5 were used to describe changes in quality parameters of color, pH and microbial population for a set of processing and packaging variables of postmortem time, gas exchange time, distribution gas composition and retail gas composition during retail display, 1 to 5 days, of beef loin steaks with a very low sum of residual errors at 4C. The DGM and the normalization methods developed in this paper can be powerful tools for modeling of complex dynamic gas exchange MAP systems as well as similar food and biological systems. The modeling and control methodology presented has specific use for design, prediction and optimization of dynamic gas exchange MAP systems.

NOMENCLATURE

C	Controller matrix
$c_{xj,i}$	Coefficients of i'th quality parameter value
$c_{xj,oi}$	Coefficients of initial value of i'th quality parameter
d	Differential operator
D	Dynamic gain matrix
$D_{ij}(t)$	Dynamic gain (function of display time t) between i'th quality variable and j'th packaging and processing variable
d_{ij}, d'_{ij}, d''_{ij}	Coefficients of dynamic gain function between i'th quality variable and j'th packaging and processing variable
t	Display time
X_j	j'th packaging and processing variable value
$X_j^{(new)}$	New value of j'th packaging and processing variable
$Y_{i,t}$	i'th quality variable value at display time t
$Y_{i,t}^{(new)}$	New value of i'th quality parameter for display time t
Y_i	i'th quality parameter value
Y_{oi}	Initial value of i'th quality parameter

Greek Letters and Other Symbols

Δ	Increment
$\Delta\varepsilon_{i,t}$	Relative error in i'th quality variable value at retail display time t
$\Delta\varepsilon$	Relative error matrix
Λ	Bristol's Relative Gain Array matrix
λ	Relative gain
$\Delta\mathbf{X}$	Quality parameter changes matrix

Subscripts

i	Quality parameter index
ij	Dynamic gain index of i'th quality variable and j'th packaging and processing variable
j	Packaging and processing variable index
oi	Quality parameter index for initial value
t	Index to indicate display time
xj	Quality parameter coefficient index

Superscript

new	Indicates the new value of quality parameter or processing and packaging variable

APPENDIX

Three examples using actual data are presented to explain and demonstrate the theoretical considerations in detail.

Example A1. Sample Calculation for a Gain

The gain between the 4'th quality parameter and the 2'nd packaging and processing variable for the 3'rd day of retail display is expressed as $D_{42}(3)$. The relative change, $\Delta Y_{4,3}/Y_{4,3}$, for the processing and packaging variable change, ΔX_2, is found using the set of experimental data such that the sum of residuals is zero. From Table 3

$$D_{42}(3) = \frac{(\Delta Y_{4,3} / Y_{4,3})}{\Delta X_2} = 15.703 \times 10^{-4}(\text{mol } N_2/\text{mol } CO_2)^{-1} \quad \text{(A1)}$$

gives the relation between the relative change in pH for a change in distribution gas composition for the third day of display.

Example A2. Interaction Analysis and Pairing

There are sixty 2 by 2 possible sets for the 5 outputs and 4 inputs for pairwise interaction and pairing analysis with BRGA. Consider two quality variables, color b value and microbial population, to be controlled simultaneously for the third day of display by manipulation of two processing variables of distribution and retail gas compositions. Using Eq. (7) and (8), the values from Table 3 results in $\lambda \cong 0.67$. The model for that specific 2 by 2 case is

$$\begin{bmatrix} \Delta \dfrac{Y_{3,3}}{Y_{3,3}} \\ \dfrac{\Delta Y_{5,3}}{Y_{5,3}} \end{bmatrix} = \begin{bmatrix} -0.0095836 & 0.0026577 \\ -0.0083775 & -0.0047633 \end{bmatrix} \begin{bmatrix} \Delta X_1 \\ \Delta X_2 \end{bmatrix} \quad \text{(A2)}$$

There is considerable interaction since two control loops interact when $0 < \lambda < 1$ and interaction is most severe when $\lambda = 0.5$ (Seborg *et al.* 1989). The controlled output should be paired with the first manipulated input only if $\lambda \geq 0.5$ (Seborg *et al.* 1989). Retail gas composition is more effective in controlling color value b while the distribution gas concentration is more appropriate to control microbial population.

Example A3. Calculation of Optimum Processing and Packaging Values

If it is also desired to control the outcomes of color b and microbial growth

for the third day of display by manipulation of retail gas concentrations, then the equation to relate the desired change in quality for the third day of display to the needed change in processing and packaging variables to achieve the desired outcome will be the model inverse. Therefore,

$$\begin{bmatrix} \Delta X_1 \\ \Delta X_2 \end{bmatrix} = \frac{1}{D_{31}(3)\ D_{52}(3)\ -\ D_{32}(3)\ D_{51}(3)} \begin{bmatrix} D_{52}(3) & -D_{32}(3) \\ -D_{51}(3) & D_{31}(3) \end{bmatrix} \begin{bmatrix} \varepsilon_{Y3,3} \\ \varepsilon_{Y5,3} \end{bmatrix} \quad \text{(A3)}$$

where

$$\begin{aligned} \Delta X_1 &= X_1^{(new)} - X_1 \\ \Delta X_2 &= X_2^{(new)} - X_2 \\ \varepsilon_{Y3,3} &= (Y_{3,3}^{(new)} - Y_{3,3})/Y_{3,3} \\ \varepsilon_{Y5,3} &= (Y_{5,3}^{(new)} - Y_{5,3})/Y_{5,3} \end{aligned} \quad \text{(A4)}$$

For a targeted 2.5% decrease in microbial content at the third display day with only a 1.0% increase in value of color b (regardless of the values of other quality variables), X_1 (retail gas composition) must be increased by 0.277 O_2/CO_2 and X_2 (distribution gas composition) must be increased by 4.761 N_2/CO_2. If the previous value of X_1 was 1 (50% O_2: 50% CO_2) then the new value should be 1.277 (56.08% O_2: 43.92% CO_2).

REFERENCES

APHA. 1976. *Compendium of Methods for the Microbiological Examination of Foods*. Am. Publ. Health Assn., Washington, D.C.

BRISTOL, E.H. 1966. On a new measure of interactions for multivariable process control, IEEE Trans. Auto. Control, AC-11, 133.

CHANDRA, P.K. and SINGH, R.P. 1995. *Applied Numerical Methods for Food and Agricultural Engineers*. CRC Press Inc., Boca Raton.

EISEN, M. 1988. *Mathematical Methods and Models in the Biological Sciences: Nonlinear and Multidimensional Theory*. Prentice Hall, New Jersey.

GARCIA, E.C. and MORARI, M. 1985. Internal Model Control 2: Design Procedure for Multivariable Systems. Ind. Eng. Chem. Process Des. Dev. *24*, 472–484.

GOLD, H.J. 1977. *Mathematical Modeling of Biological Systems*. John Wiley & Sons, New York.

LEE, F.A. 1983. *Basic Food Chemistry*. Chapman & Hall, New York.

LUYBEN, W.L. 1990. *Process Modeling, Simulation and Control for Chemical Engineers*. 2nd Ed., McGraw Hill, New York.

MARSHALL, D.L., WIESE-LEHIGH, P.L., WELLS, J.H. and FARR, A.J. 1991. Comparative growth of Listeria monocytogenes and Pseudomonas fluorescence on precooked chicken nuggets stored under modified atmospheres. J. Food Prot. *54*(11), 841–843, 851.

McAVOY, T.J. 1983. Interaction analysis theory and application. Instrum. Soc. of America, Research Triangle Park, NC.

McMILLIN, K.W. 1994. Gas-exchange systems for fresh meat in modified atmosphere packaging. In *Modified Atmosphere Packaging*, (A.L. Brady, ed.) pp. 85–108, Institute of Packaging Professionals, Herndong, VA.

McMILLIN, K.W., BIDNER, T.D., WELLS, J.H., KOH, K.C. and INGHAM, S.C. 1990. Increasing shelf life of ground beef with modified atmosphere packaging. Louisiana Agriculture *33*, 3–4.

McMILLIN, K.W., HO, C.P., HUANG, N.Y. and SMITH, B.S. 1994. Characteristics of beef loin steaks in modified atmosphere packaging with differing fabrication times, gases and gas exchange times. J. Anim. Sci. *72* (Suppl. 1), 271.

McMILLIN, K.W. *et al.* 1991. Retail shelf-life of meat patties in modified atmosphere packaging with dynamic gas exchange. Paper No. 89, 51st annual meeting of Inst. of Food Technologists, Dallas, TX.

NUNES, K. 1992. MAP for the future. Meat and Poultry *38*(10), 16–19.

PENNYCUICK, C.J. 1992. *Newton Rules Biology: A Physical Approach to Biological Problems*. Oxford University Press, New York.

PONS, M.N. 1992. *Bioprocess Monitoring and Control*. Oxford University Press, New York.

SEARLE, S.R. 1982. *Matrix Algebra Useful for Statistics*. John Wiley & Sons, New York.

SEBORG, D.E., EDGAR, T.F. and MELLICHAMP, D.A. 1989. *Process Dynamics and Control*. 1st Ed., Wiley, New York.

STEPHANOPOULOS, G. 1984. *Chemical Process Control: An Introduction to Theory and Practice*. Prentice-Hall Inc., New Jersey.

SWAN, G.W. 1984. *Applications of Optimal Control Theory in Biomedicine*. Marcel Dekker, New York.

WELLS, J.H. and McMILLIN, K.W. 1990. Dynamic packaging systems for fresh meats. FPEI News, *24*(2), 6–7.

ZHAO, Y., WELLS, J.H. and McMILLIN, K.W. 1994. Applications of dynamic modified atmosphere packaging systems for fresh red meats: review. J. Muscle Foods *5*, 299–328.

ZHAO, Y., WELLS, J.H. and McMILLIN, K.W. 1995. Dynamic changes of headspace gases in CO_2 and N_2 packaged fresh beef. J. Food Sci. *60*(3): 571–575, 591.

PHYSICAL AND COOKING PROPERTIES OF MICRONIZED LENTILS

STEFAN CENKOWSKI

Department of Biosystems Engineering
University of Manitoba
Winnipeg, MB, Canada R3T 2N2

AND

FRANK W. SOSULSKI

Department of Crop Science and Plant Ecology
University of Saskatchewan
Saskatoon, SK, Canada S7N 0W0

Accepted for Publication July 9, 1996

ABSTRACT

The potential for reducing the cooking time of lentils by micronization was studied. The effect of infrared heat and initial seed moisture on the internal temperature of lentil seeds was monitored up to the stage of seed browning. The seed physical properties, water uptake by seeds, cooking time and starch properties were determined. The cooking time was shortened from 30 min for the control seeds to 15 min for lentils adjusted to 25.8% wb moisture content and micronized for 55s to 18.0% wb moisture. Micronization was effective in gelatinizing and solubilizing 45 to 65% of the starch in the lentil seed, depending on the initial seed moisture content.

INTRODUCTION

Grain legumes are considered to be excellent sources of dietary protein, lysine, fiber and essential minerals, but their utilization in North American markets is limited (Bhatty 1995). Lentils are well adapted to growing conditions in Western Canada and the United States, and production would be increased if domestic consumption of this wholesome nutritional crop could be enhanced. One of the principal factors limiting the utilization of grain legumes is their slow and variable cooking times (Buckle and Sambudi 1990; Iyer *et al.* 1980; Bhatty

[1] Address correspondence to: Stefan Cenkowski, Department of Biosystems Engineering, University of Manitoba, Winnipeg, MB, Canada R3T 2N2

Journal of Food Process Engineering **20** (1997) 249–264.

1988). Considerable research has been conducted on the 'hard-to-cook' phenomenon associated with storage of beans under tropical conditions of high temperature and humidity (Aguilera and Stanley 1985; del Valle *et al.* 1992; Liu *et al.* 1993). Even under temperate climatic conditions, lentils may exhibit the slow cooking phenomena, although the causative factors appear to be associated with soils and mineral metabolism (Bhatty 1995).

Because of their thinner seedcoat, lentil seeds absorb water and cook more rapidly than common beans (Swanson *et al.* 1985; Stanley *et al.* 1989). However, cooking times are still in range of 30 to 70 min (Bhatty 1995). If lentils could be made available in a quick-cooking form, there is potential for growth in domestic ingredient and retail markets. Precooked lentils are currently utilized in convenience foods on a limited basis, but the technology for low-cost production of quick-cooking lentils has not been developed.

Micronizing or infrared (IR) processing has been developed commercially for the heat treatment of bulk feeds to increase their digestibility and inactivate enzymes and antinutrients (Lawrence 1975; Fernandes *et al.* 1975; Kouzeh-Kanani *et al.* 1984; Murray 1987). The generation of heat in absorbent materials is caused by near-infrared rays with wavelengths of about 1000 to 3500 nm. The cost of IR processing varies widely but operation efficiencies average about 90%. In practical applications the overall efficiency (dependent on the degree of absorption of radiant energy in the material being heated) could be about 65% (Shuman and Staley 1950). Still, a properly designed IR system can be less expensive than a convention heating system. Commercial equipment is available for applying this dry heat treatment on a continuous basis to grain products without excess damage to heat-sensitive amino acids and vitamins. However, precise control of temperature and moisture is essential to avoid browning, Maillard-type reactions and excessive gelatinization and expansion of the starch granule (Lawrence 1975).

The objective of the present study was to determine the potential for reducing the cooking time of lentils by micronization. In this preliminary study, the effect of IR heat and initial seed moisture on the internal temperature of lentil seeds was monitored up to the stage of seed browning. The effects of micronizing on seed physical properties, water uptake by seeds, cooking time and starch properties were determined.

MATERIALS AND METHODS

Seed Source and Treatment

A 10-kg lot of the large-seeded lentil cultivar, Laird, obtained from InfraReady Products Ltd., Saskatoon, SK, was determined to have a cooking

time of 30 min that was typical of the 1994 commercial crop. The moisture content (mc) of the seed was 10.1% wet basis (wb) based on the AACC (1995) (method 44-15A) procedure. On a dry basis (db), following the AACC (1995) analytical methods, these lentils contained 23.6% crude protein (N × 6.25) (method 46-12), 18.1% total dietary fiber (method 32-05), 3.2% ash (method 08-01) and 1.2% oil (method 30-25). The starch content (43.6% db) and free sugars (1.9% db) were quantified using the YSI method as outlined by Budke (1984).

The wetting treatments were selected on the basis that 25% moisture content was the upper limit for ease of seed flow from the hopper and spreading onto the vibrating belt of the commercial micronizer. Initial seed moisture contents of 19.0, 25.6, 38.6% wb were selected to represent the safe, maximum and excess moisture levels to be evaluated by micronization. Seed samples were wetted by spraying distilled water onto the seeds while tumbling. The dampened samples were tempered for 48 h at 4C prior to micronizing.

Micronization of Lentils

A schematic diagram of the infrared equipment used in micronization of lentils is shown in Fig. 1a. The infrared lamp used was a tubular quartz (T3) tungsten filament lamp (General Electric Co., Cleveland, OH) rated at 500 W and 120 V. The peak emission wavelengths of the filament wire were 1150 and 1580 nm at 120 and 60 V, respectively. The lamp was capable of converting up to 88% of its input power into infrared radiant energy with filament temperature reaching 2200C at the rated voltage. The lamp was mounted on a strip heater Model 5305 (Research Inc., Minneapolis, MN). The heater concentrated the radiant energy onto a target strip 38 mm wide, using a parabolic specular aluminum reflector over the 64 mm length of the IR lamp (Fig. 1b).

Samples of approximately 4.0 g were placed in one layer on a 35 × 60 mm white tray which was positioned on a scale for determination of drying characteristics during the IR treatments. The scale was protected from the IR rays by a screen, and was connected to a data acquisition (D/A) system to monitor changes in mass during micronization. The temperature changes during micronization were monitored by inserting a thermocouple into the center of two seeds which were placed under the IR lamp (Fig. 1b) for each test. All tests were conducted in duplicates. In preliminary experiments, the samples were placed at distances of 85, 105 and 125 mm from the IR lamp. The 105 mm height was selected for subsequent tests.

Measurement of Cooking Quality

The lentil samples prepared for the cooking tests were always micronized to the same final moisture content of 18% wb as kernel discoloration was

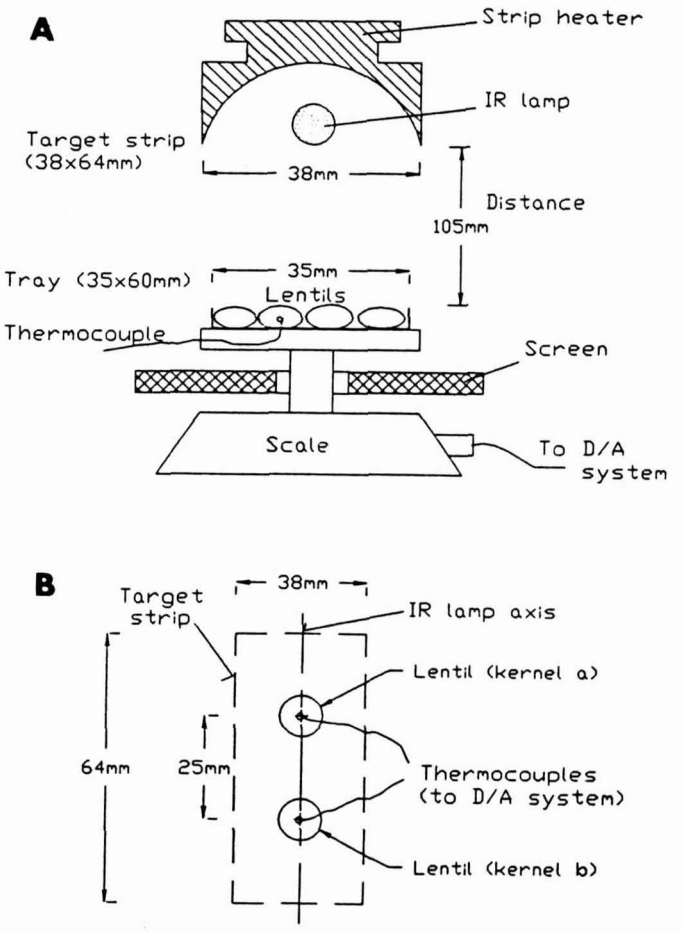

FIG. 1. DESIGN OF THE EXPERIMENTAL APPARATUS FOR IR PROCESSING OF LENTILS AND THE POSITIONING OF TWO SEEDS WITH IMBEDDED THERMOCOUPLES UNDER THE IR LAMP

observed during heating to lower moisture contents. Therefore, lentils tempered to 19.0% initial moisture contents were not included in the cooking tests. For initial moisture contents of 25.8 and 38.6% wb, micronization times of 55 and 85 s, respectively, were applied for micronization at the 105 mm distance from the IR lamp. After micronization, the heated samples were allowed to cool and dry at room temperature to approximately 10.0% wb moisture.

The 250 mL Erlenmeyer flasks containing 125 mL of distilled water were immersed in a covered boiling water bath (98C) and brought to a boil. Then, 20 g samples of micronized lentils were poured into the flask and cooked for 5, 10 and 15 min. The control samples were cooked for 5, 10, 15, 20, 30 and 40 min. After cooking, the water was drained off through a fine sieve and the lentils cooled and weighed. The gain in weight gave an estimate of water uptake. The samples were placed in sealed containers and stored at 4C.

The texture of the individual seeds of freshly-cooked lentils was measured with a texture analyzer, Model TX.XT2 (Texture Technology Corp., Scarsdale, NY). The texture analyzer was equipped with a TA7 standard probe knife. The thickness and length of the knife were 1.73 and 10.8 mm, respectively. The radius of the cutting edge was half of the thickness of the knife. The knife speed was set to 0.5 mm/s and the depth of penetration was 2.5 mm into the kernel. Ten to twelve kernels, randomly selected from a cooked sample, were tested. Eleven samples were examined so a total of 115 kernels were tested.

Isolation of Starch

To measure the extent of starch granule gelatinization during micronization and cooking, the residual intact starch granules were isolated from homogenized seeds by the procedure of Hoover *et al.* (1993). The 20 g of lentils were steeped in 200 mL 0.5% sodium bisulphate ($NaHSO_3$) solution for 24 h in a 4C chamber. Then, the seeds were thoroughly rinsed with distilled water and homogenized in a Waring blender for 2 min at low speed and then for 2 min at high speed. The homogenate was passed through a 210 μm nylon screen. The residue was homogenized two more times as described above but only at high speed and the final extract was passed through a 70 μm nylon screen. The filtrate was allowed to sediment at 4C for 16 h and the supernatant was discarded. The sedimented starch cake was suspended in an excess of 0.05N sodium hydroxide (NaOH) solution, stirred and centrifuged at 10,000 rpm for 15 min three times, followed by neutralization with hydrochloric acid (HCl) to pH 6 and washed three times with distilled water. Finally, the starch cake was washed over a Buchner filter with 95% ethanol. After drying at room temperature, the final moisture content of all starch samples was 8.0 $\pm$ 0.1% wb.

Differential Scanning Calorimetry

Differential Scanning Calorimetry (DSC) of starch was determined using a Mettler TA4000 DSC system. Approximately 4 mg of starch were weighed into stainless steel pans and approximately 13 μL of water was added. The amount of water added to a sample was calculated based on the volume ratio set to an optimum value of 0.85 following the relationship (Hoover and Sosulski 1985):

$$\frac{V_w}{\frac{m_s}{\rho_s}+V_w}=0.85$$

where: V_w = volume of water, μL; m_s = mass of starch, mg db; ρ_s = density of starch, ρ_s = 1.5 mg/μL.

The starch was sealed in the stainless steel pan, heated from 30 to 110C at a scan rate of 10C/min. The area under the peak as heat of transition of gelatinization (ΔH), and the onset (T_o), end (T_e) and peak (T_p) temperatures were determined with the Mettler TA4000 system.

RESULTS

Micronizing of Lentils

The effect of duration of IR lamp heating on the temperature within lentil seeds is illustrated in Fig. 2. The curves show the average temperatures of the two seeds positioned under the IR lamp as illustrated in Fig. 1b. Beginning at the 105 s micronization time, the two dashed lines correspond to the temperature history of the two (a and b) individual seeds. In general, temperatures increased with heating time until seeds cracked and became charred. During IR heating, three distinct stages in the temperature pattern could be detected: a rapid heating period, a temperature stabilization period and an overheating stage. For samples that were micronized at 85, 105 and 125 mm from the IR lamp, the temperature stabilization periods were between 30 to 50 s, 50 to 100 s and 80 to 120 s, respectively. Fluctuations in the curves were due to random splitting of the hulls. When the cracks were sufficiently deep to reach the center of the seed and the thermocouple, a rapid temperature drop, back to the saturation point for vapor ($\approx$ 100C), was observed. This is shown after 105 s of micronization for one seed micronized at the distance of 125 mm from the IR lamp. Then the temperature increase resumed, but at a slower rate than for more intact seeds. Presumably, more rapid evaporation through the large fissure had a cooling effect on the seed and thermocouple.

Because of the short temperature stabilization period for the 85 mm distance, and the slow temperature increase at the 125 mm micronization distance, the subsequent experiments were conducted at the 105 mm distance from the heat source.

The maximum duration of IR heating that could be applied was delineated by the discoloration and browning of the hulls. This occurred after 55, 120 and 180 s for the 85, 105 and 125 mm micronization distance from the IR lamp

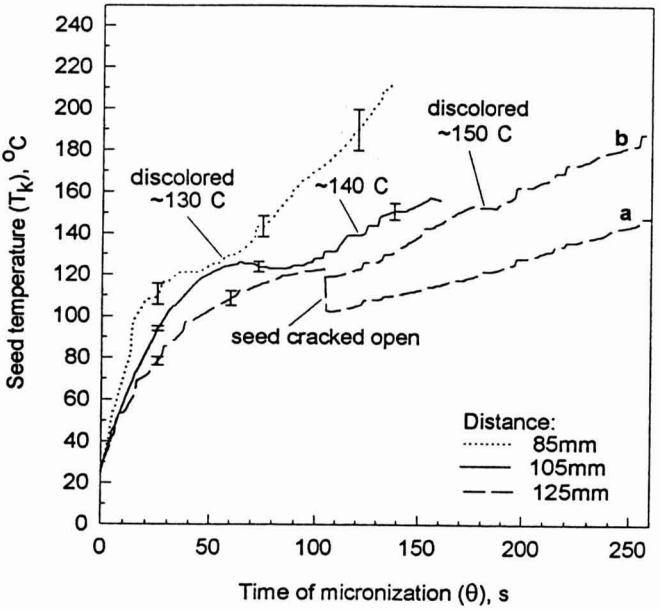

FIG. 2. THE EFFECT OF DURATION OF MICRONIZATION ON TEMPERATURE OF LENTIL SEEDS AT 34.0% wb INITIAL MOISTURE BASED ON DISTANCE FROM THE IR LAMP

Average of duplicate determinations except for the cracked (a) and uncracked seeds (b) at the 125 mm distance from the IR lamp. The vertical bars indicate standard deviations.

when temperatures had reached 130, 140 and 150C, respectively, for seeds at 34.0% wb tempered moisture content (Fig. 2). These temperatures were reached shortly after the temperature stabilization period, and so the third phase of increasing temperature was termed the overheating stage.

To determine the variability in the onset of discoloration, duplicate sets of two seeds at positions a and b (Fig. 1b) were heated simultaneously at the 105 mm distance using initial seed moisture contents of 19.0, 25.8 and 38.6% wb. The individual temperature profiles for duplicate seeds at each position are plotted in Fig. 3. They show considerable variability among seed position and replicates at 19.0% initial moisture content, but the variation decreased with increasing seed moisture. The onsets of the plateau in temperature curves occurred at about 25, 25 and 40 s, respectively, for the 19.0, 25.8 and 38.6% wb moisture levels. Based on visual monitoring of each seed, the first indication of discoloration occurred at 137 to 150C for all moisture levels. But, at the highest moisture level, one seed did not begin browning until 160C was reached. The maximum time that lentil seeds could be micronized, before discoloration started, was 38, 60 and 105 s, respectively, for 19.0, 25.8 and 38.6% wb initial seed moisture levels. On the other hand, the time span over which browning

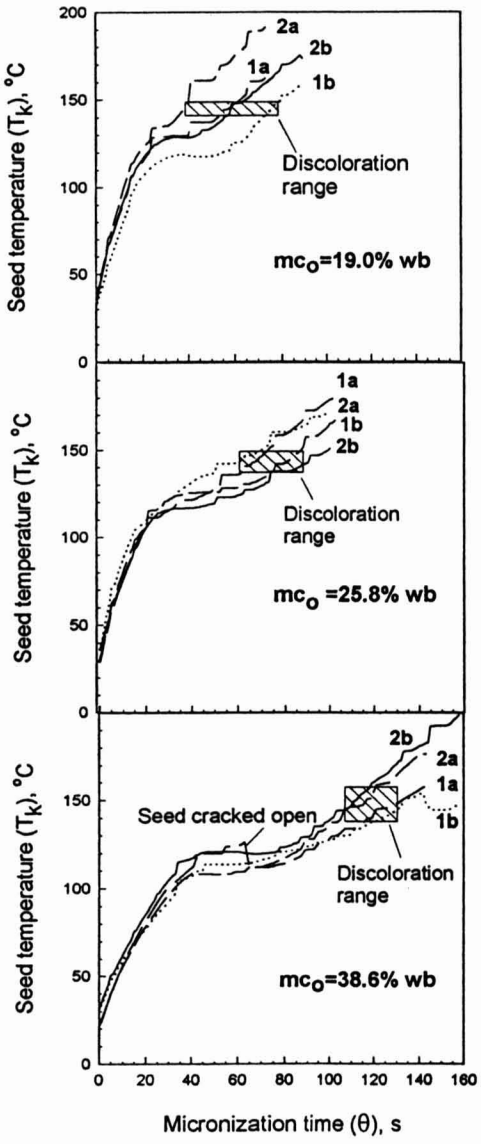

FIG. 3. TEMPERATURE HISTORY IN FOUR SEEDS AND THE DISCOLORATION RANGE DURING THE MICRONIZATION OF LENTILS CONDITIONED TO 19.0, 25.8, AND 38.6% wb INITIAL MOISTURE CONTENTS

Symbols a and b indicate a location of a kernel under the IR lamp while the numbers 1 and 2 refer to replicates.

first started among the lentil seeds was 35, 25 and 20 s, respectively, for the three initial moisture levels. Thus, the onset of browning could be predicted more accurately for the seeds tempered to the highest moisture level.

Seed cracking in these studies appeared to occur randomly among treatments (Figs. 2 and 3) and appeared to be an individual seed characteristic, rather than being due primarily to the treatments applied in this study.

Drying Curves

The drying characteristics of lentils at 22.5, 25.8 and 38.6 % wb initial moisture content were measured on single layers of seeds covering the entire sample tray (Fig. 1). The moisture changes in the samples, as recorded by the D/A system, are reported in Fig. 4.

The best fit lines of the drying data were incorporated into Fig. 4. These lines allowed for a graphical differentiation of the drying curves and determination of drying rates as a function of moisture content for the entire micronization period of the three treatments. These characteristics are shown on the left side of Fig 4. A drying rate is characterized as the slope of a drying curve at selected moisture contents. As the temperature of seeds increased during the first stage of micronization (Fig. 3), the slope of the drying curve showed progressive change (Fig. 4). This change was observed during the initial 40 s of micronization. A constant drying rate of -0.35 s^{-1} was obtained for all three samples in the

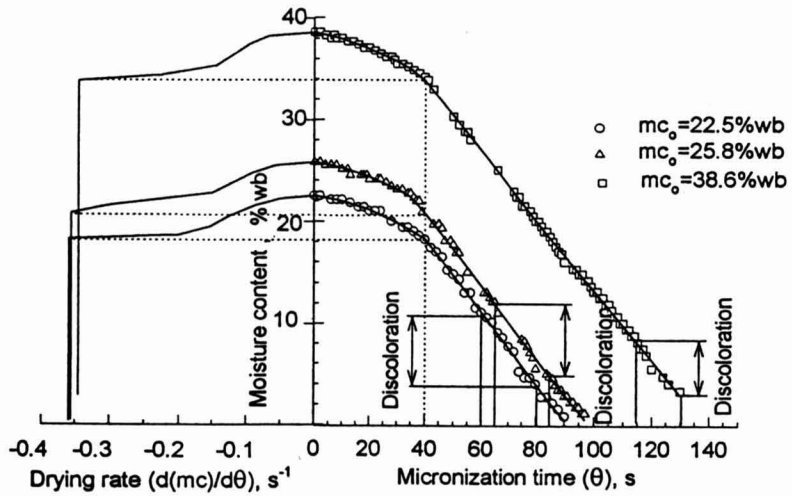

FIG. 4. MOISTURE CHANGES AND DRYING RATES DURING MICRONIZATION OF LENTILS CONDITIONED TO THREE INITIAL MOISTURE CONTENTS (mc_o)
The three vertical arrows show the moisture range at which the discoloration of kernels began to occur.

second and third stage of IR processing, regardless of the initial moisture content of the sample.

The discoloration range for each initial seed moisture content was superimposed onto Fig. 4 to show that seeds at 22.5 and 25.8% wb initial moisture content began to brown in the range of 4 to 12% wb moisture. Seeds at 38.6% wb moisture initially began to change color over the range of 3 to 8% wb moisture content.

Cooking Quality

For the following cooking tests, micronization was done on lentils at initial moisture contents of 25.8 and 38.6% wb mc but micronization times were adjusted to give a final moisture content of 18% wb. Thus, micronization times were 55 and 85 s, respectively, for the two treatments. After micronization, the samples were allowed to dry at room temperature to approximate 10.0% wb moisture.

Water uptake by control and micronized lentils was very rapid during the first 5 min of cooking, reaching 42, 47 and 52% wb, respectively, for the control and samples micronized at 25.8 and 38.6% wb mc (Fig. 5). At 15 min cooking time, the water uptake of the micronized samples increased another 10%, at which stage the seeds were fully cooked. The control lentils also reached 60% wb mc when fully cooked at 30 min.

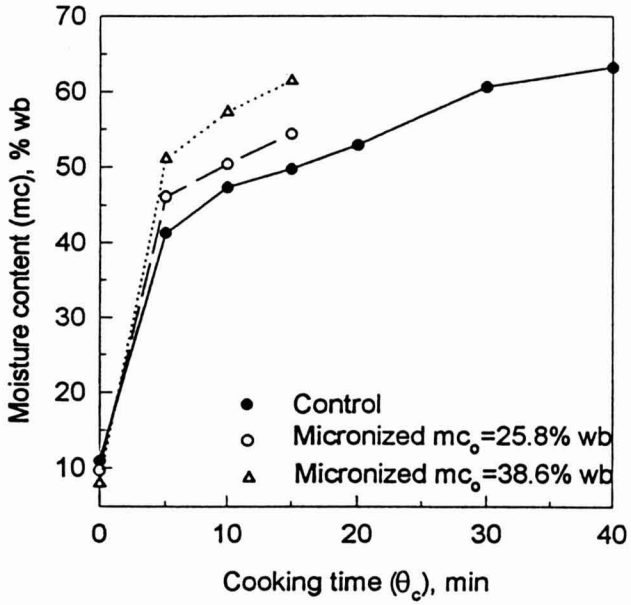

FIG. 5. WATER UPTAKE BY THE CONTROL AND MICRONIZED LENTILS DURING COOKING

The texture of lentils during cooking was measured using a penetrating probe knife on a texture analyzer. A typical force/deformation curve obtained during penetration a single seed with 3.16 mm thickness to a depth of 2.5 mm is shown in Fig. 6 (dashed line). The initial highest peak was the force required to penetrate the hull while the subsequent lesser peaks reflected variations in hardness of the consecutive inner layers of the seed until the probe was withdrawn. Only initial peak heights are reported in Fig. 6 (solid lines with symbols), where the average first peak of crushing force for fully cooked lentils was 13 $\pm$ 1.7 N with 95% confidence limit (dotted line). Each data point in the figure represents the mean of the first peaks for 10 to 12 seeds. The vertical bars indicate the 95% confidence limits.

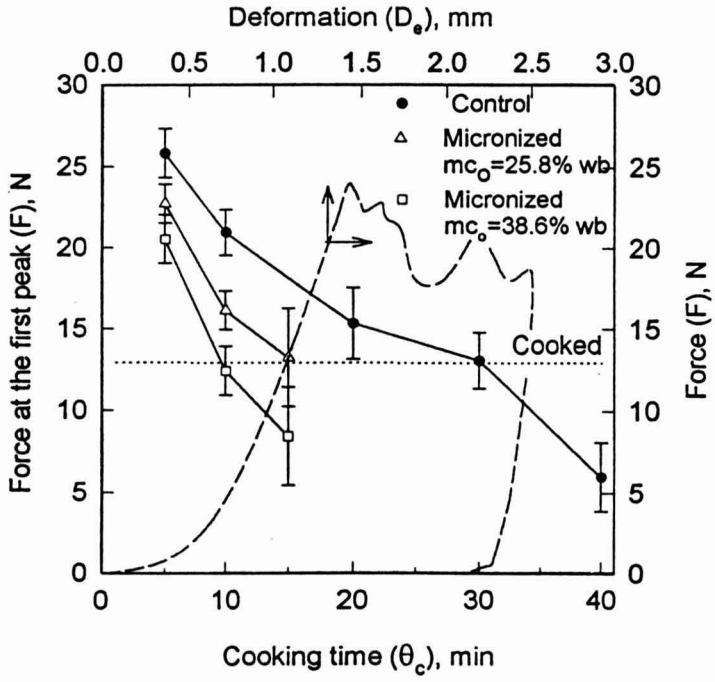

FIG. 6. EFFECT OF THE COOKING TIME ON THE INITIAL PEAK OF THE PENETRATION PROBE ANALYSIS FOR THE CONTROL AND SAMPLES MICRONIZED AT 25.8 AND 38.6% wb mc (SOLID LINES WITH SYMBOLS)
The dashed line curve shows a typical force/deformation characteristic obtained during the penetration test for a single control seed cooked for 10 min and tested on a texture analyzer. Dimensions of the seed: diameter = 7.90 mm, thickness = 3.16 mm, The deformation speed was 0.5 mm/s.

The cooking times were shortened from 30 min for the control to 15 min for the 25.8% wb mc sample and to 10 min for the 38.6% wb mc treatment. The 38.6% wb mc samples was overcooked at the 15 min interval, as was the control at 40 min. From the practical standpoint, micronization at 25.8% wb mc for 55 s could be used commercially to shorten the cooking time by half for this Laird lentil sample, which was reported to be typical of the 1994 commercial crop.

The frequency of the variability in the mean penetrating force for 115 experiments (all data including control and micronized seeds) is shown on a frequency histogram in Fig. 7 (see bars). The sample mean and standard deviation of the histogram were used to compute and superimpose a Gaussian distribution (solid line) on the histogram graph. The Gaussian distribution gives the measure of variability in the entire population of the processed lentils. No tendency was observed in the narrowing of the variability of the cooked or micronized and cooked lentils. Therefore, the data of all the experiments were combined in Fig. 7. Even after overcooking, as in the case of control samples cooked for 40 min (Fig. 6), some seeds were still quite tough, requiring a maximum peak force up to 10 N above the mean value in order to achieve penetration. This behavior could be attributed to the hard-to-cook phenomenon in lentil (Bhatty 1988; Liu *et al.* 1993).

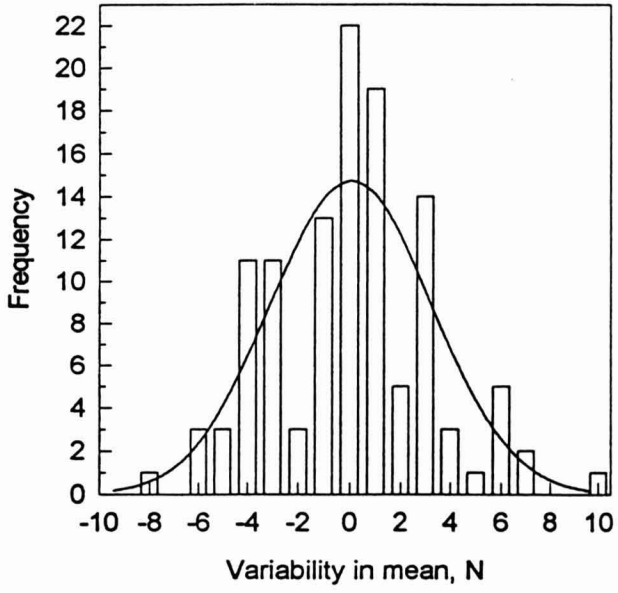

FIG. 7. HISTOGRAM OF THE FREQUENCY OF THE VARIABILITY FROM THE MEAN OF THE FIRST PEAK OF THE PENETRATING PROBE ANALYSIS

DSC Thermographs

Starch was extracted from control and micronized 25.8% and 38.6% wb mc lentils, before and after cooking for 5 min, to evaluate the effect of micronizing on the thermal characteristics of starch. Starch granules were intact in the raw control lentil and starch recovery during isolation was 90% (Table 1). During 5 min cooking, about 50% of starch granules were gelatinized and disintegrated sufficiently to be lost during starch washing. Micronization at 25.8% wb and 38.6% wb mc also gelatinized much of the starch so that insoluble starch granule yields were 55% and 35%, respectively. The cooked micronized lentils contained only 20% and <10% intact starch, so thermal analysis were only done on the intact starch granules isolated from the 25.8% wb mc sample.

TABLE 1.
APPROXIMATE YIELD OF INSOLUBLE STARCH GRANULES FROM CONTROL, MICRONIZED AND COOKED LENTILS AND THEIR DSC PROPERTIES

	Native					5 min cook				
Treatment	Yld %	T_p °C	Std	ΔH J/g	Std	Yld %	T_p °C	Std	ΔH J/g	Std
Control	90	65.9	0.2	9.2	0.5	45	67.6	0.2	7.5	0.3
Micronized	55	74.8	0.0	2.6	0.9	20	72.5	0.1	1.9	0.2
mc_o=25.8% wb										
Micronized	35	74.2	5.8	0.9	0.7	<10	-	-	-	-
mc_o=38.6% wb										

The DSC thermograms are illustrated in Fig. 8, and data on the endothermic peak transitions and transition enthalpies are given in Table 1. Raw control lentil starch had a peak gelatinization temperature (T_p) of 65.9C, and the total heat absorbed by the sample during the transition (gelatinization) period (ΔH) was 9.2 J/g. These values are similar to the values of 65C and ΔH=7.1 J/g, respectively, for native lentil starch reported by Sosulski *et al.* (1985). Cooking for 5 min increased the T_p slightly to 67.6C and the ΔH became smaller, 7.5 J/g.

Micronizing the lentils at 25.8% wb mc and, especially, at 38.6% wb mc severely reduced the ΔH to 2.6 and 0.9 J/g, respectively, and gave multiple small peaks in the range of 70 to 80C (Fig. 8, Table 1). Cooking the micronized

25.8% wb mc starch reduced the ΔH further but multiple small peaks were still present.

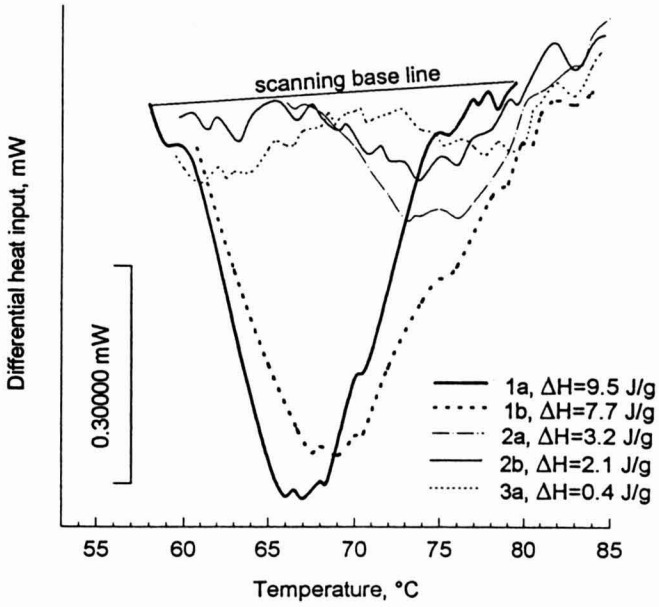

FIG. 8. DSC THERMOGRAMS OF LENTIL STARCHES FROM RAW (a) AND COOKED 5 MIN (b) CONTROL (1), MICRONIZED 25.8% wb mc (2) AND MICRONIZED 36.8% wb mc (3) SAMPLES
The ΔH values refer to the selected tests.

These results demonstrate that micronizing served to gelatinize and solubilize 45 to 65% of the lentil starch in the seed, depending on initial seed moisture content. The remaining residual (insoluble) starch in the seed was highly gelatinized and modified in its thermogram properties. Cooking for 5 min gelatinized one-half of the control starch with little change in the thermogram of the residual starch. Cooking of micronized starches for 5 min served to gelatinize most of starch and residual starches had markedly reduced thermograms.

CONCLUSIONS

During IR heating of lentils three distinct stages in the temperature pattern were detected: a rapid heating period, a temperature stabilization period and an overheating stage. The duration of the stages depended on the distance between

the seeds and the IR lamp. The first indication of discoloration of seeds during IR heating occurred at 130 to 150C for lentils of initial moisture content from 19.0 to 38.6% wb. A constant drying rate in the range of -0.35 s^{-1} was reached after the first 40 s of micronization regardless of the initial moisture content of the micronized lentils.

The cooking time was shortened from 30 min for control to 15 min for lentils adjusted to 25.8% wb mc and micronized for 55 s to the final moisture of 18.0% wb. Lentils brought to 38.6% wb moisture and then micronized for 85 s to the final moisture of 18.0% wb required only 10 min of cooking to reach the same range of crushing force that was required for the control sample cooked for 30 min. Micronization served to solubilize and gelatinize 45 to 65% of the starch in the lentil seed. Cooking of micronized seeds for 5 min served to gelatinize most of the remaining starch and the residual starches had markedly reduced thermograms. Cooking for 5 min gelatinized one-half of the control starch with little change in the thermogram of the residual (insoluble) starch.

ACKNOWLEDGMENT

The authors acknowledge the Natural Sciences and Engineering Research Council of Canada for providing partial financial support for this research. The technical support of Dr. S. Sokhansanj from the Department of Bioresource and Agricultural Engineering, University of Saskatchewan, is appreciated.

REFERENCES

AACC. 1995. Methods: 08-01, 30-25, 32-05, 44-15A and 46-12. (Am. Assoc. Cereal Chem.) St. Paul, MN.

AGUILERA, J.M. and STANLEY, D.W. 1985. A review of textural defects in cooked reconstituted legumes - the influence of storage and processing. J. Food Processing & Preservation *9*, 145–169.

BHATTY, R.S. 1988. Composition and quality of lentil (Lens culinaris Medik): A review. Can. Inst. Food Sci. Technol. J. *21*, 144–160.

BHATTY, R.S. 1995. Lentils as a dietary cereal component. Cereal Foods World *40*, 387–392.

BUCKLE, K.A. and SAMBUDI, H. 1990. Effect of soaking and boiling treatments on the quality of Winged bean seed. J. Sci. Food Agric. *53*, 379–388.

BUDKE, C.C. 1984. Determination of total available glucose in corn base materials. J. Agric. Food Chem. *32*, 34–37.

DEL VALLE, J.M., COTTRELL, T.J., JACKMAN, R.L. and STANLEY, D.W. 1992. Hard-to-cook defect in black beans: the contribution of proteins to salt soaking effects. Food Res. Int. *25*, 429–436.

FERNANDES, T.H., HUTTON, K. and SMITH, W.C. 1975. A note on the use of micronized barley for growing pigs. Animal Prod. *20*, 307–310.

HOOVER, R. and SOSULSKI, F. 1985. Studies on the functional characteristics and digestibility of starches from Phaseolus vulgaris biotypes. Starch/Stärke *37*, 181–191.

HOOVER, R., SWAMIDAS, G. and VASANATHAN, T. 1993. Studies on the physiochemical properties of native, defatted, and heat-moisture treated pigeon pea (Cajanus cajan L) starch. Carbohydrate Res. *246*, 185–203.

IYER, V., SALUNKHE, D.U., SATHE, S.K. and ROCKLAND, L.B. 1980. Quick-cooking beans (Phaseolus vulgaris L.): I. Investigations on quality. Qual. Plant. Plant Foods Human Nutrit. *30*, 27–43.

KOUZEH-KANANI, M., VAN ZUILICHEM, D.J., ROOZEN, J.P. and PILNIK, W. 1981. A modified procedure for low temperature infrared radiation of soybeans. Part III: Pretreatment of whole beans in relation to oil quality and yield. Lebensmittel-Wissenschaft und-Technologie *17*, 39–41.

LAWRENCE, T.L.J. 1975. An evaluation of the micronization process for preparing cereals for the growing pig. A note on the effect of micronization temperature on the nutritive value of wheat. Animal Prod. *20*, 167–170.

LIU, K., PHILLIPS, R.D. and MCWATTERS, K.H. 1993. Induced hard-to-cook state in cowpeas by freeze-thawing and calcium chloride soaking. Cereal Chem. *70*, 193–195.

MURRAY, J. 1987. Unlocking new product opportunities with infra-red processing. The 2nd Int. Conf. on Design and Engng New Food Plants. Sept. 23-25 1987, Lincolnshire (Chicago), IL.

SHUMAN, A.C. and STALEY, C.H. 1950. Drying by infra-red radiation. Food Techn. *4*, 481–484.

SOSULSKI, F.W., HOOVER, R., TYLER, R.T., MURRAY, E.D. and ARNTFIELD, S.D. 1985. Differential scanning calorimetry of air-classified starch and protein fractions from eight legume species. Starch/Stärke. *8*, 257–262.

STANLEY, D.W., WU, X. and PLHAK, L.C. 1989. Seed coat effects in cooked reconstituted bean texture. J. Texture Studies *20*, 419–429.

SWANSON, B.G., HUGHES, J.S. and RASMUSSEN, H.P. 1985. Seed microstructure: Review of water imbibition in legumes. Food Microstruct. *4*, 115–124.

F N P PUBLICATIONS IN FOOD SCIENCE AND NUTRITION

Journals

JOURNAL OF FOOD LIPIDS, F. Shahidi
JOURNAL OF RAPID METHODS AND AUTOMATION IN MICROBIOLOGY, D.Y.C. Fung and M.C. Goldschmidt
JOURNAL OF MUSCLE FOODS, N.G. Marriott, G.J. Flick, Jr. and J.R. Claus
JOURNAL OF SENSORY STUDIES, M.C. Gacula, Jr.
JOURNAL OF FOODSERVICE SYSTEMS, C.A. Sawyer
JOURNAL OF FOOD BIOCHEMISTRY, N.F. Haard, H. Swaisgood and B. Wasserman
JOURNAL OF FOOD PROCESS ENGINEERING, D.R. Heldman and R.P. Singh
JOURNAL OF FOOD PROCESSING AND PRESERVATION, D.B. Lund
JOURNAL OF FOOD QUALITY, J.J. Powers
JOURNAL OF FOOD SAFETY, T.J. Montville and D.G. Hoover
JOURNAL OF TEXTURE STUDIES, M.C. Bourne and M.A. Rao

Books

APPETITE FOR LIFE: AN AUTOBIOGRAPHY, S.A. Goldblith
HACCP: MICROBIOLOGICAL SAFETY OF MEAT AND POULTRY, J.J. Sheridan, R.L. Buchanan and T.J. Montville
OF MICROBES AND MOLECULES: FOOD TECHNOLOGY AT M.I.T., S.A. Goldblith
MEAT PRESERVATION: PREVENTING LOSSES AND ASSURING SAFETY, R.G. Cassens
S.C. PRESCOTT, M.I.T. DEAN AND PIONEER FOOD TECHNOLOGIST, S.A. Goldblith
FOOD CONCEPTS AND PRODUCTS: JUST-IN-TIME DEVELOPMENT, H.R. Moskowitz
MICROWAVE FOODS: NEW PRODUCT DEVELOPMENT, R.V. Decareau
DESIGN AND ANALYSIS OF SENSORY OPTIMIZATION, M.C. Gacula, Jr.
NUTRIENT ADDITIONS TO FOOD, J.C. Bauernfeind and P.A. Lachance
NITRITE-CURED MEAT, R.G. Cassens
POTENTIAL FOR NUTRITIONAL MODULATION OF AGING, D.K. Ingram *et al.*
CONTROLLED/MODIFIED ATMOSPHERE/VACUUM PACKAGING OF FOODS, A.L. Brody
NUTRITIONAL STATUS ASSESSMENT OF THE INDIVIDUAL, G.E. Livingston
QUALITY ASSURANCE OF FOODS, J.E. Stauffer
THE SCIENCE OF MEAT AND MEAT PRODUCTS, 3RD ED., J.F. Price and B.S. Schweigert
HANDBOOK OF FOOD COLORANT PATENTS, F.J. Francis
ROLE OF CHEMISTRY IN PROCESSED FOODS, O.R. Fennema *et al.*
NEW DIRECTIONS FOR PRODUCT TESTING OF FOODS, H.R. Moskowitz
ENVIRONMENTAL ASPECTS OF CANCER: ROLE OF FOODS, E.L. Wynder *et al.*
FOOD PRODUCT DEVELOPMENT AND DIETARY GUIDELINES, G.E. Livingston, R.J. Moshy and C.M. Chang
SHELF-LIFE DATING OF FOODS, T.P. Labuza
ANTINUTRIENTS AND NATURAL TOXICANTS IN FOOD, R.L. Ory
UTILIZATION OF PROTEIN RESOURCES, D.W. Stanley *et al.*
POSTHARVEST BIOLOGY AND BIOTECHNOLOGY, H.O. Hultin and M. Milner

Newsletters

MICROWAVES AND FOOD, R.V. Decareau
FOOD INDUSTRY REPORT, G.C. Melson
FOOD, NUTRITION AND HEALTH, P.A. Lachance and M.C. Fisher

GUIDE FOR AUTHORS

If the manuscript has been produced by a word processor, a disk containing the manuscript would be greatly appreciated. Word Perfect 5.1 is the preferred word processing program. The original and THREE copies of the manuscript should be sent along with the disk to the editorial office. The typing should be double-spaced throughout with one-inch margins on all sides.

Page one should contain: the title, which should be concise and informative; the complete name(s) of the author(s); affiliation of the author(s); a running title of 40 characters or less; and the name and mail address to whom correspondence should be sent.

Page two should contain an abstract of not more than 150 words. This abstract should be intelligible by itself.

The main text should begin on page three and will ordinarily have the following arrangement:

Introduction: This should be brief and state the reason for the work in relation to the field. It should indicate what new contribution is made by the work described.

Materials and Methods: Enough information should be provided to allow other investigators to repeat the work. Avoid repeating the details of procedures that have already been published elsewhere.

Results: The results should be presented as concisely as possible. Do not use tables *and* figures for presentation of the same data.

Discussion: The discussion section should be used for the interpretation of results. The results should not be repeated.

In some cases it might be desirable to combine results and discussion sections.

References: References should be given in the text by the surname of the authors and the year. *Et al.* should be used in the text when there are more than two authors. All authors should be given in the Reference section. In the Reference section the references should be listed alphabetically. See below for style to be used.

RIZVI, S.S.H. 1986. Thermodynamic properties of foods in dehydration. In *Engineering Properties of Foods*, (M.A. Rao and S.S.H. Rizvi, eds.) pp. 133-214, Marcel Dekker, New York.

MICHAELS, S.L. 1989. Crossflow microfilters ins and outs. Chem. Eng. *96*, 84-91.

LABUZA, T.P. 1982. *Shelf-Life Dating of Foods*, pp. 66-120, Food & Nutrition Press, Trumbull, CT.

Journal abbreviations should follow those used in Chemical Abstracts. Responsibility for the accuracy of citations rests entirely with the author(s). References to papers in press should indicate the name of the journal and should only be used for papers that have been accepted for publication. Submitted papers should be referred to by such terms as "unpublished observations" or "private communication." However, these last should be used only when absolutely necessary.

Tables should be numbered consecutively with Arabic numerals. The title of the table should appear as below:

TABLE 1.
ACTIVITY OF POTATO ACYL-HYDROLASES ON NEUTRAL LIPIDS, GALACTOLIPIDS AND PHOSPHOLIPIDS

Description of experimental work or explanation of symbols should go below the table proper. Type tables neatly and correctly as tables are considered art and are not typeset. Single-space tables.

Figures should be listed in order in the text using Arabic numbers. Figure legends should be typed on a separate page. Figures and tables should be intelligible without reference to the text. Authors should indicate where the tables and figures should be placed in the text. Photographs must be supplied as glossy black and white prints. Line diagrams should be drawn with black waterproof ink on white paper or board. The lettering should be of such a size that it is easily legible after reduction. Each diagram and photograph should be clearly labeled on the reverse side with the name(s) of author(s), and title of paper. When not obvious, each photograph and diagram should be labeled on the back to show the top of the photograph or diagram.

Acknowledgments: Acknowledgments should be listed on a separate page.

Short notes will be published where the information is deemed sufficiently important to warrant rapid publication. The format for short papers may be similar to that for regular papers but more concisely written. Short notes may be of a less general nature and written principally for specialists in the particular area with which the manuscript is dealing. Manuscripts that do not meet the requirement of importance and necessity for rapid publication will, after notification of the author(s), be treated as regular papers. Regular papers may be very short.

Standard nomenclature as used in the engineering literature should be followed. Avoid laboratory jargon. If abbreviations or trade names are used, define the material or compound the first time that it is mentioned.

EDITORIAL OFFICE: DR. D.R. HELDMAN, COEDITOR, *Journal of Food Process Engineering*, University of Missouri-Columbia, 214 Agricultural Engineering Bldg., Columbia, MO 65211 USA; or DR. R.P. SINGH, COEDITOR, *Journal of Food Process Engineering*, University of California, Davis, Department of Agricultural Engineering, Davis, CA 95616 USA.

JOURNAL OF FOOD PROCESS ENGINEERING VOLUME 20, NUMBER 3

CONTENTS